

# Posterior Conformal Prediction

Yao Zhang\* and Emmanuel J. Candès†

October 1, 2024

## Abstract

Conformal prediction is a popular technique for constructing prediction intervals with distribution-free coverage guarantees. The coverage is marginal, meaning it only holds *on average* over the entire population but not necessarily for any specific subgroup. This article introduces a new method, *posterior conformal prediction* (PCP), which generates prediction intervals with both marginal and approximate conditional validity for clusters (or subgroups) naturally discovered in the data. PCP achieves these guarantees by modelling the conditional conformity score distribution as a mixture of cluster distributions. Compared to other methods with approximate conditional validity, this approach produces tighter intervals, particularly when the test data is drawn from clusters that are well represented in the validation data. PCP can also be applied to guarantee conditional coverage on user-specified subgroups, in which case it achieves robust coverage on smaller subgroups within the specified subgroups. In classification, the theory underlying PCP allows for adjusting the coverage level based on the classifier’s confidence, achieving significantly smaller sets than standard conformal prediction sets. We evaluate the performance of PCP on diverse datasets from socio-economic, scientific and healthcare applications.

## 1 Introduction

Conformal prediction [Vovk et al., 2005] is a modern technique for distribution-free uncertainty quantification. It allows generating prediction intervals with a desired coverage level while making minimal assumptions about the data distribution and

---

\*Department of Statistics, Stanford University

†Departments of Statistics and Mathematics, Stanford University

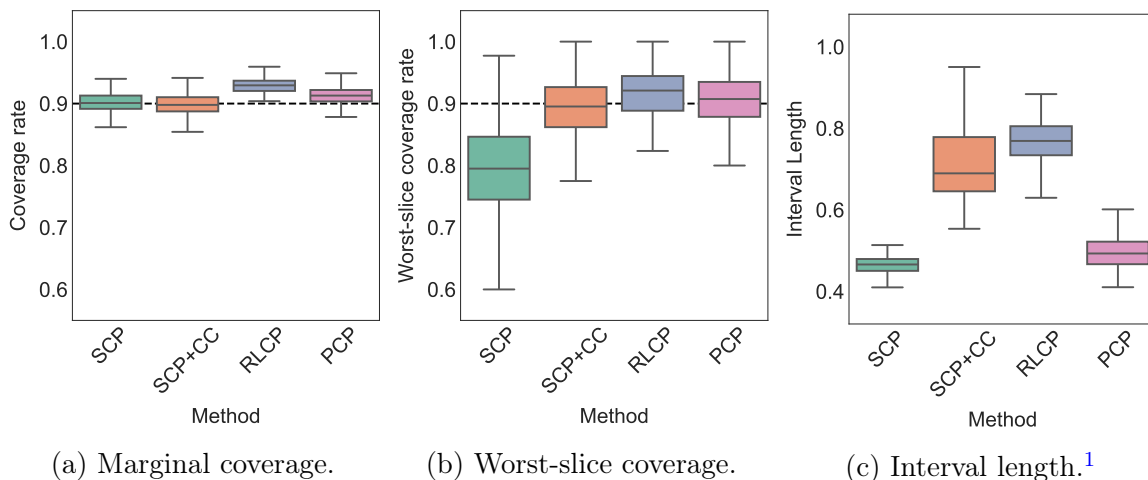


Figure 1: Marginal coverage rate, worst-slice conditional coverage rate [Cauchois et al., 2020; Romano et al., 2020b] and interval length of conformal prediction methods on the communities and crime dataset. The results are from 200 runs of the experiments.

predictive model. Due to this flexibility, researchers have applied conformal prediction to various domains, such as drug discovery [Cortés-Ciriano and Bender, 2020] and election forecasting [Cherian and Bronner, 2020].

Conformal prediction ensures *marginal* coverage, meaning the coverage holds on average over the population. However, this may be inadequate for real-world applications requiring coverage on subpopulations of interest. For instance, if a predictive model performs well overall but underperforms on racial minorities, then conformal prediction intervals might have poor coverage on those minority groups, despite achieving marginal coverage. Achieving coverage guarantees *conditional on individual-level information* is necessary to enable reliable decisions for everyone.

To address this issue, researchers have recently proposed new methods to achieve different types of conditional guarantees. These methods improve conditional coverage but may increase the interval length. To illustrate this tradeoff, we preview an experiment on the community and crime dataset [Redmond, 2009], which we shall return to in later sections. We train a random forest model to predict the per capita violent crime rate of communities from 99 features mostly providing demographic, socioeconomic, and crime-related information. To assess marginal coverage, we compute the coverage rate over all communities in the test portion of the dataset. To assess conditional coverage in finite samples, we follow Cauchois et al. [2020]; Romano et al. [2020b] to compute the “worst-slice” conditional coverage. This roughly corresponds to the worst coverage over all small subpopulations given by  $\{x : v^\top x \in$

<sup>1</sup>If an interval is infinite, we replace its length with twice the largest absolute prediction error in the test set, which represents the range of the prediction error.

$[a, b]$ , where  $a$ ,  $b$ , and  $v$  can vary arbitrarily. When  $v$  is a basis vector, the “worst-slice” method considers the local coverage for a particular feature in  $x$ . When  $v$  combines multiple features (e.g., unemployment and poverty rates), it can represent the economic condition of communities, as well as social and public security conditions. In this sense, the “worst-slice” method also assesses the local coverage rate across communities under a variety of conditions.

Figure 1a shows that all conformal prediction methods achieve a marginal coverage rate close to the target rate of 0.9. Split conformal prediction (SCP) [Vovk et al., 2005] has a worst-slice conditional coverage rate of around 0.8 (Figure 1b). More advanced methods, including SCP+conditional calibration (CC) [Gibbs et al., 2023], randomly-localized conformal prediction (RLCP) [Hore and Barber, 2023], and our proposed method, *posterior conformal prediction* (PCP), achieve a worst-slice conditional coverage rate close to 0.9. Among these advanced methods, only PCP can maintain an interval length comparable to that of SCP, as shown in Figure 1c. Code for implementing PCP and reproducing the experiments and figures in our article is available at <https://github.com/yaozhang24/pcp>.

The key difference between PCP and existing baselines is that PCP adapts its coverage guarantee to the residuals, i.e. the absolute differences between the observed crime rates and the corresponding predictions. PCP models the residuals to pinpoint regions where the random forest performs poorly, and then widens the interval until the desired coverage guarantee is achieved in those regions. By doing so, PCP balances the trade-off between conditional coverage and interval length. We next formalize the guarantees of conformal prediction and summarize our key idea.

## 1.1 Marginal and conditional validity

Suppose we have a pre-fitted predictive model  $\hat{\mu}$  mapping features  $X_{n+1} \in \mathcal{X}$  to predict the unseen response  $Y_{n+1} \in \mathcal{Y}$ . Given a separate set of validation data  $Z_{[n]} = (Z_1, \dots, Z_n) = ((X_i, Y_i), \dots, (X_n, Y_n))$ , the split conformal prediction (SCP) method constructs the following prediction interval for  $Y_{n+1}$ :

$$\hat{C}_n^{\text{SCP}}(X_{n+1}) = \left[ \hat{\mu}(X_{n+1}) \pm Q_{1-\alpha} \left( \sum_{i=1}^n \frac{1}{n+1} \delta_{R_i} + \frac{1}{n+1} \delta_{+\infty} \right) \right], \quad (1)$$

where  $Q_{1-\alpha}(\cdot)$  denotes the  $(1-\alpha)$ -quantile of the distribution in its argument and  $\delta_{R_i}$  denotes the point mass at  $R_i = |Y_i - \hat{\mu}(X_i)|$ . The interval (1) is centered at  $\hat{\mu}(X_{n+1})$ , and its width is given by an empirical quantile of the residuals. More generally, conformal prediction methods, including ours, can be based on any conformity score; see examples of conformity scores in Lei et al. [2018]; Romano et al. [2019]; Chernozhukov et al. [2021]. In most of this paper, except in the section where we consider classification problems, we will use the residual magnitude  $R_i$  as our conformity score.

Assume that  $Z_{[n+1]}$  is a sequence of i.i.d (or more generally, exchangeable) random variables. It is well known [Papadopoulos et al., 2002, Proposition 1] that the SCP interval in (1) has *marginal validity*, in the sense that

$$\mathbb{P}\{Y_{n+1} \notin \hat{C}_n^{\text{SCP}}(X_{n+1})\} \leq \alpha. \quad (2)$$

While marginal validity holds, the conditional coverage of SCP can fall below  $1 - \alpha$ . For instance, if the predictions for elderly individuals are less accurate, then the interval using residuals from individuals of all ages would have a coverage rate below  $1 - \alpha$  for the elderly population. To address such issues, we may consider generating a prediction interval with *conditional validity*:

$$\mathbb{P}\{Y_{n+1} \notin \hat{C}_n(X_{n+1}) \mid X_{n+1}\} \leq \alpha. \quad (3)$$

If age is a feature in  $X_{n+1}$ , conditional validity ensures that the coverage rate for individuals at any age is at least  $1 - \alpha$ . Unfortunately, it is known that in distribution-free settings, any interval satisfying (3) must have an infinite expected length [Vovk, 2012; Lei and Wasserman, 2014]. This hardness result follows from the fact that we never get to observe two features  $X_i$  and  $X_{n+1}$  at the same non-atomic point  $x \in \mathcal{X}$  in finite samples. Consequently, any observation located at  $X_i \neq x$  provides no information about the distribution of  $Y_{n+1} \mid X_{n+1} = x$ , unless the response distribution satisfies some smoothness assumption. Hence, conditional validity is only achievable via the infinite interval. Similarly, Theorem 2 in Barber et al. [2021] shows that if an interval can achieve a relaxed guarantee conditional on  $X_{n+1} \in \mathcal{S}$  for any subset  $\mathcal{S} \subseteq \mathcal{X}$  satisfying  $\mathbb{P}_X\{X \in \mathcal{S}\} \geq \delta$ , the expected length of this interval is comparable to the length of the SCP interval at level  $\delta\alpha$ . This means that achieving an accurate approximation of conditional validity inevitably increases the interval length.

## 1.2 Relaxation through mixture modeling

To overcome the challenges we have just reviewed, we introduce a relaxed notion of conditional validity that is both simple and flexible. The idea is to model the residuals  $R_{[n+1]}$  via a finite mixture model:

$$R_i \mid X_i \sim \sum_{k=1}^{K^*} \pi_k^*(X_i) f_k^*, \quad (4)$$

where  $K^* \in [n + 1]$ ,  $\pi^*(X_i)$  is a  $K^*$ -dimensional probability vector that sum to 1 and  $f_1^*, \dots, f_{K^*}^*$  are  $K^*$  distinct probability density or mass functions. For ease of exposition, we shall refer to  $\pi^*(X_i)$  as (cluster) membership probabilities and to  $f_k^*$ 's as cluster distributions. A mixture model can be used to represent residual distributions in many applications. For example, in a sales dataset, we may have more

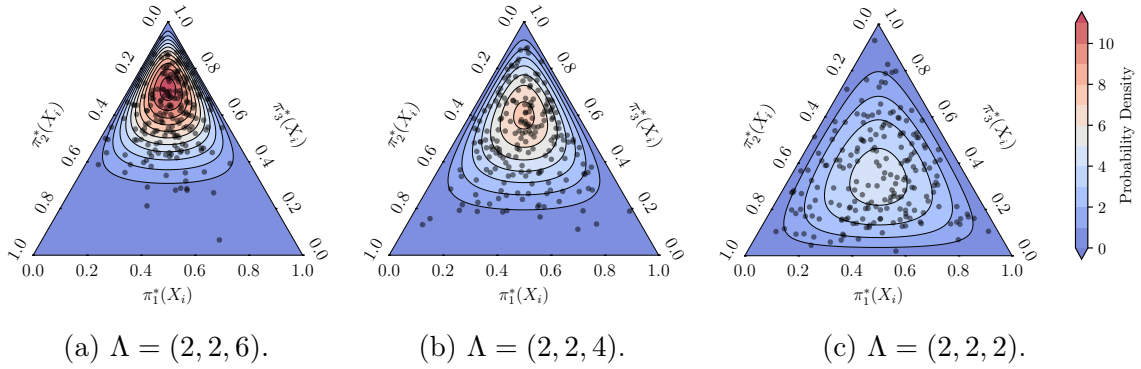


Figure 2: Dirichlet distributions  $\text{Dir}(\Lambda)$  of  $\pi^*(X_i)$  for three different values of  $\Lambda$ .

data on regular days than on promotion days, or the data on promotion days may be noisier than usual. Similarly, in a job hiring dataset, we may have less data for racial minorities. These data imbalance issues result in uneven performance of the predictive model across the feature space. The finite mixture in (4) can model the residuals in these situations by varying the membership probabilities across the feature space.

If  $\pi^*$  and  $f_1^*, \dots, f_{K^*}^*$  in the model (4) are known, the  $(1 - \alpha)$ -quantile of the residual  $R_{n+1} | X_{n+1}$  can be computed directly. Replacing the empirical quantile in (1) with this true quantile produces a conditionally valid interval for  $Y_{n+1}$ . When the cluster distributions are unknown,  $\pi^*$  can inform us about which  $f_k^*$  is most likely to generate  $R_i$  given  $X_i$ . By matching  $\pi^*(X_i)$  and  $\pi^*(X_{n+1})$ , we can identify the residuals  $R_i$  that share a conditional distribution similar to that of the test residual  $R_{n+1}$ . Running SCP on these residuals can generate a prediction interval for  $Y_{n+1}$  with approximate conditional validity as follows:

$$\hat{C}_n^*(X_{n+1}) = \left[ \hat{\mu}(X_{n+1}) \pm Q_{1-\alpha} \left( \sum_{i=1}^n w_i^* \delta_{R_i} + w_{n+1}^* \delta_{+\infty} \right) \right]; \quad (5)$$

here we use the quantiles of a weighted empirical distribution, where  $w_i^*$  takes the form  $\phi^*(X_i, X_{n+1}) / \sum_{j=1}^{n+1} \phi^*(X_j, X_{n+1})$  and  $\phi^*(X_i, X_{n+1})$  measures the similarity between  $\pi^*(X_i)$  and  $\pi^*(X_{n+1})$ , depending solely on their values. One of our formal results shows that the interval  $\hat{C}_n^*(X_{n+1})$  in (5) satisfies

$$\mathbb{P} \left\{ Y_{n+1} \notin \hat{C}_n^*(X_{n+1}) \mid X_1, \dots, X_{n+1} \right\} \leq \alpha + 2 \sum_{i=1}^{n+1} w_i^* \|\pi^*(X_i) - \pi^*(X_{n+1})\|_1. \quad (6)$$

Minimizing the  $\ell_1$  distances in (6) over  $w_i^*$  can be challenging if the membership probabilities  $\pi^*(X_1), \dots, \pi^*(X_{n+1})$  are widely dispersed across the probability simplex  $\Delta^{K^*-1}$ , as illustrated in Figure 2c. On the other hand, if the  $\pi^*(X_i)$ 's are tightly

clustered as in Figures 2a and 2b, many of the  $\pi^*(X_i)$ 's are clustered near  $\pi^*(X_{n+1})$ . Increasing the corresponding  $w_i^*$ 's and slightly lowering  $\alpha$  in (5) yields a finite and conditionally valid interval for  $Y_{n+1}$ . Moreover, we show that if the model (4) holds, conditional validity in (3) is implied by

$$\mathbb{P}\{Y_{n+1} \notin \hat{C}_n^*(X_{n+1}) \mid \pi^*(X_{n+1})\} \leq \alpha. \quad (7)$$

Conditional on  $\pi^*(X_{n+1})$ , the guarantee in (7) is an automatic interpolation between *no conditioning*, as in (2), and *full conditioning*, as in (3). For example, when the predictive model  $\hat{\mu}$  performs equally well across the feature space, we may only need a single cluster ( $K^* \approx 1$ ) and the interval obeying (7) can resemble that of SCP. In contrast, when  $\hat{\mu}$  performs unevenly for different instances, the interval needs to become increasingly adaptive to the test point. Building on this observation, we will introduce a new approach to approximate conditional validity by relaxing the guarantee in (7).

### 1.3 Outline

In Section 2, we introduce our posterior conformal prediction (PCP) method, which generates prediction intervals using a mixture model fitted to the residuals. While maintaining marginal validity, our interval has a coverage guarantee conditional on the membership probabilities from the mixture model. Our additional theoretical results focus on quantifying the probability that our interval has a finite length and assessing its worst-case coverage gap compared to conditional validity.

Apart from the standard conditional coverage problem, PCP finds applications in other calibration problems, such as equalizing coverage across subgroups and calibrating black-box classifiers, which will be described in Sections 3 and 4, respectively. In these applications, we focus on the fairness and adaptivity aspects of prediction intervals. In the former, we want our interval to achieve a group-conditional coverage guarantee while not harming any individuals within subgroups. In the latter, we aim to adjust the level of our prediction set so that it usually only contains a classifier's top-class prediction and correctly predicts the true label with a guarantee.

### 1.4 Related work

We next compare PCP with existing methods that achieve approximate conditional validity. These methods can be broadly categorized into localization and grouping.

Localization modifies the SCP interval in (1) by using a weighted empirical quantile, where the weight on  $\delta_{R_i}$  is proportional to a similarity measure between  $X_i$  and  $X_{n+1}$ ,

e.g.,  $w(X_i, X_{n+1}) \propto \exp\{-\beta\|X_i - X_{n+1}\|^2/2\}$  in the localized conformal prediction (LCP) method proposed by Guan [2023]. LCP needs to recalibrate the level  $\alpha$  of the quantile to maintain marginal validity. Conceptually, we can view LCP as running SCP in the neighbourhood of  $X_{n+1}$ , thereby improving the conditional coverage of  $Y_{n+1}$ . Hore and Barber [2023] proposed an extension of LCP called randomly-localized conformal prediction (RLCP), where they replace  $X_{n+1}$  in the LCP weights by a random draw  $\tilde{X}_{n+1} \sim \mathcal{N}(X_{n+1}, \beta^{-1}I)$ . This randomization step makes RLCP marginally valid without any level adjustment. However, even if  $X_i$  and  $X_{n+1}$  are relatively close in Euclidean distance, they may still differ in those important features that determine the distribution of  $R_{n+1} | X_{n+1}$ . Increasing  $\beta$  in (R)LCP can match  $X_i$  and  $X_{n+1}$  in every feature, but it may widen the interval by shrinking the sample size. In comparison, our construction is quite different since we use weights based on a similarity measure between the cluster membership probabilities at  $X_i$  and  $X_{n+1}$ . When our mixture model can accurately describe the conditional residual distribution with a few cluster distributions, our method can improve conditional coverage with tighter intervals compared to localization methods.

Grouping is often used to attain coverage guarantees for subgroups defined in terms of some sensitive attributes such as gender and age. When these subgroups form a partition of the feature space  $\mathcal{X}$ , running SCP with the data points from the same group as  $X_{n+1}$  can generate a group-conditional valid prediction interval for  $Y_{n+1}$  [Vovk et al., 2003; Lei and Wasserman, 2014; Romano et al., 2020a]. Jung et al. [2022] introduces a more direct method for grouping called multi-calibration, which involves fitting a linear quantile regression model to the validation data. This method can asymptotically achieve a coverage guarantee for overlapping subgroups. Gibbs et al. [2023] propose a conditional calibration (CC) method for SCP to generate intervals with exact finite-sample guarantees for any pre-specified function class, subsuming a class of subgroups as a special case. In comparison, our method offers no coverage guarantee for any pre-determined functions or subgroups.

## 2 Posterior conformal prediction (PCP)

Let  $\mathcal{D}_{\mathbf{z}} = \{z_i = (x_i, y_i) : i \in [n+1]\}$  be a set consisting of  $n+1$  distinct values of the data points  $Z_1, \dots, Z_{n+1}$ . Recall that the validity of conformal prediction relies on the data points  $Z_{[n+1]}$  being i.i.d. (or, more generally, exchangeable). This assumption implies that, conditional on  $Z_{[n+1]} \in \mathcal{D}_{\mathbf{z}}$ ,  $Z_{n+1}$  follows a uniform distribution,

$$\mathbb{P}\{Z_{n+1} = z_i \mid Z_{[n+1]} \in \mathcal{D}_{\mathbf{z}}\} = \frac{1}{n+1}, \quad \forall i \in [n+1]. \quad (8)$$

If the residuals  $r_i = |y_i - \hat{\mu}(x_i)|$  are distinct across  $i \in [n+1]$ , the test residual  $R_{n+1}$  takes on the value  $r_i$  with equal probability  $1/(n+1)$  for every  $i \in [n+1]$ . Thus,  $R_{n+1}$



is upper bounded by the empirical quantile in (1) with probability at least  $1 - \alpha$ . This argument establishes marginal validity of the SCP interval for  $Y_{n+1}$  in (2).

Let us now try extending the exchangeability argument to construct a conditionally valid prediction interval for  $Y_{n+1}$ . We then have

$$\mathbb{P}\{Z_{n+1} = z_i \mid Z_{[n+1]} \in \mathcal{D}_z, X_{n+1} = x_{n+1}\} = \begin{cases} 0, & \text{if } i \in [n], \\ 1, & \text{if } i = n + 1. \end{cases} \quad (9)$$

This is because the condition  $X_{n+1} = x_{n+1}$  only holds for  $z_{n+1} = (x_{n+1}, y_{n+1}) \in \mathcal{D}_z$ . In other words, eq. (9) suggests that  $Z_{n+1}$  is conditionally only exchangeable with itself. Thus, to achieve conditional validity, we must exclude the residuals  $R_1, \dots, R_n$  in (1), which unfortunately results in an infinite interval.

We next address this issue by aiming at the guarantee conditional on  $\pi^*(X_{n+1})$ . As discussed below (7), the choice of  $\pi^*(X_{n+1})$  automatically chooses the adaptivity to the test point  $X_{n+1}$ . Importantly, it also ensures that if the coverage rate conditional on  $\pi^*(X_{n+1})$  is upper bounded by  $\alpha$ , then so is the coverage rate conditional on  $X_{n+1}$ .

**Proposition 1.** *If the mixture model (4) holds, the interval  $\hat{C}_n^*(X_{n+1})$  in (5) satisfies*

$$\mathbb{P}\{Y_{n+1} \notin \hat{C}_n^*(X_{n+1}) \mid X_{n+1}\} = \mathbb{P}\{Y_{n+1} \notin \hat{C}_n^*(X_{n+1}) \mid \pi^*(X_{n+1})\}.^2 \quad (10)$$

We first note that if the  $\pi^*(X_i)$ 's are distinct across  $i \in [n + 1]$ , replacing the condition  $X_{n+1} = x_{n+1}$  with  $\pi^*(X_{n+1}) = \pi^*(x_{n+1})$  does not change the equality in (9). However,  $\pi^*(X_{n+1})$  is a vector of probabilities rather than arbitrary features. This characteristic allows us to relax the guarantee conditional on  $\pi^*(X_{n+1})$  by sampling: first, draw a sample of size  $m$  from the multinomial distribution based on  $\pi^*(X_{n+1})$ , and then compute the sample mean  $\tilde{\pi}^*(X_{n+1})$  to estimate  $\pi^*(X_{n+1})$ , i.e.,

$$\tilde{L} = (\tilde{L}_1, \dots, \tilde{L}_{K^*}) \sim \text{Multi}(m, \pi^*(X_{n+1})) \quad \text{and} \quad \tilde{\pi}^*(X_{n+1}) = \tilde{L}/m. \quad (11)$$

We shall refer to  $m$  as the precision parameter in our interval defined below since increasing  $m$  makes  $\tilde{\pi}^*(X_{n+1})$  a more accurate estimate of  $\pi^*(X_{n+1})$ . Next, we update the uniform distribution in (8) by conditioning on the estimator  $\tilde{\pi}^*(X_{n+1})$  or the sample  $\tilde{L}$ . By Bayes' rule, we obtain the posterior distribution,

$$\mathbb{P}\{Z_{n+1} = z_i \mid Z_{[n+1]} \in \mathcal{D}_z, \tilde{\pi}^*(X_{n+1})\} \propto \prod_{k=1}^{K^*} [\pi_k^*(x_i)]^{\tilde{L}_k}, \quad \forall i \in [n + 1], \quad (12)$$

which is the likelihood function  $\text{Multi}(m, \pi^*(x_i))$  evaluated at  $\tilde{L}$ . The (concentrated) posterior in (12) serves as our approximation of the point mass distribution in (9).

---

<sup>2</sup>Even though we can use  $\pi^*(X_{n+1})$  to predict the true membership of  $X_{n+1}$ , the coverage rate conditional on the prediction is not the same as the coverage rate conditional on  $X_{n+1}$ .



We define our interval  $\hat{C}_n^*(X_{n+1})$  as in (5) with  $\phi^*(X_i, X_{n+1})$  as the likelihood function in (12). The weight  $w_i^*$  in the interval is proportional to the likelihood ratio  $\phi^*(X_i, X_{n+1})/\phi^*(X_{n+1}, X_{n+1})$ , which can be expressed as

$$w_i^* \propto \exp \left\{ - \sum_{k=1}^{K^*} \tilde{L}_k \log \frac{\pi_k^*(X_{n+1})}{\pi_k^*(X_i)} \right\} \approx \exp \left\{ -m D_{\text{KL}}(\pi^*(X_{n+1}) \parallel \pi^*(X_i)) \right\}, \quad (13)$$

where the approximation holds for large  $m$ , and  $D_{\text{KL}}(\cdot \parallel \cdot)$  is the Kullback-Leibler (KL) divergence between  $\pi^*(X_i)$  and  $\pi^*(X_{n+1})$ . By matching  $\pi^*(X_i)$  and  $\pi^*(X_{n+1})$ , the weight  $w_i^*$  reduces the coverage gap in (6) and achieves the following relaxed guarantee.

**Theorem 1.** *If  $Z_i = (X_i, Y_i), i \in [n + 1]$ , are exchangeable, the interval  $\hat{C}_n^*(X_{n+1})$  in (5) based on the weights in the left-hand side (LHS) of (13) satisfies*

$$\mathbb{P}\{Y_{n+1} \notin \hat{C}_n^*(X_{n+1}) \mid \tilde{\pi}^*(X_{n+1})\} \leq \alpha. \quad (14)$$

Marginalizing out  $\tilde{\pi}^*(X_{n+1})$  in (14) shows that the interval  $\hat{C}_n^*(X_{n+1})$  has marginal validity. In Appendix A, we prove that the interval loses marginal validity if it uses the non-randomized weights in the right-hand side (RHS) of (13). Controlling the coverage gap between the randomized and non-randomized intervals requires additional assumptions, while randomization allows us to establish distribution-free validity.

One way to interpret (14) is through the latent membership of the residuals under the mixture model (4), which can be expressed as follows: conditional on  $X$ , sample a latent variable  $U$  from  $\sum_{k=1}^{K^*} \pi_k^*(X) \delta_k$ , and then conditional on  $U$ , generate a residual from the cluster distribution  $f_U^*$ . To give a concrete example, imagine we are using a model  $\hat{\mu}$  to predict a diabetes risk score  $Y$ . The model  $\hat{\mu}$  may perform poorly and generate large residuals for a small subpopulation with insulin resistance ( $U = 1$ ) due to limited training data. Although  $U$  is unobserved, it may be correlated with observed features, including metabolic and lifestyle factors. To satisfy the guarantee in (14), the interval  $\hat{C}_n^*(X_{n+1})$  assigns large weights to individuals with  $\pi(X_i) \approx \tilde{\pi}^*(X_{n+1})$ , where we interpret the membership probabilities  $\tilde{\pi}^*(X_{n+1})$  as a “soft” prediction of  $U_{n+1}$ . When  $\tilde{\pi}_1^*(X_{n+1}) \approx 1$ , the interval upweights individuals who are likely to have insulin resistance ( $U_i = 1$ ). When  $\tilde{\pi}_1^*(X_{n+1}) \approx 0.5$ , the interval gives more weight to individuals whose insulin resistance status is rather uncertain. In comparison, using a “hard” prediction of  $U_{n+1}$  may yield a significantly different interval. For example, whenever the prediction is  $U_{n+1} = 1$ , we compute the interval  $\hat{C}_n^*(X_{n+1})$  as if  $\tilde{\pi}_1^*(X_{n+1}) = 1$ . This approach may lead to substantial coverage loss, especially when  $U_{n+1}$  is uncertain and thus difficult to predict from  $X_{n+1}$ .

As the precision parameter  $m$  increases, the coverage guarantee in (14) approaches conditional validity, with the RHS of (10) being nearly upper bounded by  $\alpha$ .<sup>3</sup> However,

---

<sup>3</sup>The mean squared error of  $\tilde{\pi}^*(X_{n+1})$  in estimating  $\pi^*(X_{n+1})$  is upper bounded by  $1/m$ .

if we let  $m$  grow excessively, the interval may become infinite, as most of the  $w_i^*$ 's in (13) diminish while  $w_{n+1}^*$  exceeds  $\alpha$ . In the next subsection, we will discuss how we choose  $m$  to balance the trade-off between conditional coverage and interval length. Here, we illustrate scenarios in which our interval can remain finite even for large  $m$ .

**Theorem 2.** *If the model (4) holds,  $\pi^*(X_{n+1}) \sim \text{Dir}(\Lambda_1, \Lambda_2, \Lambda_3)$  and  $\bar{\Lambda} = \sum_{k=1}^3 \Lambda_k$ , the interval  $\hat{C}_n^*(X_{n+1})$  in (5) using the weights in the LHS of (13) satisfies*

$$\begin{aligned} & \mathbb{P}\{|\hat{C}_n^*(X_{n+1})| < \infty \mid X_1, X_1, \dots, X_n, \tilde{\pi}^*(X_{n+1}) = \Lambda/\bar{\Lambda}\} \\ &= \min \left\{ \frac{\alpha}{1-\alpha} \sum_{i=1}^n \exp \left( -m \sum_{k=1}^3 D_{\text{KL}}(\tilde{\pi}^*(X_{n+1}) \parallel \pi^*(X_i)) \right), 1 \right\}^{(m+\bar{\Lambda})/m} + O(1/m).^4 \end{aligned}$$

For example, in Figure 2a, the mean  $\Lambda/\bar{\Lambda}$  of the distribution  $\text{Dir}(\Lambda)$  is located in the top red region of the simplex. This region contains many samples  $\pi^*(X_i)$  that have a small KL divergence from  $\Lambda/\bar{\Lambda}$ . If  $\pi^*(X_{n+1})$  is also located in this region such that  $\pi^*(X_{n+1}) \approx \tilde{\pi}^*(X_{n+1}) = \Lambda/\bar{\Lambda}$ , the sum of the  $n$  exponential functions in Theorem 2 exceeds  $(1-\alpha)/\alpha$ , implying that our interval is finite with probability 1. This result highlights that when  $\pi^*(X_{n+1})$  is located in the high-density region of the distribution of  $\pi^*(X_i)$ , our interval can be finite even for a large value of  $m$ . In comparison, as discussed in Section 1.4, localization can match  $X_i$  and  $X_{n+1}$  to achieve approximate conditional validity, but it may produce infinite intervals as the features disperse in moderate- or high-dimensional spaces. Grouping, on the other hand, may provide a poor approximation of conditional validity if the pre-specified subgroups fail to capture changes in the conditional residual distribution. Increasing the number of subgroups may result in wide intervals due to smaller sample sizes within each group.

In what follows, assuming that  $\pi^*$  is unknown, PCP constructs intervals by fitting a mixture model to the residuals. This approach discovers subgroups with distinct residual distributions. As illustrated in Theorem 2, if a test point shares similar membership probabilities with many points in a large subgroup, PCP can improve the conditional coverage of its interval by increasing the precision parameter  $m$ .

## 2.1 PCP interval

Given a fixed number of cluster distributions  $K$ , the fitting algorithm  $\mathcal{A}$  is a mapping from an imputed dataset  $\mathcal{D}_{[n+1]}^y = \{(X_1, Y_1), \dots, (X_n, Y_n), (X_{n+1}, y)\}$  to the member-

---

<sup>4</sup>The proof in Appendix C.4 is based on an interesting observation that, after some transformation, the non-normalized weight of the point mass  $\delta_{+\infty}$  in  $\hat{C}_n^*(X_{n+1})$  approximately follows an exponential distribution. We also provide a set of numerical experiments to verify this theory across various  $\Lambda$ .

ship probabilities  $\pi^y$  in the model. We require  $\mathcal{A}$  to satisfy

$$\mathcal{A}((x_{\sigma(1)}, y_{\sigma(1)}), \dots, (x_{\sigma(n+1)}, y_{\sigma(n+1)})) \stackrel{d}{=} \mathcal{A}((x_1, y_1), \dots, (x_{n+1}, y_{n+1})), \quad (15)$$

for all  $n \geq 1$ , permutations  $\sigma$  on the index set  $[n+1]$ , and  $\{(x_i, y_i) : i \in [n+1]\}$ . The equality in distribution means we can use a randomized algorithm  $\mathcal{A}$ , but the randomization step in  $\mathcal{A}$  should be independent of the data order. The imputation  $y$  and the symmetry of  $\mathcal{A}$  are introduced to preserve the exchangeability of the validation and test samples, which is crucial for the validity result below.

The prediction interval of PCP is defined as

$$\hat{C}_n^{\text{PCP}}(X_{n+1}) = \left\{ y \in \mathcal{Y} : P_n^{\text{PCP}}(y) := \sum_{i=1}^{n+1} \tilde{w}_i(\mathcal{D}_{[n+1]}^y) \mathbb{1}\{R_i \geq R_{n+1}^y\} > \alpha \right\}, \quad (16)$$

where  $R_{n+1}^y = |y - \hat{\mu}(X_{n+1})|$ . The weight  $\tilde{w}_i(\mathcal{D}_{[n+1]}^y)$  is given by

$$\tilde{w}_i(\mathcal{D}_{[n+1]}^y) \propto \prod_{k=1}^K [\pi_k^y(X_i)]^{m \tilde{\pi}_k^y(X_{n+1})} \propto \exp \left\{ -m \sum_{k=1}^K \tilde{\pi}_k^y(X_{n+1}) \log \frac{\pi_k^y(X_{n+1})}{\pi_k^y(X_i)} \right\}, \quad (17)$$

where  $\tilde{\pi}^y(X_{n+1}) = \tilde{L}^y/m$  and  $\tilde{L}^y \sim \text{Multi}(m, \pi^y(X_{n+1}))$ . When computing the interval in (16), we need to estimate  $\pi^y$  for all  $y \in \mathcal{Y}$  and avoid overfitting the mixture model to  $R_{n+1}^y$ . We address these challenges by developing an efficient algorithm  $\mathcal{A}$ , which has linear complexity in the sample size  $n$ . This algorithm is not required for the applications of PCP in Sections 3 and 4, so we defer its introduction to Appendix B. In what follows, we let  $\mathcal{D}_{[n+1]} = \mathcal{D}_{[n+1]}^{Y_{n+1}}$  and  $\tilde{\pi}(X_{n+1}) = \tilde{\pi}^{Y_{n+1}}(X_{n+1})$  given that  $\mathcal{A}$  is a symmetric function of its arguments, as described in (15).

**Proposition 2.** *Suppose that  $Z_i = (X_i, Y_i), i \in [n+1]$ , are exchangeable, and the algorithm  $\mathcal{A}$  treats the examples in  $\mathcal{D}_{[n+1]}$  symmetrically as in (15). Then for any  $m \in \mathbb{N}^+$ , the posterior conformal prediction (PCP) interval in (16) satisfies*

$$\mathbb{P}\left\{ Y_{n+1} \notin \hat{C}_n^{\text{PCP}}(X_{n+1}) \mid \tilde{\pi}(X_{n+1}) \right\} \leq \alpha. \quad (18)$$

Furthermore, if all the residuals  $R_{[n+1]}$  are distinct with probability 1,

$$\mathbb{P}\left\{ Y_{n+1} \notin \hat{C}_n^{\text{PCP}}(X_{n+1}) \mid \tilde{\pi}(X_{n+1}) \right\} \geq \alpha - \mathbb{E}\left\{ \max_{i \in [n+1]} \tilde{w}_i(\mathcal{D}_{[n+1]}) \mid \tilde{\pi}(X_{n+1}) \right\}. \quad (19)$$

If the maximum weight in (19) is small, our interval is finite and has a coverage rate close to  $\alpha$ . This occurs when sufficiently many  $\pi^y(X_i)$ 's are similar to  $\pi^y(X_{n+1})$  in (17), which resembles the condition for obtaining a finite interval in Theorem 2. To control the magnitude of the weights, we select the number  $K$  of cluster distributions and

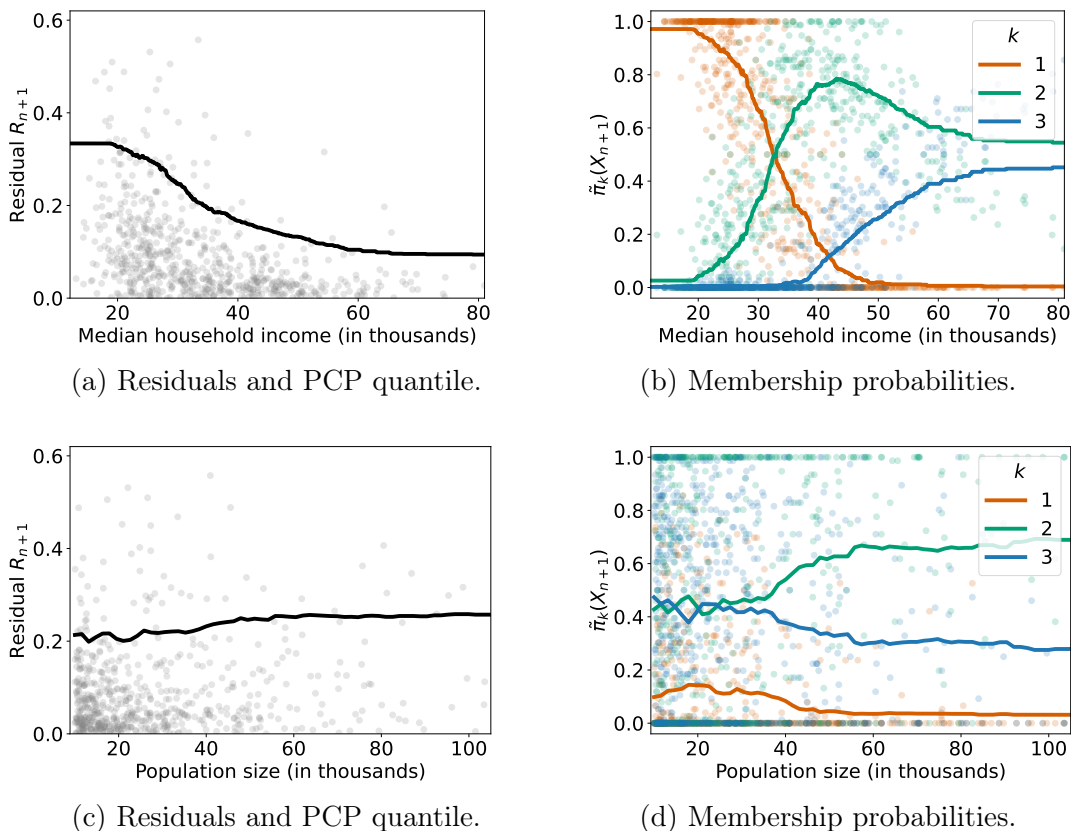


Figure 3: Illustration of PCP quantiles and membership probabilities over the population and income features in the communities and crime dataset.

the precision parameter  $m$  using the dataset for fitting the model  $\hat{\mu}$ . Specifically, we use this dataset to generate a separate set of residuals by cross-validation. We select the smallest mixture model that can explain most of the variations in the residuals. We then use these residuals to construct PCP intervals and select the largest value of  $m$  that can keep the intervals finite and stable. Further details on this selection procedure can be found in Appendix B.

The guarantee in Proposition 2 can be interpreted as that in Theorem 1. Using  $\tilde{\pi}(X_{n+1})$  as a “soft” prediction of the test point’s membership, it can improve conditional coverage if the distribution of  $R | X$  can be accurately described by

$$R | X \sim \sum_{k=1}^K \tilde{\pi}_k(X) f_k \quad (20)$$

for some arbitrary cluster distributions  $f_1, \dots, f_K$ . We illustrate this using the communities and crime dataset [Redmond, 2009] above.

Figures 3a and 3c show how the test residuals vary across two features, “Median house-

hold income” and “Population size”, respectively. The black curves are the local averages of the finite residual quantiles produced by PCP over the nearest 100 test points.<sup>5</sup> Figures 3b and 3d depict the probabilities  $\tilde{\pi}(X_{n+1}) = [\tilde{\pi}_1(X_{n+1}), \tilde{\pi}_2(X_{n+1}), \tilde{\pi}_3(X_{n+1})]$  and their local averages as solid curves.

When the residuals increase in low-income communities, as shown in Figure 3a, the membership probability  $\tilde{\pi}_1(X_{n+1})$  also rises with decreasing income, as depicted in Figure 3b. The first subgroup primarily consists of low-income communities, while the other two groups comprise higher-income communities. In contrast, the residual distribution is nearly invariant across population size in Figure 3c, and consequently,  $\tilde{\pi}(X_{n+1})$  only exhibits minor variations across population size in Figure 3d. The probabilities  $\tilde{\pi}(X_{n+1})$  effectively summarize the feature information related to the residual distribution while marginalizing out the irrelevant factors. Therefore, the income- and population-conditional residual distributions (Figures 3a and 3c) can be approximately expressed as (20). Consequently, PCP has approximately valid coverage over these features.

Proposition 2 offers a guarantee based on a mixture model learnt from the data. We next assume that the residuals follow a true mixture model (4), and then bound the conditional coverage gap of our interval, without requiring the number of cluster distributions to be specified correctly. Our bounds are inspired by those in Barber et al. [2023]. In the theorems below, we consider the KL limit of our interval in (13).

**Theorem 3.** *If the mixture model (4) holds, the PCP interval defined in (16) using weights  $w_{\text{KL},i} \propto \exp\{-mD_{\text{KL}}(\pi(X_{n+1})||\pi(X_i))\}$  for some fixed  $\pi$  satisfies*

$$\mathbb{P}\{Y_{n+1} \notin \hat{C}_n^{\text{PCP}}(X_{n+1}) \mid X_1, \dots, X_{n+1}\} \leq \alpha + 2 \sum_{i=1}^{n+1} w_{\text{KL},i} \|\pi^*(X_i) - \pi^*(X_{n+1})\|_1.$$
<sup>6</sup>

**Theorem 4.** *In the setting of Theorem 3, it holds that*

$$\mathbb{P}\{Y_{n+1} \notin \hat{C}_n^{\text{PCP}}(X_{n+1}) \mid X_1, \dots, X_{n+1}\} \leq \alpha \sum_{k=1}^{K^*} \frac{\pi_k^*(X_{n+1})}{\sum_{i=1}^n w_{\text{KL},i} \pi_k^*(X_i)}.$$

As demonstrated above, PCP fits a mixture model to the residuals, allowing the membership probabilities  $\pi$  to identify the key features of the true probabilities  $\pi^*$  in (4). The KL divergence based on  $\pi$  captures the similarity between  $\pi^*(X_i)$  and  $\pi^*(X_{n+1})$ , enabling the weight  $w_{\text{KL},i}$  to reduce the coverage gap of our interval.

<sup>5</sup>The quantile is the  $R_{n+1}^y$  in (16) for the largest  $y$  satisfying that  $P_n^{\text{PCP}}(y) \geq \alpha$ , i.e.,  $y$  is the upper bound in  $\hat{C}_n^{\text{PCP}}(X_{n+1})$ . We only show the local average to keep the residuals visible.

<sup>6</sup>We also allow the weights to depend on the residuals in the proof of Theorem 3 in Appendix C.5.

Theorem 4 offers a tighter bound for the coverage gap when  $\pi^*$  is sparse. For instance, if  $\pi_k^*(X_{n+1}) = 1$  and  $\pi_{k'}^*(X_{n+1}) = 0$  for  $k' \neq k$ , the bound can be written as

$$\alpha / \sum_{i=1}^n w_{\text{KL},i} \pi_k^*(X_i) \approx \alpha + \alpha \left[ \pi_k^*(X_{n+1}) - \sum_{i=1}^n w_{\text{KL},i} \pi_k^*(X_i) \right] \approx \alpha.$$

To summarize, the theorems above show that PCP can improve conditional coverage, especially when  $\pi^*(X_i)$  are concentrated and/or sparse.

## 2.2 Empirical results

We next provide more experiments to compare PCP with the other methods in Figure 1. Implementation details of all the methods can be found in Appendix E.

### 2.2.1 Experiments on synthetic data

Our data experiment here has two settings. We discuss the first setting in this subsection and defer the second to the Appendix. We first create a 6-dimensional feature vector  $X$  by sampling each feature from the uniform distribution on  $[0, 8]$ . We let  $V$  and  $W$  denote the first and second features in  $X$  respectively. We define a drift function  $f(V) = -3V + V^2 - 5V \sin(V)$  and use it to generate the response,

$$Y = f(V) + [4 + 2(V - 2)^2] \epsilon_i \quad \text{and} \quad \epsilon_i \sim \mathcal{N}(0, 1).$$

We generate 5000 random copies of  $(X, Y)$  as our training, validation, and test sets, respectively. We then use the training set to fit a random forest model  $\hat{\mu}$  to predict the responses in the validation and test set. Since  $\hat{\mu}$  can accurately approximate  $f(V)$ , most of the variations in the residual  $R = |Y - \hat{\mu}(X)|$  given  $X$  come from the variance function of  $Y$ . We can imagine that  $R$  roughly follows a mixture model in (4) with a small  $K^*$ . Since the variance of  $Y$  only depends on  $V$ , the distribution of  $\pi^*(X)$  has small variability over  $X$ . This is the scenario where our interval can be finite for a large value of  $m$  in Theorem 2, and achieve a small coverage gap in Theorem 3.

Figure 4 depicts the test responses in grey, along with their prediction intervals. Figure 5 shows the local average coverage rates of the conformal prediction methods over the 250 nearest test points based on the feature  $V$ . SCP computes intervals without using the feature  $V$ , resulting in a local coverage rate deviating significantly from the target rate of 0.9. SCP+CC computes intervals using a linear quantile regression model of the residuals. These intervals lose coverage when the model fails to capture the nonlinear changes in the conditional residual distribution. RLCP also suffers coverage loss, which shows that matching all the features may overlook the

variations primarily caused by the first feature  $V$ . In comparison, PCP maintains a coverage rate near 0.9 by effectively modelling the smooth variation in the conditional residual distribution. The hyperparameter selection method in Appendix B.1 chooses the number  $K = 3$  of cluster distributions and the precision parameter  $m = 276$  to construct the PCP intervals. Figure 6 shows that the PCP (local average) membership probabilities vary smoothly over  $V$  while fluctuating randomly over  $W$ . This indicates that our mixture model identifies  $V$  as the key feature driving the changes in the conditional residual distribution. In Appendix E.1, we demonstrate PCP can also deal with nonsmooth variations in the second setting of our experiment.

### 2.2.2 Experiments on real data

We next discuss experiments on the following two real-world datasets:

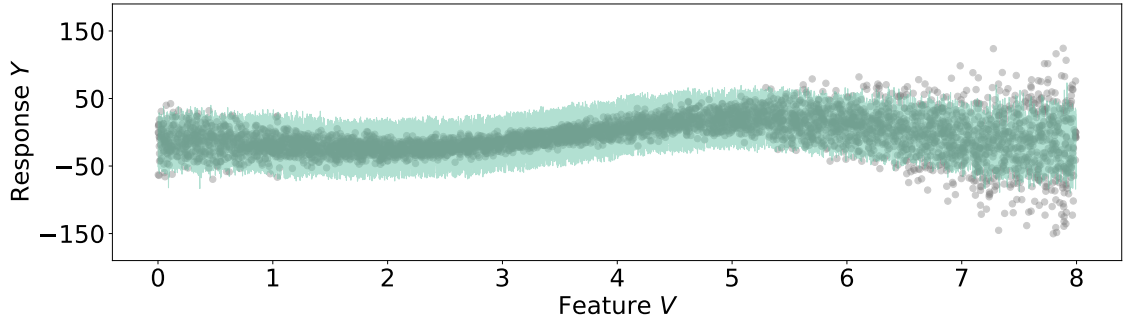
- The online news popularity dataset [Fernandes et al., 2015] includes 58 features describing the content of articles, such as word counts and the number of images, to predict the number of shares each article receives on social networks.
- The superconductivity dataset [Hamidieh, 2018] contains 81 features about materials and their properties, such as mean atomic mass and radius, to predict the critical temperature ( $T_c$ ) at which a material becomes superconductive.

We reduce the dimensionality of both datasets to 30 using principal component analysis (PCA) and use ridge regression as the predictive model  $\hat{\mu}$ . We compare the coverage rates and interval length of the conformal prediction methods across 200 independent runs of our experiments, each using a subsample of 2,000 data points.

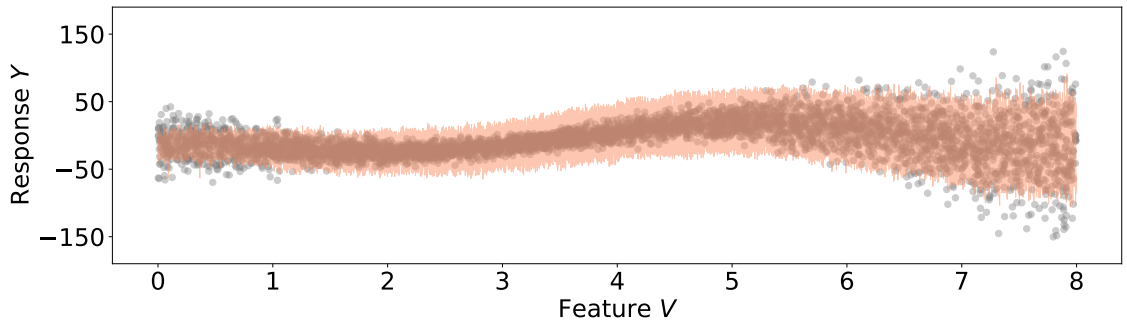
The results for the popularity dataset are reported in Figure 7. All methods achieve a marginal coverage rate near the target rate of 0.9. However, the worst-slice conditional coverage rate (WSCR) of SCP falls significantly below 0.9, while the WSCRs of RLCP, SCP+CC, and PCP are approximately 0.9. In terms of interval length, RLCP produces much wider intervals than SCP+CC and PCP. Although SCP+CC generates shorter intervals than PCP, it does so at the cost of slightly lower WSCR.

The results for the superconductivity dataset are shown in Figure 8. Here, the WSCR of SCP is slightly below 0.9, leaving a small gap for other methods to fill. Among the advanced methods, only PCP can close the gap without significantly increasing interval length. Using a linear quantile regression model, SCP+CC achieves a pre-specified coverage guarantee across all linear functions of the features. In comparison, PCP improves coverage more effectively by adapting its guarantee to the residuals.

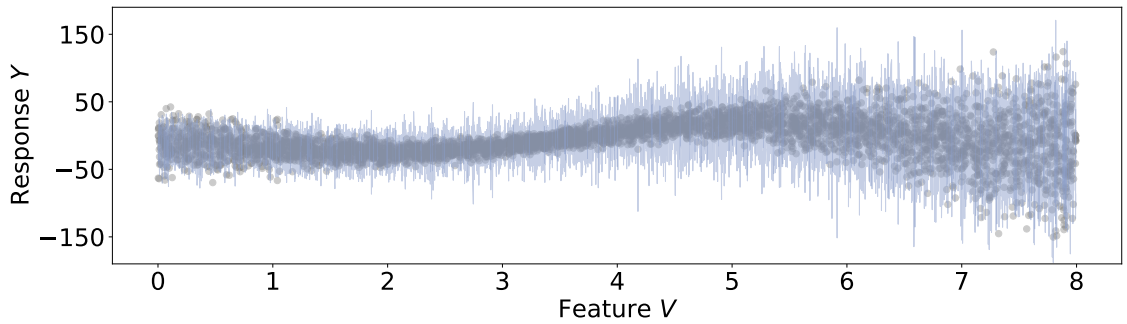




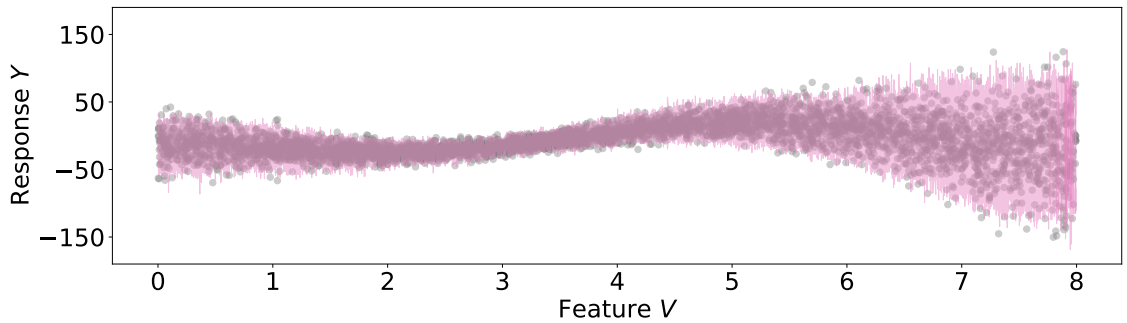
(a) Split conformal prediction (SCP).



(b) SCP+conditional calibration (SCP+CC).



(c) Randomly-localized conformal prediction (RLCP).



(d) Posterior conformal prediction (PCP).

Figure 4: Prediction intervals of conformal prediction methods in Setting 1.

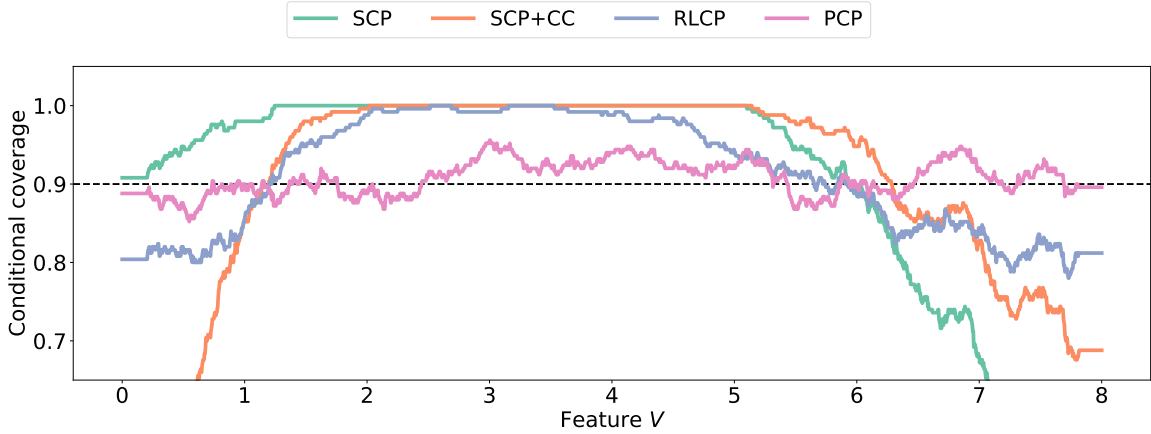


Figure 5: Local average coverage rates of conformal prediction methods in Setting 1.

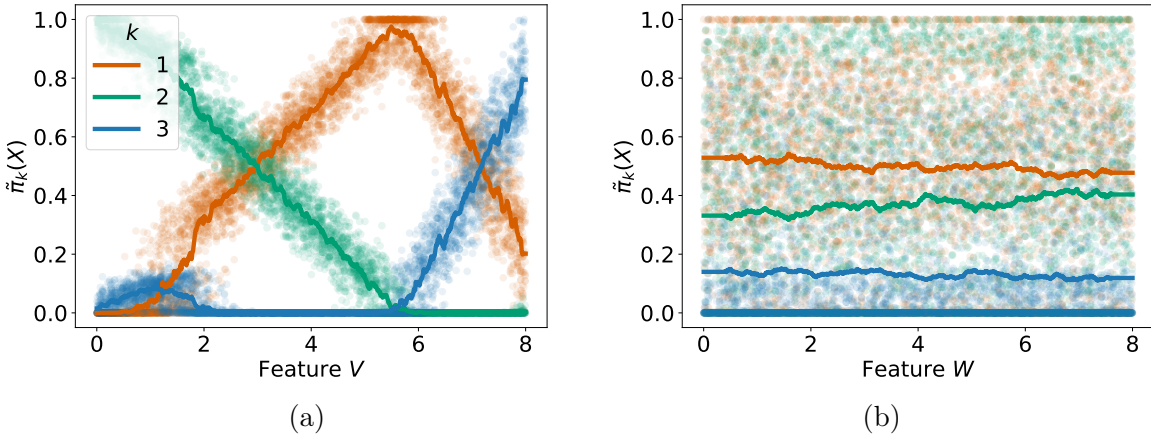


Figure 6: PCP membership probabilities in Setting 1.

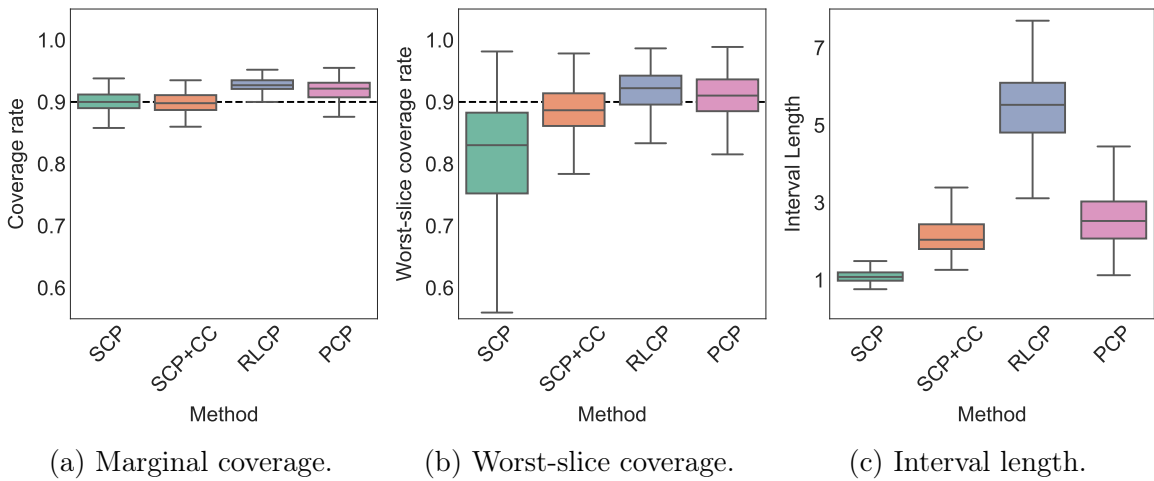


Figure 7: Comparison of conformal prediction methods on the online news popularity dataset.

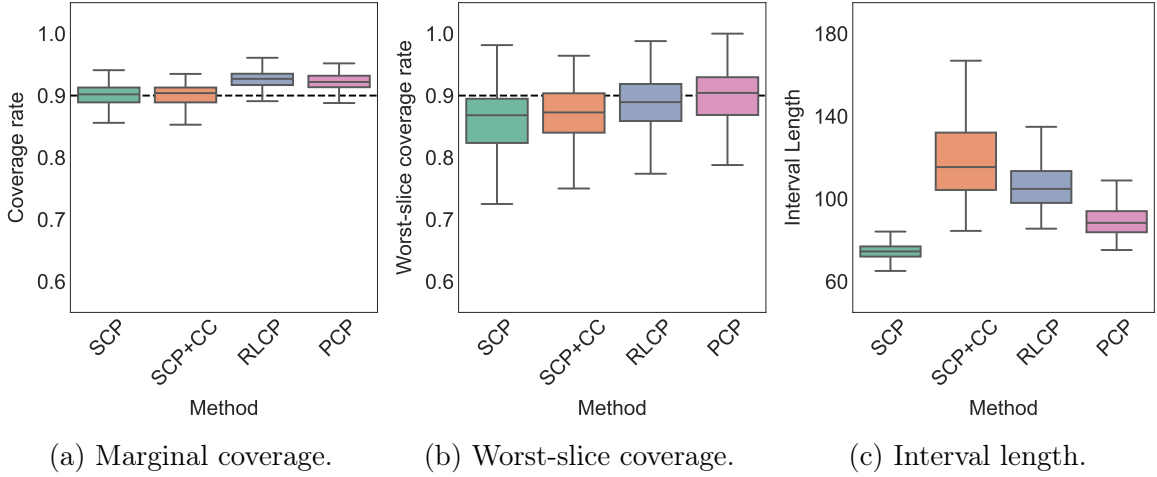


Figure 8: Comparison of conformal prediction methods on the superconductivity dataset.

### 3 Equalized conditional coverage

In conformal prediction, the partition method [Lei and Wasserman, 2014; Romano et al., 2020a] is often used to generate prediction intervals with group-conditional coverage guarantees. We next show that this partition-based approach may lead to a loss of coverage for some individuals within the subgroups. In response, we apply PCP to achieve the same group-conditional coverage guarantees while making the interval nearly independent of the test point’s subgroup membership. By doing so, PCP eliminates the coverage gap arising from the partition.

To begin with a concrete example, imagine that we have a medical dataset from a study of a disease where male patients are predominant. In this dataset, it is crucial to obtain a group conditional coverage guarantee for gender  $A_{n+1} \in \{0, 1\}$ , as the predictive model may underperform for females due to limited training data. In this situation, we often run SCP for males and females separately. Specifically, we let  $\mathcal{I}_n = \{i \in [n + 1] : A_i = A_{n+1}\}$  collect all the individuals who have the same gender as the test point. Running SCP solely on  $Z_{\mathcal{I}_n}$  produces the interval,

$$\hat{C}_n^{\text{SCP+Partition}}(X_{n+1}, A_{n+1}) = \left[ \hat{\mu}(X_{n+1}, A_{n+1}) \pm Q_{1-\alpha} \left( \sum_{i \in \mathcal{I}_n} \frac{1}{|\mathcal{I}_n|} \delta_{R_i} + \frac{1}{|\mathcal{I}_n|} \delta_{+\infty} \right) \right],$$

which satisfies the group-conditional coverage guarantee,

$$\mathbb{P}\{Y_{n+1} \notin \hat{C}_n^{\text{SCP+Partition}}(X_{n+1}, A_{n+1}) \mid A_{n+1}\} \leq \alpha. \quad (21)$$

Despite the guarantee in (21), generating intervals based on a partition may decrease the coverage rate for some minorities within the subgroups. This general phenomenon

can be illustrated using the probabilities of  $A = 1$  (female),

$$\theta = \mathbb{P}\{A = 1\} \quad \text{and} \quad e(X) = \mathbb{P}\{A = 1 \mid X\}.$$

For any value of  $\theta \in (0, 1)$ , it holds that

$$\underbrace{\mathbb{P}\{e(X) \geq \theta \mid A = 1\}}_{\text{Female population}} - \underbrace{\mathbb{P}\{e(X) \geq \theta\}}_{\text{Full population}} = \mathbb{E}[\mathbb{1}\{e(X) \geq \theta\} (e(X)/\theta - 1)] \geq 0. \quad (22)$$

Equation (22) highlights that the female population ( $A = 1$ ) is more likely to have  $e(X) \geq \theta$  than the full population. In other words, a test point with  $A_{n+1} = 1$  but  $e(X_{n+1}) < \theta$  is less likely in the female population than in the full population. For instance, females who are taller than the average height of the full population are even more minoritized in the female population than in the full population. Consequently, the SCP+Partition interval defined above will achieve a worse coverage rate for these tall females, compared to the original SCP interval computed using full data.

To demonstrate this coverage loss, we compare the methods on the Medical Expenditure Panel Survey (MEPS) 2019 dataset [Romano et al., 2019, 2020a], provided by the Agency for Healthcare Research and Quality. In this experiment, we predict individuals' utilization of medical services from their personal information, such as age, race, poverty status, health status, etc. We randomly draw 6000 individuals from the MEPS dataset and divide them into three folds. We fit two random forests  $\hat{e}$  and  $\hat{\mu}$  using the first fold. The female proportion  $\theta$  in (22) is approximately 0.5 in the MEPS dataset. We further divide the female group ( $A_{n+1} = 1$ ) in the test set into two subgroups based on whether the estimator  $\tilde{e}(X_{n+1})$  defined below is larger than 0.5 or not. Figure 9a shows that SCP+Partition achieves a lower coverage rate than SCP in the first subgroup, where  $A_{n+1} = 1$  and  $\tilde{e}(X_{n+1}) < 0.5$ , aligning with our discussion above.<sup>7</sup>

Next, we apply PCP to remedy the coverage loss of SCP+Partition. We exclude gender from  $\hat{\mu}$  and modify the SCP+Partition interval using weights generated by  $\hat{e}$  :

$$\hat{C}_n^{\text{PCP}}(X_{n+1}, A_{n+1}) = \left[ \hat{\mu}(X_{n+1}) \pm Q_{1-\alpha} \left( \sum_{i \in \mathcal{I}_n} \tilde{w}_i \delta_{R_i} + \tilde{w}_{n+1} \delta_{+\infty} \right) \right], \quad (23)$$

where we sample  $\tilde{A}_1, \dots, \tilde{A}_m \stackrel{\text{i.i.d.}}{\sim} \text{Ber}(\hat{e}(X_{n+1}))$ , compute their sum as  $\tilde{L}$ , and then let

$$\tilde{w}_i \propto \prod_{t=1}^m [\hat{e}(X_i)]^{\tilde{L}} [1 - \hat{e}(X_i)]^{m - \tilde{L}} \quad \text{and} \quad \tilde{e}(X_{n+1}) = \tilde{L}/m.$$

The PCP interval in (23) satisfies an augmented group-conditional guarantee:

---

<sup>7</sup>In Appendix E.2, we repeat the same experiment, with  $A_{n+1}$  indicating whether a person is white or non-white. The results there are consistent with the ones here.

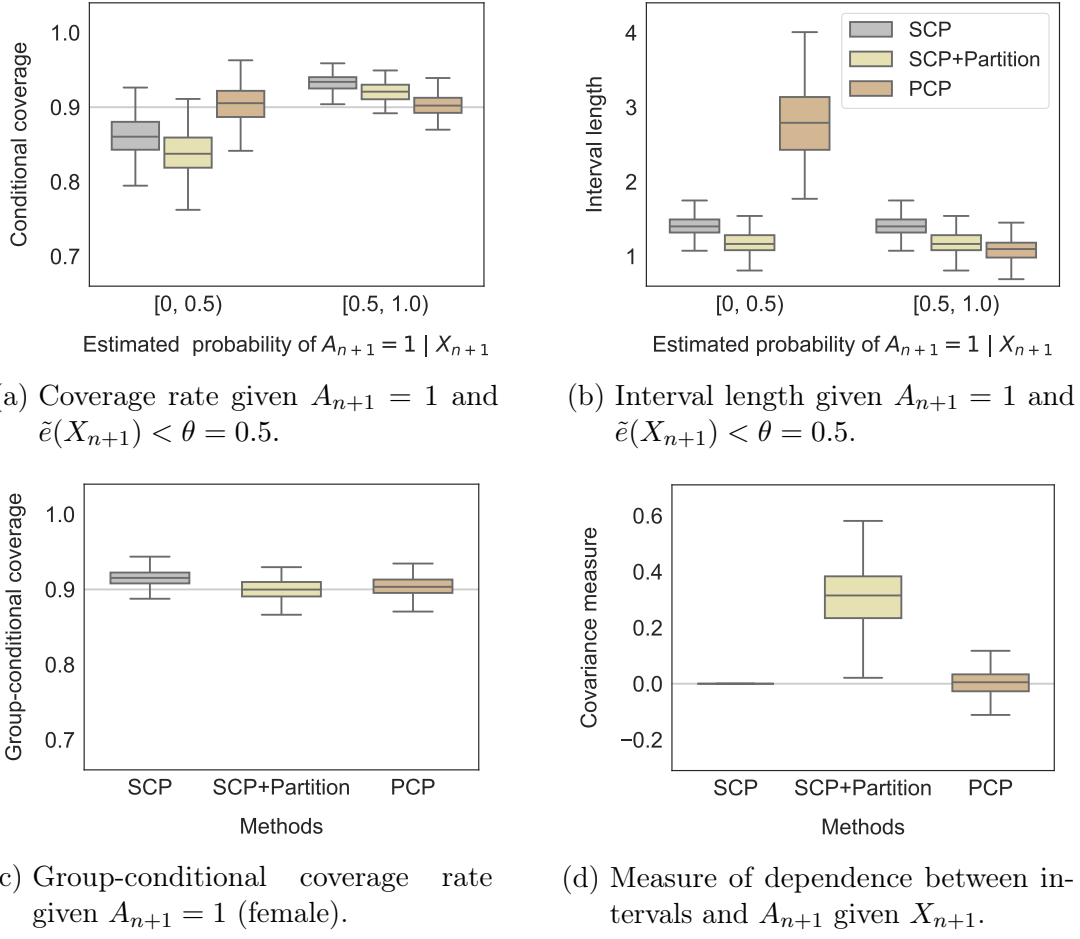


Figure 9: Comparison of conformal prediction methods on the Medical Expenditure Panel Survey (MEPS) 19. The results are from 200 runs of the experiments.

**Proposition 3.** *Suppose that the data points  $(X_i, A_i, Y_i), i \in [n + 1]$ , are i.i.d.. Then the prediction interval in (23) satisfies*

$$\mathbb{P}\{Y_{n+1} \notin \hat{C}_n^{\text{PCP}}(X_{n+1}, A_{n+1}) \mid A_{n+1}, \tilde{e}(X_{n+1})\} \leq \alpha. \quad (24)$$

*Assume that with probability 1,  $e \in (0, 1)$  and  $\sup_{x \in \mathcal{X}} |\hat{e}(x) - e(x)| \rightarrow 0$  as  $n \rightarrow \infty$ . Then, as  $n \rightarrow \infty$  and  $m(n) \rightarrow \infty$ , we have*

$$\hat{C}_n^{\text{PCP}}(X_{n+1}, A_{n+1}) \perp\!\!\!\perp A_{n+1} \mid X_{n+1}. \quad (25)$$

The guarantee in (24) follows from Theorem 1. Imagine that a female group primarily consists of individuals with large values of  $\tilde{e}(X) \approx e(X) = \mathbb{P}\{A = 1 \mid X\}$ , while minorities in the group, such as tall females in the example above, have smaller values of  $\tilde{e}(X)$ . The smaller  $\tilde{e}(X_{n+1})$  is, the less represented an individual is within the female

group. In this sense, the guarantee in (24) means that PCP has valid coverage across individuals regardless of *how represented they are in their gender group*.

This guarantee is demonstrated through the results in Figure 9a, where PCP has coverage of approximately 0.9 for both subgroups. We also see from Figure 9b that the interval length of PCP is highly adaptive: it increases significantly to close the coverage gap of SCP+Partition for the underrepresented individuals with  $\tilde{e}(X_{n+1}) < 0.5$ , while decreasing for the well-presented individuals with  $\tilde{e}(X_{n+1}) \geq 0.5$ , where  $\hat{\mu}$  is relatively accurate due to sufficient training data. Finally, we note that, by (24), PCP also has the group-conditional guarantee of SCP+Partition, as shown in Figure 9c.

Asymptotically, the guarantee in (24) leads to the conditional independence in (25), by the consistency assumption of  $\hat{e}$  and  $A_{n+1} \perp\!\!\!\perp X_{n+1} \mid e(X_{n+1})$ . The independence means PCP will generate the same interval for two individuals who differ only in gender but share all other features, thereby eliminating the effect of partition on any individual’s interval. Furthermore, if  $Y_{n+1} \perp\!\!\!\perp A_{n+1} \mid X_{n+1}$ , the independence in (25) implies that the coverage rate of our interval is also independent of  $A_{n+1}$  given  $X_{n+1}$ .

To empirically verify the independence in (25), we measure the generalized covariance [Shah and Peters, 2020, Section 3]<sup>8</sup> between the upper bounds of the prediction intervals and the gender feature. As shown in Figure 9d, the covariance for PCP is approximately 0, which is significantly smaller than the covariance for SCP+Partition. The covariance for SCP is 0 because its interval does not depend on gender. This result confirms that the dependence of our interval on gender can vanish asymptotically.

Finally, we note that the equalized coverage problem studied in this section is related to the covariate shifts problem in Tibshirani et al. [2019]. However, the difference of PCP is that it maintains the group-conditional guarantee of SCP+Partition and provides the new guarantees in Proposition 3.

## 4 Level-adaptive conditional coverage

Next, we consider classification problems and apply PCP to create level-adaptive prediction sets. The adaptivity ensures that the top-class coverage rate of our prediction set aligns with the classifier’s top-class predictive probability. This new feature is useful in applications that require small and well-calibrated prediction sets. For example, PCP can recommend a more focused set of products to users when the classifier is uncertain about their preferences. Similarly, PCP can aid clinicians by narrowing down potential diagnoses, expediting decisions and improving patient care.

---

<sup>8</sup>We additionally sample 2000 data points to estimate the conditional expectations in the covariance. The estimators are two random forest models applied to compute the empirical covariance.

Suppose that a pre-fitted classifier predicts  $Y_{n+1} \in \mathcal{Y} = \{1, 2, \dots, K\}$  based on a probability vector  $\hat{\eta}(X_{n+1})$ , where  $\hat{\eta}_k(X_{n+1})$  is the predictive probability of  $Y_{n+1} = k$ . We define the top-class prediction and the top-class predictive probability as

$$\hat{\mu}(X_{n+1}) = \arg \max_{k \in [K]} \hat{\eta}_k(X_{n+1}) \quad \text{and} \quad \hat{p}(X_{n+1}) = \max_{k \in [K]} \hat{\eta}_k(X_{n+1}).$$

We call the classifier top-class calibrated if it obeys

$$\mathbb{P}\{Y_{n+1} = \hat{\mu}(X_{n+1}) \mid \hat{p}(X_{n+1}), \hat{\mu}(X_{n+1})\} = \hat{p}(X_{n+1}), \quad (26)$$

i.e., the true probability of  $Y_{n+1} = \hat{\mu}(X_{n+1})$  is exactly  $\hat{p}(X_{n+1})$  when the classifier predicts  $Y_{n+1} = \hat{\mu}(X_{n+1})$  holds with probability  $\hat{p}(X_{n+1})$ . In other words, the accuracy of the top-class prediction  $\hat{\mu}(X_{n+1})$  stays consistent with the top-class probability  $\hat{p}(X_{n+1})$ . Before calibration, the original classifier often overfits the training data and fails to satisfy the guarantee in (26). Calibration methods adjust the predictive probabilities  $\hat{\eta}(X_{n+1})$  using a nonparametric regression model fitted to the validation data, e.g., histogram binning or isotonic regression [Zadrozny and Elkan, 2001]. They enable the top-class prediction  $\hat{\mu}(X_{n+1})$  to satisfy (26) asymptotically. Additional calibration methods and guarantees can be found in Guo et al. [2017]; Kull et al. [2019]; Gupta and Ramdas [2021] and the references therein.

In comparison, existing conformal prediction sets can offer marginal and class-conditional guarantees for covering  $Y_{n+1}$  in finite samples; see examples in Sadinle et al. [2019]; Romano et al. [2020b]; Stutz et al. [2021]; Ding et al. [2023]. However, when the classifier has low predictive probability for the top class, these prediction sets would need to include many classes to achieve the target coverage rate of  $1 - \alpha$ . In medical diagnostics, a large prediction set has limited utility as it offers little information on the true outcome  $Y_{n+1}$  and may take a long time for experts to review. In comparison, a calibrated classifier satisfying (26) can offer more information about  $Y_{n+1}$  through its top-class prediction  $\hat{\mu}(X_{n+1})$  and predictive probability  $\hat{p}(X_{n+1})$ , which are easier for experts to review. Next, we use PCP to generate smaller, often singleton prediction sets, combining the benefits of top-class calibration and conformal prediction.

We define our prediction set using the conformity score proposed by Romano et al. [2020b]. For simplicity, we omit discussing the randomization step involved and note here that it occasionally generates an empty set to keep the coverage close to the target rate. We include the step in both SCP and PCP in our experiments below.

We let  $\hat{\eta}^0(X_i)$  denote the sorted version of  $\hat{\eta}(X_i)$  from the largest to the smallest, and  $K_i$  denote the rank of  $\hat{\eta}_{Y_i}(X_i)$  in  $\hat{\eta}^0(X_i)$ . For example, if  $Y_i = 3$  and  $\hat{\eta}(X_i) = [0.2, 0.5, 0.3]$ ,

$$\hat{\eta}^0(X_i) = [0.5, 0.3, 0.2] \quad \text{and} \quad K_i = 2.$$

Similarly, we let  $K_{n+1}^y$  denote the rank of  $\hat{\eta}_y(X_{n+1})$  in  $\hat{\eta}^0(X_{n+1})$  for any value  $y \in \{1, 2, \dots, K\}$ . Suppose the example above holds with  $X_i$  replaced by  $X_{n+1}$ . We have

$$K_{n+1}^1 = 3, \quad K_{n+1}^2 = 1 \quad \text{and} \quad K_{n+1}^3 = 2.$$



We define the conformity score  $S_i$  as the probability that we need to add on top of the top-class probability  $\hat{p}(X_{n+1})$  such that the top- $K_i$  prediction set can cover  $Y_i$ :

$$S_i = \sum_{k \in [K_i]} \hat{\eta}_k^{(0)}(X_i) - \hat{p}(X_{n+1}) \quad \text{and} \quad S_{n+1}^y = \sum_{k \in [K_{n+1}^y]} \hat{\eta}_k^{(0)}(X_{n+1}) - \hat{p}(X_{n+1}).$$

Our PCP prediction set for  $Y_{n+1}$  is defined as

$$\hat{C}_n^{\text{PCP}}(X_{n+1}) = \left\{ y \in \mathcal{Y} : S_{n+1}^y \leq Q_{1-\tilde{\alpha}(X_{n+1})} \left( \sum_{i=1}^n \tilde{w}_i \delta_{S_i} + \tilde{w}_{n+1} \delta_1 \right) \right\}, \quad (27)$$

where  $\tilde{w}_i \propto \prod_{k=1}^K [\hat{\eta}_k(X_i)]^{\tilde{L}_k}$  and  $\tilde{L} \sim \text{Multi}(m; \hat{\eta}(X_{n+1}))$ . If  $\hat{\eta}(X_i)$  and  $\hat{\eta}(X_{n+1})$  are similar, the score  $S_i$  receives a larger weight in the interval (27). In other words, PCP adjusts its interval according to the classifier's performance on the validation examples with similar predictive probabilities as  $\hat{\eta}(X_{n+1})$ . The proposition below follows directly from Theorem 1. The key observation here is that we can use an adaptive level  $\tilde{\alpha}(X_{n+1})$  after conditioning on  $\tilde{\eta}(X_{n+1}) = \tilde{L}/m$ .

**Proposition 4.** *Suppose that  $Z_i = (X_i, Y_i), i \in [n+1]$ , are exchangeable. The posterior conformal prediction (PCP) interval in (27) satisfies*

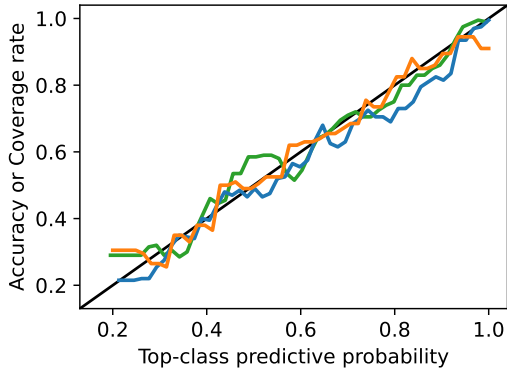
$$\mathbb{P}\{Y_{n+1} \notin \hat{C}_n^{\text{PCP}}(X_{n+1}) \mid \tilde{\eta}(X_{n+1})\} \leq \tilde{\alpha}(X_{n+1}), \quad (28)$$

where  $\tilde{\alpha}(X_{n+1}) = 1 - \tilde{p}(X_{n+1})$  and  $\tilde{p}(X_{n+1}) = \max_{k \in [K]} \tilde{\eta}_k(X_{n+1})$ .

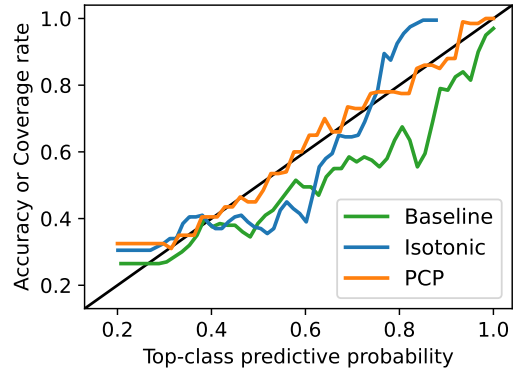
With the knowledge of  $\tilde{\eta}(X_{n+1})$ , the top class prediction and its probability  $\tilde{p}(X_{n+1})$  are known. The guarantee above means the coverage rate of our prediction set is at least  $\tilde{p}(X_{n+1})$ . Our prediction set tends to be small if  $\tilde{p}(X_{n+1})$  is low. If the classifier's accuracy can consistently match its predictive probability  $\tilde{p}(X_{n+1})$ , our prediction set is often a singleton predicting  $Y_{n+1}$  with accuracy at least  $\tilde{p}(X_{n+1})$ , which approximately satisfies the top-class calibration guarantee in (26).

In the following experiment, we compare PCP against the isotonic regression-based calibration method [Zadrozny and Elkan, 2001] and the SCP method for classification [Romano et al., 2020b]. Our evaluation is based on the HAM10000 dataset [Tschandl et al., 2018], which consists of 10,015 dermatoscopic images with seven classes of pigmented skin lesions. We consider two baseline classifiers: a convolutional neural network (CNN) and logistic regression. We split the dataset into three folds: one for training the classifier, another for validation, and the last for testing the methods.

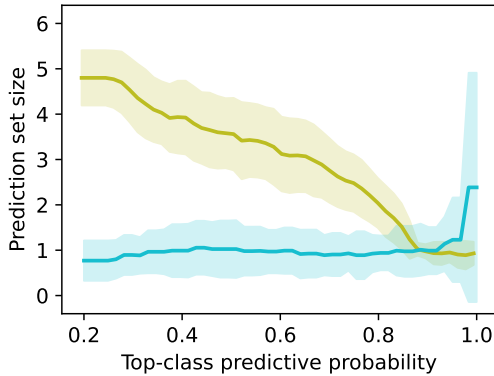
First, we compare calibration curves of PCP and isotonic regression. To construct each curve, we evenly place 50 points within the support of the top-class predictive probability and then calculate the local average accuracy or coverage rate at each



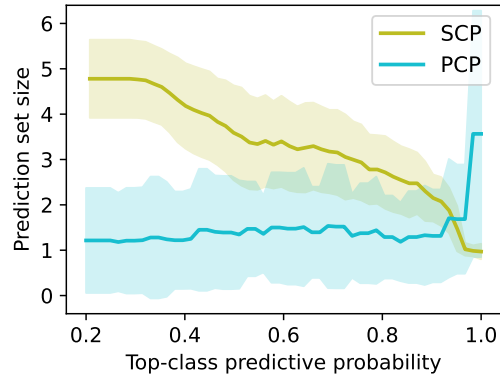
(a) Calibration curves (CNN).



(b) Calibration curves (logistic regression).



(c) Prediction set size (CNN).



(d) Prediction set size (logistic regression).

Figure 10: Comparison of calibration and conformal prediction methods for CNN and logistic regression models on the HAM10000 image dataset.

point, using the 200 nearest test points. The original CNN model is relatively well-calibrated, since the green curve approximately follows the diagonal line in Figure 10a. The logistic regression model is poorly calibrated, as shown by the green curve in Figure 10b. We can see from the same figure that our prediction sets always keep the local coverage rate close to the top-class predictive probability  $\tilde{p}(X_{n+1})$ . In contrast, the isotonic regression method fails to calibrate the logistic regression model.

By definition, our guarantee in (28) is a good approximation of the calibration guarantee in (26), if our prediction set stays close to a singleton. This is the case for the CNN model when its top-class predictive probability  $\tilde{p}(X_{n+1}) \leq 0.9$  in Figure 10c. When  $\tilde{p}(X_{n+1}) > 0.9$ , our method enlarges the prediction set to meet the target coverage rate of  $\tilde{p}(X_{n+1})$ . Figure 10d shows that our prediction set is wider for the less-calibrated logistic regression model. Nevertheless, it is smaller than the prediction set of SCP when the top-class predictive probability  $\tilde{p}(X_{n+1}) \leq 0.9$ .

## 5 Discussion

This paper introduced posterior conformal prediction (PCP), a distribution-free method to construct prediction intervals with conditional coverage guarantees. We showed that PCP can improve conditional coverage by modelling the conditional residual distributions, equalize coverage across subgroups by classifying sensitivity attributes, and adapt the level of prediction sets by calibrating the predictive probabilities. In the following, we discuss a few limitations and extensions of PCP.

**PAC guarantee.** For large  $n$ , we may also want a marginal guarantee such as (2) and (18) to hold conditional on  $Z_{[n]}$  with high probability such that

$$\mathbb{P} \left\{ \alpha(Z_{[n]}) := \mathbb{P}\{Y_{n+1} \notin \hat{C}_n(X_{n+1}) \mid Z_{[n]}\} \leq \alpha + o(1) \right\} \geq 1 - o(1). \quad (29)$$

A prediction set  $\hat{C}_n$  satisfying (29) is called ‘‘Probably Approximately Correct’’ (PAC) [Wilks, 1941; Vovk, 2012]. When marginal validity fails to hold, i.e.,  $\mathbb{E}[\alpha(Z_{[n]})] > \alpha$ , it is less likely that  $\alpha(Z_{[n]}) \leq \alpha$  can hold with high probability as in (29). On the contrary, when marginal validity holds, it is relatively straightforward to prove the PAC guarantee in (29). For PCP intervals with data-dependent weights, the proof requires a mild stability assumption on our mixture learning algorithm. We refer to Appendix D for more details on our PAC guarantee.

**Distributional shifts.** Recently, there has been growing interest in extending conformal prediction to applications with distributional shifts, such as election forecasting [Cherian and Bronner, 2020; Barber et al., 2023] and time series modelling [Xu and Xie, 2021; Gibbs and Candès, 2022; Zaffran et al., 2022]. PCP can be extended to these applications, by fitting a mixture model to residuals, or fitting a classifier to predict the variable that causes the distributional shift. The advantage of PCP is that it guarantees marginal validity when there is no distributional shift. When using our method in online or dynamic settings, we can let the number of cluster distributions grow as more data distributions emerge over time or space.

**Utility maximization.** In Section 4, we applied our method to generate level-adaptive prediction sets. This adaptivity is useful when increasing uncertainty is costly. For example, suppose  $h(X)$  is a decision rule that determines whether recommending the movies in our prediction set  $\hat{C}_n^{\text{PCP}}(X)$  to a user with features  $X$ . If the user randomly selects one movie to watch, the expected benefit of our recommendation is

$$\mathbb{E} \left\{ h(X) \times \left[ r_1(X) \frac{\mathbb{1}\{Y \in \hat{C}_n^{\text{PCP}}(X)\}}{|\hat{C}_n^{\text{PCP}}(X)|} - r_2(X) \left( 1 - \frac{\mathbb{1}\{Y \in \hat{C}_n^{\text{PCP}}(X)\}}{|\hat{C}_n^{\text{PCP}}(X)|} \right) \right] \right\},$$

where  $r_1(X)$  is the reward function for watching the favourite movie and  $r_2(X)$  is the risk function for watching the others. Recommending a large prediction set may result

in more risk than reward. Maximizing the expected benefits by choosing the decision rule  $h$  is an interesting problem for future research.

## 6 Acknowledgements

Y.Z thanks John Cherian, Ying Jin, Daniel LeJeune, Jinzhou Li, and Tijana Zrnic for their valuable feedback on this article. Y.Z and E.J.C. were supported by the Office of Naval Research under Grant No. N00014-24-1-2305 and the National Science Foundation under Grant No. DMS2032014. Additionally, E.J.C. acknowledges support from the Office of Naval Research under Grant No. N00014-20-1-2157, the Simons Foundation under Award 814641, and the Army Research Office under Grant No. 2003514594.

## References

- David Arthur and Sergei Vassilvitskii. K-means++ the advantages of careful seeding. In *Proceedings of the eighteenth annual ACM-SIAM symposium on Discrete algorithms*, pages 1027–1035, 2007.
- Rina Foygel Barber, Emmanuel J Candes, Aaditya Ramdas, and Ryan J Tibshirani. The limits of distribution-free conditional predictive inference. *Information and Inference: A Journal of the IMA*, 10(2):455–482, 2021.
- Rina Foygel Barber, Emmanuel J Candes, Aaditya Ramdas, and Ryan J Tibshirani. Conformal prediction beyond exchangeability. *The Annals of Statistics*, 51(2): 816–845, 2023.
- Michael Bian and Rina Foygel Barber. Training-conditional coverage for distribution-free predictive inference. *Electronic Journal of Statistics*, 17(2):2044–2066, 2023.
- Evgeny Burnaev and Vladimir Vovk. Efficiency of conformalized ridge regression. In *Conference on Learning Theory*, pages 605–622. PMLR, 2014.
- Maxime Cauchois, Suyash Gupta, and John C Duchi. Knowing what you know: valid confidence sets in multiclass and multilabel prediction. *stat*, 1050:24, 2020.
- John Cherian and Lenny Bronner. How the washington post estimates outstanding votes for the 2020 presidential election, 2020.
- Victor Chernozhukov, Kaspar Wüthrich, and Yinchu Zhu. Distributional conformal prediction. *Proceedings of the National Academy of Sciences*, 118(48):e2107794118, 2021.

- Isidro Cortés-Ciriano and Andreas Bender. Concepts and Applications of Conformal Prediction in Computational Drug Discovery. In *Artificial Intelligence in Drug Discovery*. The Royal Society of Chemistry, 11 2020. ISBN 978-1-78801-547-9.
- Tiffany Ding, Anastasios N Angelopoulos, Stephen Bates, Michael I Jordan, and Ryan J Tibshirani. Class-conditional conformal prediction with many classes. *arXiv preprint arXiv:2306.09335*, 2023.
- Kelwin Fernandes, Pedro Vinagre, Paulo Cortez, and Pedro Sernadela. Online News Popularity. UCI Machine Learning Repository, 2015.
- Isaac Gibbs and Emmanuel Candès. Conformal inference for online prediction with arbitrary distribution shifts. *arXiv preprint arXiv:2208.08401*, 2022.
- Isaac Gibbs, John J Cherian, and Emmanuel J Candès. Conformal prediction with conditional guarantees. *arXiv preprint arXiv:2305.12616*, 2023.
- Arthur Gretton, Alex Smola, Jiayuan Huang, Marcel Schmittfull, Karsten Borgwardt, Bernhard Schölkopf, et al. Covariate shift by kernel mean matching. *Dataset shift in machine learning*, 3(4):5, 2009.
- Leying Guan. Localized conformal prediction: A generalized inference framework for conformal prediction. *Biometrika*, 110(1):33–50, 2023.
- Chuan Guo, Geoff Pleiss, Yu Sun, and Kilian Q Weinberger. On calibration of modern neural networks. In *International conference on machine learning*, pages 1321–1330. PMLR, 2017.
- Chirag Gupta and Aaditya Ramdas. Top-label calibration and multiclass-to-binary reductions. *arXiv preprint arXiv:2107.08353*, 2021.
- Kam Hamidieh. Superconductivity Data. UCI Machine Learning Repository, 2018.
- Matthew T Harrison. Conservative hypothesis tests and confidence intervals using importance sampling. *Biometrika*, 99(1):57–69, 2012.
- Rohan Hore and Rina Foygel Barber. Conformal prediction with local weights: randomization enables local guarantees. *arXiv preprint arXiv:2310.07850*, 2023.
- Christopher Jung, Georgy Noarov, Ramya Ramalingam, and Aaron Roth. Batch multivald conformal prediction. *arXiv preprint arXiv:2209.15145*, 2022.
- Takafumi Kanamori, Shohei Hido, and Masashi Sugiyama. A least-squares approach to direct importance estimation. *The Journal of Machine Learning Research*, 10: 1391–1445, 2009.

- Meelis Kull, Miquel Perello Nieto, Markus Kängsepp, Telmo Silva Filho, Hao Song, and Peter Flach. Beyond temperature scaling: Obtaining well-calibrated multi-class probabilities with dirichlet calibration. *Advances in neural information processing systems*, 32, 2019.
- Jing Lei. Fast exact conformalization of the lasso using piecewise linear homotopy. *Biometrika*, 106(4):749–764, 2019.
- Jing Lei and Larry Wasserman. Distribution-free prediction bands for non-parametric regression. *Journal of the Royal Statistical Society Series B: Statistical Methodology*, 76(1):71–96, 2014.
- Jing Lei, Max G’Sell, Alessandro Rinaldo, Ryan J Tibshirani, and Larry Wasserman. Distribution-free predictive inference for regression. *Journal of the American Statistical Association*, 113(523):1094–1111, 2018.
- Ruiting Liang and Rina Foygel Barber. Algorithmic stability implies training-conditional coverage for distribution-free prediction methods. *arXiv preprint arXiv:2311.04295*, 2023.
- Pascal Massart. The tight constant in the dvoretzky-kiefer-wolfowitz inequality. *The annals of Probability*, pages 1269–1283, 1990.
- Harris Papadopoulos, Kostas Proedrou, Volodya Vovk, and Alex Gammerman. Inductive confidence machines for regression. In *Machine learning: ECML 2002: 13th European conference on machine learning Helsinki, Finland, August 19–23, 2002 proceedings 13*, pages 345–356. Springer, 2002.
- Aaditya K. Ramdas, Rina F. Barber, Martin J. Wainwright, and Michael I. Jordan. A unified treatment of multiple testing with prior knowledge using the p-filter. *The Annals of Statistics*, 47(5):2790 – 2821, 2019.
- Sashank Reddi, Barnabas Poczos, and Alex Smola. Doubly robust covariate shift correction. In *Proceedings of the AAAI Conference on Artificial Intelligence*, 2015.
- Michael Redmond. Communities and Crime. UCI Machine Learning Repository, 2009.
- Yaniv Romano, Evan Patterson, and Emmanuel Candes. Conformalized quantile regression. *Advances in neural information processing systems*, 32, 2019.
- Yaniv Romano, Rina Foygel Barber, Chiara Sabatti, and Emmanuel Candès. With malice toward none: Assessing uncertainty via equalized coverage. *Harvard Data Science Review*, 2(2):4, 2020a.
- Yaniv Romano, Matteo Sesia, and Emmanuel Candes. Classification with valid and adaptive coverage. *Advances in Neural Information Processing Systems*, 33: 3581–3591, 2020b.

- Mauricio Sadinle, Jing Lei, and Larry Wasserman. Least ambiguous set-valued classifiers with bounded error levels. *Journal of the American Statistical Association*, 114(525):223–234, 2019.
- Rajen D. Shah and Jonas Peters. The hardness of conditional independence testing and the generalised covariance measure. *The Annals of Statistics*, 48(3):1514 – 1538, 2020.
- David Stutz, Ali Taylan Cemgil, Arnaud Doucet, et al. Learning optimal conformal classifiers. *arXiv preprint arXiv:2110.09192*, 2021.
- Masashi Sugiyama, Taiji Suzuki, and Takafumi Kanamori. Density-ratio matching under the bregman divergence: a unified framework of density-ratio estimation. *Annals of the Institute of Statistical Mathematics*, 64:1009–1044, 2012.
- Michel Talagrand. Concentration of measure and isoperimetric inequalities in product spaces. *Publications Mathématiques de l’Institut des Hautes Etudes Scientifiques*, 81:73–205, 1995.
- Ryan J Tibshirani, Rina Foygel Barber, Emmanuel Candes, and Aaditya Ramdas. Conformal prediction under covariate shift. *Advances in neural information processing systems*, 32, 2019.
- Philipp Tschandl, Cliff Rosendahl, and Harald Kittler. The ham10000 dataset, a large collection of multi-source dermatoscopic images of common pigmented skin lesions. *Scientific data*, 5(1):1–9, 2018.
- Vladimir Vovk. Conditional validity of inductive conformal predictors. In *Asian conference on machine learning*, pages 475–490. PMLR, 2012.
- Vladimir Vovk, David Lindsay, Ilija Nourtdinov, and Alex Gammerman. Mondrian confidence machine. *Technical Report*, 2003.
- Vladimir Vovk, Alexander Gammerman, and Glenn Shafer. *Algorithmic learning in a random world*. Springer Science & Business Media, 2005.
- S. S. Wilks. Determination of Sample Sizes for Setting Tolerance Limits. *The Annals of Mathematical Statistics*, 12(1):91 – 96, 1941.
- Chen Xu and Yao Xie. Conformal prediction interval for dynamic time-series. In *International Conference on Machine Learning*, pages 11559–11569. PMLR, 2021.
- Bianca Zadrozny and Charles Elkan. Obtaining calibrated probability estimates from decision trees and naive bayesian classifiers. In *Icml*, volume 1, pages 609–616, 2001.
- Margaux Zaffran, Olivier Féron, Yannig Goude, Julie Josse, and Aymeric Dieuleveut. Adaptive conformal predictions for time series. In *International Conference on Machine Learning*, pages 25834–25866. PMLR, 2022.



# Appendices

## A Randomized versus non-randomized intervals

This section first presents a counterexample to prove that non-randomized intervals may lose marginal validity. Following this, we discuss the difference between the randomized and non-randomized PCP interval as the precision parameter  $m$  increases.

Previously, Proposition 2 in Guan [2023] demonstrated the loss of marginal validity in localized conformal prediction intervals. In the example there, every feature  $X_{ij} \in \{-1, 0, 1\}$  for  $j \in [d]$ . The residuals at the origin ( $X_i = 0$ ) are 0. When  $X_i = 0$  holds with high probability, the interval mainly uses zero residuals and achieves a poor coverage rate. The loss of coverage in this example is primarily due to the choice of weight function  $w_i \propto \exp(-d(X_i, X_{n+1}))$  in the interval, where

$$d(X_i, X_{n+1}) = \begin{cases} 0, & \text{if } X_i \in \{0, X_{n+1}\}, \\ +\infty, & \text{otherwise.} \end{cases}$$

Equality in the distance metric  $d(\cdot, \cdot)$  is non-transitive, i.e.,

$$d(0, X_{n+1}) = 0 \text{ and } d(0, X_{n+2}) = 0 \not\Rightarrow d(X_{n+1}, X_{n+2}) = 0,$$

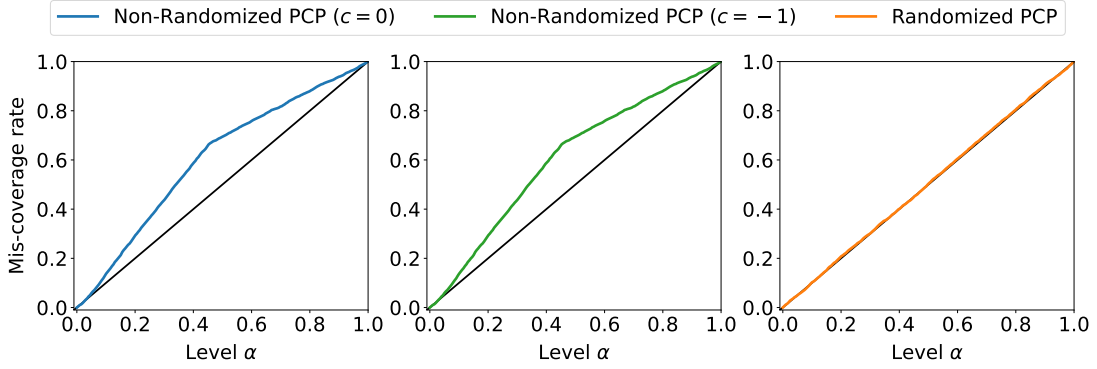
whereas most distance metrics are transitive in measuring similarity between data points. Transitivity is also essential for other metric properties, such as the triangle inequality. In the following, we provide a new example to illustrate that non-randomized intervals using standard distance metrics may still fail to achieve marginal validity. In distribution-free settings, we assume that the feature space can be divided into two disjoint subsets with significantly different residuals.

**Example 1.** Without loss of generality, we assume that the residuals for  $X_i > 0$  are larger than those for  $X_i \leq 0$  with probability 1. We also assume that  $(X_1, R_1), \dots, (X_{n+1}, R_{n+1})$  are distinct with probability 1. We define a prediction interval with weights only depending on whether  $X_i, X_{n+1} > 0$  as follows:

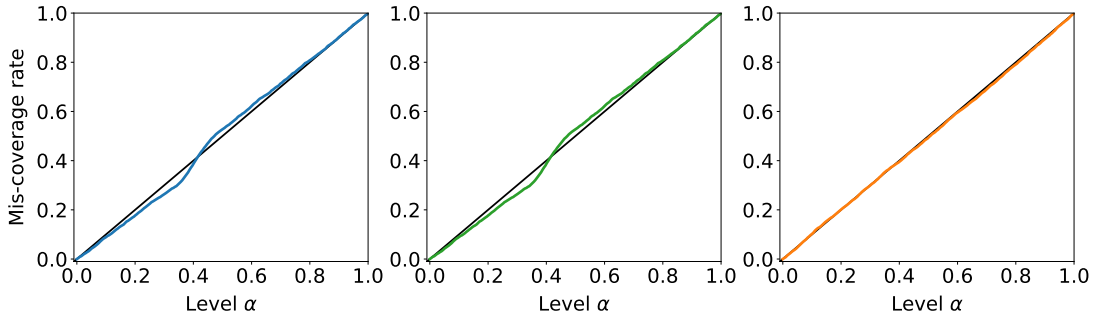
$$\hat{C}_n(X_{n+1}) = \left[ \hat{\mu}(X_{n+1}) \pm Q_{1-\alpha} \left( \sum_{i=1}^n w_i \delta_{R_i} + w_{n+1} \delta_{+\infty} \right) \right], \quad (30)$$

where  $w_i = \phi(X_i, X_{n+1}) / \sum_{j=1}^{n+1} \phi(X_j, X_{n+1})$  for  $\phi(X_{n+1}, X_{n+1}) = 1 + c$  and

$$\phi(X_i, X_{n+1}) = \begin{cases} a, & \text{if } X_i \leq 0, X_{n+1} > 0, \\ b, & \text{if } X_i > 0, X_{n+1} \leq 0, \\ 1, & \text{otherwise.} \end{cases} \quad (31)$$



(a) Asymmetric similarity measure  $\phi$ .



(b) Symmetric similarity measure  $\phi$ .

Figure 11: Comparison of the randomized and non-randomized PCP intervals in Simulation 1.

where  $a, b \in [0, 1]$ . Choosing different values for  $a$  and  $b$  can make the distance metric in  $\phi$  asymmetric, e.g., the KL divergence in our PCP interval. In (31), the  $X_i$ 's with the same sign as  $X_{n+1}$  receive greater weight than those with a different sign. If  $c$  is positive,  $X_{n+1}$  itself receives a larger weight than others. If  $c = -1$ , we remove the point mass  $\delta_{+\infty}$  in (30), which defines the interval  $\hat{C}_n(X_{n+1})$  solely using the residuals  $R_{[n]}$ . In the proposition below,  $\rho = \mathbb{P}\{X_i > 0\}$  and we omit terms that vanish exponentially as the sample size  $n$  increases.

**Proposition 5.** *Suppose that  $Z_i = (X_i, Y_i), i \in [n + 1]$ , are exchangeable. In the setup of Example 1, the interval  $\hat{C}_n(X_{n+1})$  in (30) using the weights in (31) satisfies*

$$\mathbb{P}\{Y_{n+1} \notin \hat{C}_n(X_{n+1})\} \geq \alpha + \alpha a(1 - \rho) - (1 - \alpha)b\rho - \frac{2(1 - \alpha)c + 2}{n + 1}. \quad (32)$$

The proof of the proposition can be found in Appendix C.1. In the lower bound, the term  $\alpha a(1 - \rho)$  is the coverage loss for  $X_{n+1} > 0$  where the test residual  $R_{n+1}$  is

large, while  $(1 - \alpha)b\rho$  is the coverage gain for  $X_{n+1} \leq 0$  where  $R_{n+1}$  is small. The mis-coverage rate in (32) is above  $\alpha$  if

$$\frac{\alpha}{1 - \alpha}a - \frac{\rho}{1 - \rho}b \geq \frac{2(1 - \alpha)c + 2}{(n + 1)(1 - \alpha)(1 - \rho)}. \quad (33)$$

This condition holds if the interval uses an asymmetric distance metric with  $a > b$  in (31). It becomes more difficult to satisfy if  $\alpha$  is small and the distance metric is symmetric with  $a = b$ , for example, with Gaussian or uniform kernels.

**Simulation 1.** We next verify Proposition 5 by comparing the mis-coverage rates of the randomized and non-randomized PCP intervals on a synthetic dataset. We generate  $X_i \sim \text{Bern}(\rho = 0.4)$  and the residual  $R_i | X_i = 0 \sim \mathcal{N}(5, 1)$  and  $R_i | X_i = 1 \sim \mathcal{N}(10, 1)$ . Suppose that  $\pi(0) = [0.8, 0.2]$  and  $\pi(1) = [1, 0]$ . In (31), we let

$$a = \exp\{-D_{\text{KL}}(\pi(1) \parallel \pi(0))\} \approx 0.8 \quad \text{and} \quad b = \exp\{-D_{\text{KL}}(\pi(0) \parallel \pi(1))\} \approx 0.$$

We generate 10000 data points  $(X_i, R_i)$  to construct the interval  $\hat{C}_n(X_{n+1})$  in (30) and the randomized PCP intervals described in (12) and (13), using  $\pi$  and  $m = 1$ . Another 10000 data points are generated to evaluate the coverage rates of these intervals. As shown in Figure 11a, the non-randomized intervals exhibit coverage gaps across all values of  $\alpha$ , while the randomized interval maintains a miscoverage rate consistent with  $\alpha$ . In Figure 11b, we let  $\pi(0) = [0.5, 0.5]$  to make both  $a$  and  $b$  close to 0.8. Using this nearly symmetric distance metric, the non-randomized PCP intervals have significantly smaller coverage gaps. The gap is approximately 0 when  $\alpha \approx 0.4 = \rho$ . This result aligns with our lower bound in (32) when  $\alpha = \rho$  and  $a = b$ .

**PCP intervals.** Thus far, we have demonstrated that non-randomized weighted intervals lack distribution-free marginal validity. Next, we bound the difference between randomized and non-randomized PCP intervals as the precision parameter  $m$  increases. For any fixed  $\pi$ , the weights in the non-randomized interval are defined as

$$w_i \propto \phi_i := \prod_{k=1}^K [\pi_k(X_i)]^{m\pi_k(X_{n+1})} \propto \exp\{-mD_{\text{KL}}(\pi(X_{n+1}) \parallel \pi(X_i))\},$$

while in the randomized interval, the weights  $\tilde{w}_i \propto \tilde{\phi}_i := \prod_{k=1}^K [\pi_k(X_i)]^{\tilde{L}_k}$  are computed using a sample  $\tilde{L}$  from the multinomial distribution based on  $\pi(X_{n+1})$ . We know that

$$Y_{n+1} \notin \hat{C}_n(X_{n+1}) \Leftrightarrow \sum_{i=1}^{n+1} w_i \mathbb{1}\{R_i \geq R_{n+1}\} \leq \alpha.$$

Let  $\psi = \sum_{i=1}^{n+1} \phi_i$  and  $\tilde{\psi} = \sum_{i=1}^{n+1} \tilde{\phi}_i$ . In the decomposition

$$w_i - \tilde{w}_i = \phi_i/\psi - \tilde{\phi}_i/\psi + \tilde{\phi}_i/\psi - \tilde{\phi}_i/\tilde{\psi},$$

we can rewrite the first difference as  $(\phi_i - \tilde{\phi}_i)/\psi = w_i(1 - \tilde{\phi}_i/\phi_i)$ . Using this expression, we can rewrite the second difference as

$$\tilde{\phi}_i/\psi - \tilde{\phi}_i/\tilde{\psi} = \tilde{w}_i(\tilde{\psi} - \psi)/\psi = w_i \sum_{j=1}^{n+1} (\tilde{\phi}_j - \phi_j)/\psi = -w_i \sum_{j=1}^{n+1} w_j (1 - \tilde{\phi}_j/\phi_j).$$

Then, we can upper bound the difference between the empirical distributions as follows:

$$\begin{aligned} \sum_{i=1}^{n+1} (w_i - \tilde{w}_i) \mathbb{1}\{R_i \geq R_{n+1}\} &= \sum_{i=1}^{n+1} w_i \left[ \left(1 - \tilde{\phi}_i/\phi_i\right) - \sum_{j=1}^{n+1} w_j (1 - \tilde{\phi}_j/\phi_j) \right] \mathbb{1}\{R_i \geq R_{n+1}\} \\ &\leq \left( \sum_{i=1}^{n+1} w_i \left[ \tilde{\phi}_i/\phi_i - \sum_{j=1}^{n+1} w_j \tilde{\phi}_j/\phi_j \right]^2 \right)^{1/2}. \end{aligned}$$

The term within the last line is the weighted empirical variance of  $\tilde{\phi}_i/\phi_i$  over  $i \in [n+1]$ . Additional assumptions are required to establish its convergence rate as  $m$  increases and to control the coverage gap between the randomized and non-randomized intervals.

Finally, suppose we exclude the point mass  $\delta_{+\infty}$  from the randomized interval and denote the weights normalized over the first  $n$  data points as  $\tilde{w}_i^{-(n+1)}$ . We have

$$\begin{aligned} &\sum_{i=1}^n \tilde{w}_i^{-(n+1)} \mathbb{1}\{R_i \geq R_{n+1}\} - \sum_{i=1}^{n+1} \tilde{w}_i \mathbb{1}\{R_i \geq R_{n+1}\} \\ &= \frac{\tilde{\phi}_{n+1}}{\tilde{\psi} - \tilde{\phi}_{n+1}} \sum_{i=1}^n \tilde{w}_i \mathbb{1}\{R_i \geq R_{n+1}\} - \tilde{w}_{n+1} \leq \tilde{w}_{n+1} \frac{\tilde{\phi}_{n+1}}{\tilde{\psi} - \tilde{\phi}_{n+1}} = \frac{\tilde{w}_{n+1}^2}{1 - \tilde{w}_{n+1}}, \end{aligned}$$

which indicates that not including  $\delta_{+\infty}$  yields different randomized and non-randomized intervals, even for a large value of the precision parameter  $m$ .

## B Matching algorithm

Estimating mixture models is a nontrivial nonconvex optimization problem. Computing the PCP interval in (16) requires refitting  $\pi^y$  for all  $y \in \mathcal{Y}$ . In this section, we introduce a mixture learning algorithm to address this computational challenge.

Our algorithm is motivated by two observations. First, given a pre-fitted model  $\hat{\mu}$ , it is easy to impute  $R_{n+1}^y = |y - \hat{\mu}(X_{n+1})|$  for all  $y \in \mathcal{Y}$ . Second, to compute the weights in (16), we only need to estimate the membership probabilities, not the entire mixture model. The conditional cumulative distribution functions (CDFs) of the residuals are monotone and right-continuous. We learn the probabilities by matching the CDFs at some fixed points in the support of the marginal residual distribution.

In what follows, we introduce our algorithm  $\mathcal{A}$  in three steps: gridding, fitting, and clustering. After the introduction, we provide a numerical experiment to confirm that our algorithm’s complexity for computing a single PCP interval is linear in  $n$ .

**Gridding.** In the gridding step, we choose a fixed number of points to match the residual CDFs. This process requires re-running the training algorithm  $\mathcal{A}'$  for the predictive model  $\hat{\mu} = \mathcal{A}'(\mathcal{D}'_{[n]})$  on the dataset

$$\mathcal{D}'_{[n]} = \{(X'_1, Y'_1), \dots, (X'_n, Y'_n)\}. \quad (34)$$

We only need to implement the gridding step once. We will use the same grids to compute the intervals for all the test points.

We first generate  $n$  residuals via a 20-fold cross-validation on  $\mathcal{D}'_{[n]}$ . More precisely, we divide  $[n]$  into 20 subsets  $\mathcal{I}^{(1)}, \dots, \mathcal{I}^{(20)}$  and compute 20 models

$$\hat{\mu}_{-\mathcal{I}^{(1)}} = \mathcal{A}'(\mathcal{D}'_{[n] \setminus \mathcal{I}^{(1)}}), \dots, \hat{\mu}_{-\mathcal{I}^{(20)}} = \mathcal{A}'(\mathcal{D}'_{[n] \setminus \mathcal{I}^{(20)}}).$$

For every  $(X'_j, Y'_j)$  in  $\mathcal{D}'_{[n]}$ , we let  $\hat{\mu}_{-j}(X'_j) = \sum_{t=1}^{20} \mathbb{1}\{j \notin \mathcal{I}^{(t)}\} \hat{\mu}_{-\mathcal{I}^{(t)}}(X'_j)$  denote the prediction from the model that is not fitted to  $Y'_j$ . Then we compute the residual

$$R'_j = |Y'_j - \hat{\mu}_{-j}(X'_j)|. \quad (35)$$

Every model  $\mu_{-\mathcal{I}^{(t)}}$  is trained on about 5% less data than  $\hat{\mu}$ . The residuals  $R'_{[n]} = (R'_1, \dots, R'_n)$  have a similar support compared to  $R_{[n]}$ . We choose  $s$  different quantiles  $\xi'_{[s]}$  of the empirical distribution of  $R'_{[n]}$  to represent the support of the distribution of  $R_i$ . For example, we set  $s = 9$  and choose the  $\alpha$ -quantiles for  $\alpha \in \{0.1, \dots, 0.9\}$ .

**Fitting.** For each  $t \in [s]$  and any value  $y \in \mathcal{Y}$ , we want to fit a model  $\tau_t^y(X)$  to estimate the conditional expectation  $\mathbb{P}\{R \leq \xi'_t \mid X\}$  using the imputed data

$$(X_1, \mathbb{1}\{R_1 \leq \xi'_t\}), \dots, (X_n, \mathbb{1}\{R_n \leq \xi'_t\}), (X_{n+1}, \mathbb{1}\{R_{n+1}^y \leq \xi'_t\}). \quad (36)$$

The imputed label can only take two values, 0 or 1, so we only need to compute two estimators,  $\tau_{t,0}(X_i)$  and  $\tau_{t,1}(X_i)$ , for all values  $y$ . Then, we can define

$$\tau_t^y(X_i) = \begin{cases} \tau_{t,0}(X_i), & \text{if } R_{n+1}^y \leq \xi'_t, \\ \tau_{t,1}(X_i), & \text{otherwise.} \end{cases} \quad (37)$$

To prevent  $\tau_t^y(X_{n+1})$  from over-fitting to  $\mathbb{1}\{R_{n+1}^y \leq \xi'_t\}$ , we implement a cross-fitting strategy: divide the imputed data in (36) into 20 folds and compute every estimate  $\tau_t^y(X_i)$  using the model fitted to the folds that do not contain  $(X_i, \mathbb{1}\{R_i \leq \xi'_t\})$ . To ensure our algorithm is efficient, we construct the estimators using linear models and the least-squares method proposed by [Kanamori et al. \[2009\]](#). This method is different

from logistic regression in the Bregman divergences they minimize; see Section 3.1 in [Sugiyama et al. \[2012\]](#) for more details. Here, we briefly describe the idea.

For every  $t \in [s]$ , we follow Bayes' rule to estimate  $\mathbb{P}\{R \leq \xi'_t \mid X = x\}$  as

$$\hat{\tau}_t(x) = [n_t \hat{g}_t(x)] / [n - n_t + n_t \hat{g}_t(x)], \quad (38)$$

where  $n_t = \sum_{i=1}^n \mathbb{1}\{R_n \leq \xi'_t\}$  and  $g_t(x)$  is an estimator of the conditional density ratio  $g_t(x) = f_X(x \mid R \leq \xi'_t) / f_X(x \mid R > \xi'_t)$ . The mean squared loss of  $\hat{g}_t$  can be written as

$$\begin{aligned} & \int [\hat{g}_t(x) - g_t(x)]^2 f_X(x \mid R > \xi'_t) dx \\ = & \int \hat{g}_t^2(x) f_X(x \mid R > \xi'_t) dx - 2 \int \hat{g}_t(x) f_X(x \mid R \leq \xi'_t) dx + \int g_t^2(x) f_X(x \mid R > \xi'_t) dx. \end{aligned}$$

Observe that the third term does not depend on the estimator  $\hat{g}_t$ . In other words, we can construct  $\hat{g}_t$  by minimizing the empirical version of the first two terms. When  $\hat{g}_t$  is linear, the objective function on the first  $n$  data points in (36) is given by

$$\min_{\beta} \frac{1}{n - n_t} \sum_{i=1}^n \mathbb{1}\{R_n > \xi'_t\} (X_i^\top \beta)^2 - \frac{2}{n_t} \sum_{i=1}^n \mathbb{1}\{R_n \leq \xi'_t\} X_i^\top \beta, \quad (39)$$

The solution of (39) can be expressed as

$$\hat{\beta} = \frac{n - n_t}{n_t} \left( \sum_{i=1}^n \mathbb{1}\{R_n > \xi'_t\} X_i^\top X_i \right)^{-1} \sum_{i=1}^n X_i \mathbb{1}\{R_n \leq \xi'_t\}.$$

Finally, we define  $\hat{\tau}_t(x)$  in (38) using  $\hat{g}_t(x) = \max\{\hat{\beta}^\top x, 0\}$ . Given the solution  $\hat{\beta}$ , we can efficiently compute the least-squares solutions for all the test points and  $y \in \mathcal{Y}$  using algorithms developed for full conformal prediction [[Vovk et al., 2005](#)]. The key idea is to update  $\hat{\beta}$  with the last point  $(X_{n+1}, \mathbb{1}\{R_{n+1}^y \leq \xi'_t\})$ , using the Sherman-Morrison-Woodbury (SMW) identity. The complexity of updating all the estimators for one test point is  $O(nd^2 + ndc)$ , where  $d$  is the dimension of  $\mathcal{X}$  and  $c$  is the total number of linear models to update. When we use 20-fold cross-fitting,  $c = 20 \times 2 \times 9 = 380$ . As we will explain later, the constant  $c$  can be reduced by computing our interval as a union when  $\alpha$  is small, e.g., 0.1. Using the identity, we can also efficiently update solutions in kernel regression [[Burnaev and Vovk, 2014](#)] and Lasso [[Lei, 2019](#)], as well as in our method with regularization. We can select the regularization hyperparameter by cross-validating the linear models fitted to the residuals from (35):

$$(X'_1, \mathbb{1}\{R'_1 \leq \xi'_t\}), \dots, (X'_n, \mathbb{1}\{R'_n \leq \xi'_t\}). \quad (40)$$

**Clustering.** Let  $(\xi'_0, \xi'_{s+1}) = (0, \infty)$ . The response space  $\mathcal{Y}$  is covered by

$$\mathcal{Y}^{(j)} = \{y \in \mathcal{Y} : R_{n+1}^y \in [\xi'_{j-1}, \xi'_j]\}, \forall j \in [s+1].$$

By definition,  $\xi'_0 < \xi'_1 < \dots < \xi'_s < \xi'_{s+1}$ . The estimators  $\tau_1^y, \dots, \tau_s^y$  are unchanged across  $y \in \mathcal{Y}^{(j)}$  because the binary responses in (36) remain invariant across all  $y \in \mathcal{Y}^{(j)}$ . Thus, we let  $\tau_{[s]}^{(j)}(x) = [\tau_1^y(x), \dots, \tau_s^y(x)]$  for all  $y \in \mathcal{Y}^{(j)}$  and  $j \in [s+1]$ .

We learn the probabilities  $\pi$  by solving the following reconstruction problem,

$$\pi_{[n+1],[K]}^{(j)}, \gamma_{[K]}^{(j)} = \arg \min_{\pi_{i,[K]} \in \Delta^{K-1}, \gamma_k \in \mathbb{R}^s} \sum_{i=1}^{n+1} \left\| \tau_{[s]}^{(j)}(X_i) - \sum_{k=1}^K \pi_{i,k} \gamma_k \right\|^2, \quad (41)$$

where the choice of  $K$  will be discussed in Appendix B.1. For every  $k \in [K]$ ,  $\gamma_k^{(j)}$  estimates the values of an unconditional residual CDF at the points  $\xi'_1, \dots, \xi'_s$ . Then,  $\pi_{i,[K]}^{(j)} = (\pi_{i,1}^{(j)}, \dots, \pi_{i,K}^{(j)})$  combines  $\gamma_{[K]}^{(j)} = (\gamma_1^{(j)}, \dots, \gamma_K^{(j)})$  to reconstruct the estimators  $\tau_{[s]}^{(j)}(X_i)$ . To warm start, we initialize  $(\gamma_1, \dots, \gamma_K)$  as the  $K$  cluster centers from the  $k$ -means++ algorithm [Arthur and Vassilvitskii, 2007] applied to the estimators  $\tau_{[s]}^{(j)}(X_1), \dots, \tau_{[s]}^{(j)}(X_{n+1})$ . The algorithm has complexity  $O(Knd)$ . Then, we improve the fit by alternating optimization. Fixing  $\gamma$ 's allows us to update each  $\pi_{i,[K]}$  via mirror descent. Fixing  $\pi$ 's enables us to update  $\gamma_{1,j}, \dots, \gamma_{K,j}$  with a least-squares fit, which has complexity  $O(Kns^2 + Ks^3)$ . Alternating between the two convex problems will converge to a local minimum of the problem in (41).

**PCP interval.** Finally, we compute our PCP interval by taking a union:

$$\hat{C}_n^{\text{PCP}}(X_{n+1}) = \bigcup_{j=1}^{s+1} \hat{C}_n^{(j)} \equiv \bigcup_{j=1}^{s+1} \left\{ y \in \mathcal{Y}^{(j)} : P_n^{(j)}(y) = \sum_{i=1}^{n+1} \tilde{w}_i^{(j)} \mathbb{1}\{R_i \geq R_{n+1}^y\} > \alpha \right\}.$$

where the weights  $\tilde{w}_i^{(j)}$  are computed using  $\pi_{[n+1],[K]}^{(j)} = [\pi_{1,[K]}^{(j)}, \dots, \pi_{n+1,[K]}^{(j)}]$  for  $j \in [s+1]$ . In any implementation, we can compute  $\hat{C}_n^{(1)}, \dots, \hat{C}_n^{(s+1)}$  in a backward fashion. Once we reach  $j^*$  satisfying  $\hat{C}_n^{(j^*)} \subset \mathcal{Y}^{(j^*)}$ , we can set the remaining  $\hat{C}_n^{(j)} = \mathcal{Y}^{(j)}$  for all  $j = 1, \dots, j^*$ . This simplification never yields a smaller interval and often returns the same interval that we want to compute. This is because if  $j < j^*$ , it often holds that

$$P_n^{(j)}(y) > P_n^{(j^*)}(y'), \forall y \in \mathcal{Y}^{(j)} \text{ and } y' \in \mathcal{Y}^{(j^*)}.$$

When  $\alpha = 0.1$ ,  $j^* \approx s+1$ . Suppose that  $j^* = s = 9$ . To compute the interval, we only need to compute  $\tau_{t,1}(x)$  for all  $t \in [9]$  and  $\tau_{9,0}(x)$  in (37), i.e., update  $10 \times 20 = 200$  cross-fitted linear models using the solution  $\hat{\beta}$  and the SMW identity.

**Numerical experiment.** We verify the computational complexity of our algorithm  $\mathcal{A}$  using the MEPS 19 and 20 datasets [Romano et al., 2019] with 139 features. We see from Figure 12 that the time required to compute 1000 PCP intervals increases linearly as the size  $n$  of the validation set grows from 2000 to 10000. This verifies our calculation above, which shows that the computational complexity of  $\mathcal{A}$  is linear in  $n$ .



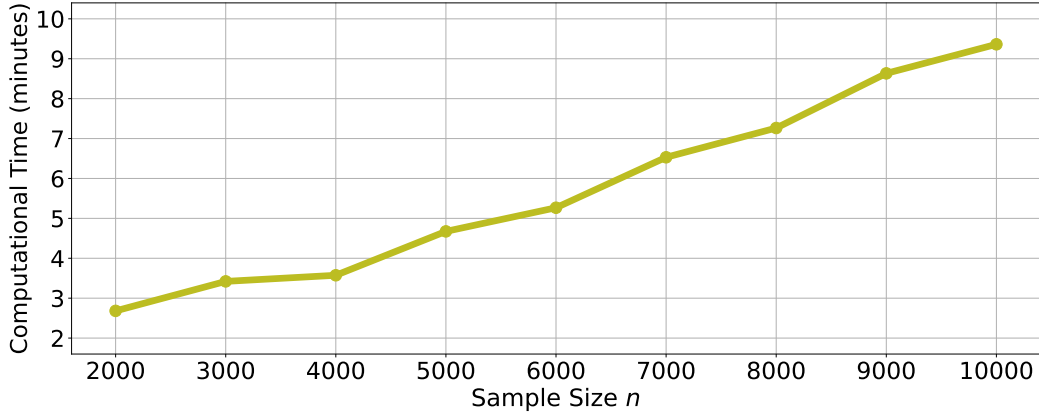


Figure 12: Computational time of generating 1000 PCP intervals.

When the validation set size  $n = 10000$ , our algorithm  $\mathcal{A}$  can generate 1000 intervals in less than 10 minutes on a MacBook Pro laptop with an Intel Core i7 processor. Given this linearly increasing complexity, we can apply PCP to large datasets, and evaluate its coverage rate and interval length through hundreds of repeated experiments.

## B.1 Hyperparameter selection

**Number of cluster distributions  $K$ .** We choose the number of cluster distributions  $K$  using the dataset  $\mathcal{D}'_{[n]}$  in (34) used to pre-fit  $\hat{\mu}$ . As described in (35), we can use  $\mathcal{D}'_{[n]}$  to generate  $n$  extra residuals  $R'_{[n]}$ . We apply the algorithm  $\mathcal{A}$  on  $\mathcal{D}'_{[n]}$  to learn a membership probabilities estimator. More precisely, using the data in (40), we fit the same model  $\tau'_t$  to estimate  $\mathbb{P}\{R \leq \xi'_t \mid X\}$  for all  $t \in [s]$ . Let  $\tau'_{[s]} = (\tau'_1, \dots, \tau'_s)$ . We learn the membership probabilities  $\pi$ 's by solving a reconstruction problem,

$$\min_{\pi_{i,[K]} \in \Delta^{K-1}, \gamma_k \in \mathbb{R}^s} \sum_{i=1}^n \left\| \tau'_{[s]}(X'_i) - \sum_{k=1}^K \pi_{i,k} \gamma_k \right\|^2.$$

The loss is difficult to minimize when  $K$  is too small. We increment  $K = 1, 2, \dots$  until the coefficient of determination improves by less than 0.05 from  $K$  to  $K + 1$ .

**Precision parameter  $m$ .** Let  $\pi'$  denote the membership probabilities estimator using the selected  $K$ . For each point  $(X'_i, Y'_i)$  in  $\mathcal{D}'_{[n]}$ , we compute its PCP interval for  $Y'_i$  using  $\pi'$  and the other points in  $\mathcal{D}'_{[n]}$  as a validation set. More specifically, we let

$$\tilde{L}' \sim \text{Multi}(m, \pi'(X'_i)) \text{ and } \tilde{\pi}'(X'_i) = \tilde{L}'/m.$$

The PCP interval for the response  $Y'_i$  is defined as

$$\hat{C}_n^{\text{PCP}}(X'_i) = \left\{ y \in \mathcal{Y} : \sum_{j=1}^n \tilde{w}_{ij} \mathbb{1}\{R'_j \geq R'_i{}^y\} > \alpha \right\},$$

where  $R_i^y = |y - \hat{\mu}_{-i}(X_i^y)|$  for the model  $\hat{\mu}_{-i}$  described above (35) and  $\tilde{w}_{ij}$  is given by

$$\tilde{w}_{ij} \propto \prod_{k=1}^K [\pi'_k(X_j^y)]^{m\tilde{\pi}'_k(X_j^y)} \propto \exp \left\{ -m \sum_{k=1}^K \tilde{\pi}'_k(X_j^y) \log \frac{\pi'_k(X_j^y)}{\tilde{\pi}'_k(X_j^y)} \right\}.$$

Let  $\|\tilde{w}_i\|^2 = \sum_{j=1}^n \tilde{w}_{ij}^2$ . We define the “effective sample size” of  $\hat{C}_n^{\text{PCP}}(X_i^y)$  as  $1/\|\tilde{w}_i\|^2$ , which is a heuristic formula used in the literature of distributional shifts [Gretton et al., 2009; Reddi et al., 2015; Tibshirani et al., 2019; Barber et al., 2023]. When the weights  $\tilde{w}_{ij} = 1/n$  for all  $j \in [n]$ , the effective sample size is  $n$ . When the weights  $\tilde{w}_{ij}$  are unequal, the effective sample size decreases as the  $\ell^2$ -norm increases. We use the bisection method to search for the largest  $m \in [5, 500]$  that achieves  $n^{-1} \sum_{i=1}^n \|\tilde{w}_i\|_2^2 \geq 100$  or  $n^{-1} \sum_{i=1}^n w_{ii} \leq 1/30$ , ensuring both the effective sample size and the precision parameter  $m$  are relatively large to compute our interval in (16).

## C Technical proofs

### C.1 Proof of Proposition 5

*Proof.* We denote  $U_i := \mathbb{1}\{X_i > 0\} \sim \text{Bern}(\rho)$ ,  $N_0 := \sum_{i=1}^n U_i \sim \text{Binomial}(n, \rho)$ , and  $N_1 = n - N_0$ . When  $X_{n+1} \leq 0$ , we have

$$\begin{aligned} \sum_{i=1}^{n+1} w_i \mathbb{1}\{R_i \geq R_{n+1}\} &= \frac{\sum_{i=1}^{n+1} [(1 - U_i) + bU_i] \mathbb{1}\{R_i \geq R_{n+1}\} + c}{N_0 + N_1 b + 1 + c} \\ &= \frac{N_0 + 1}{N_0 + N_1 b + 1 + c} \times \frac{\sum_{i=1}^{n+1} (1 - U_i) \mathbb{1}\{R_i \geq R_{n+1}\} + bN_1 + c}{N_0 + 1}. \end{aligned}$$

The second equality uses the assumption that the residual  $R_{n+1}$  at  $X_{n+1} = 0$  is smaller than the residuals  $R_i$  at  $X_i = 1$ . Then, we have

$$\begin{aligned} &\mathbb{P}\{Y_{n+1} \notin \hat{C}_n(X_{n+1}) \mid X_{n+1} \leq 0, N_0\} \\ &= \mathbb{P} \left\{ \sum_{i=1}^{n+1} w_i \mathbb{1}\{R_i \geq R_{n+1}\} \leq \alpha \mid X_{n+1} \leq 0, N_0 \right\} \\ &= \mathbb{P} \left\{ \frac{\sum_{i=1}^{n+1} (1 - U_i) \mathbb{1}\{R_i \geq R_{n+1}\}}{N_0 + 1} \leq \alpha - \frac{(1 - \alpha)(N_1 b + c)}{N_0 + 1} \mid X_{n+1} \leq 0, N_0 \right\} \quad (42) \\ &\geq \alpha - \frac{(1 - \alpha)(N_1 b + c) + 1}{N_0 + 1} \\ &= \alpha + (1 - \alpha)b - \frac{(1 - \alpha)[(n + 1)b + c] + 1}{N_0 + 1}. \end{aligned}$$

The inequality is obtained by conditioning on which of the  $N_0$  units are located at  $X_i = 0$ . For example, given  $X_1 = \dots = X_{N_0} = X_{n+1} = 1$ , the residuals  $R_1, \dots, R_{N_0}, R_{n+1}$  are drawn from the same distribution. Then, the empirical average in the second equality is a valid p-value, which satisfies the inequality in the last line when all the residuals are distinct [Lei et al., 2018, Theorem 2]. We also note that the probability,

$$\mathbb{P} \left\{ \alpha - \frac{(1-\alpha)(N_1 b + c)}{N_0 + 1} \geq 0 \right\} = \mathbb{P} \left\{ N_1 \leq \frac{\alpha(n+1) - (1-\alpha)c}{\alpha + (1-\alpha)b} \right\},$$

goes to 1 exponentially fast as  $n$  increases, indicating that the inequality above becomes increasingly accurate for larger sample size  $n$ . It follows from (42) that

$$\begin{aligned} & \mathbb{P}\{Y_{n+1} \notin \hat{C}_n(X_{n+1}) \text{ and } X_{n+1} \leq 0\} \\ & \geq (1-\rho) \times \left( \alpha + (1-\alpha)b - [(1-\alpha)[(n+1)b + c] + 1] \times \mathbb{E} \left[ \frac{1}{N_0 + 1} \right] \right) \\ & = (1-\rho)\alpha - (1-\alpha)b\rho[1 - \rho^n] - \frac{(1-\alpha)c + 1}{n+1} [1 - \rho^{n+1}]. \end{aligned} \quad (43)$$

Similarly, when  $X_{n+1} > 1$ , we have

$$\begin{aligned} \sum_{i=1}^{n+1} w_i \mathbb{1}\{R_i \geq R_{n+1}\} &= \frac{\sum_{i=1}^{n+1} [a(1-U_i) + U_i] \mathbb{1}\{R_i \geq R_{n+1}\} + c}{N_0 a + N_1 + 1 + c} \\ &= \frac{N_1 + 1}{N_0 a + N_1 + 1 + c} \times \frac{\sum_{i=1}^{n+1} U_i \mathbb{1}\{R_i \geq R_{n+1}\} + c}{N_1 + 1}. \end{aligned}$$

The mis-coverage rate of  $\hat{C}_n(X_{n+1})$  conditional on  $X_{n+1} > 1$  can be expressed as

$$\begin{aligned} & \mathbb{P}\{Y_{n+1} \notin \hat{C}_n(X_{n+1}) \mid X_{n+1} > 0, N_1\} \\ &= \mathbb{P} \left\{ \sum_{i=1}^{n+1} w_i \mathbb{1}\{R_i \geq R_{n+1}\} \leq \alpha \mid X_{n+1} > 0, N_1 \right\} \\ &= \mathbb{P} \left\{ \frac{\sum_{i=1}^{n+1} U_i \mathbb{1}\{R_i \geq R_{n+1}\}}{N_1 + 1} \leq \alpha + \frac{\alpha N_0 a - (1-\alpha)c}{N_1 + 1} \mid X_{n+1} > 0, N_1 \right\} \\ &\geq \alpha + \frac{\alpha N_0 a - (1-\alpha)c - 1}{N_1 + 1} \\ &= \alpha - \alpha a + \frac{\alpha(n+1)a - (1-\alpha)c - 1}{N_1 + 1}. \end{aligned} \quad (44)$$

As explained in (42), the inequality is tight since the probability

$$\mathbb{P} \left\{ \alpha + \frac{\alpha N_0 a - (1-\alpha)c}{N_1 + 1} \geq 0 \right\} = \mathbb{P} \left\{ N_1 \geq \frac{-\alpha(na + 1) + (1-\alpha)c}{\alpha(1-a)} \right\},$$

which goes to 1 as  $n$  increases; it is 1 if the numerator is negative. Then,

$$\begin{aligned}
& \mathbb{P}\{Y_{n+1} \notin \hat{C}_n(X_{n+1}) \text{ and } X_{n+1} > 0\} \\
& \geq \rho \times \left( \alpha - \alpha a + [\alpha(n+1)a - (1-\alpha)c - 1] \times \mathbb{E} \left[ \frac{1}{N_1 + 1} \right] \right) \\
& = \rho \alpha + \alpha a (1 - \rho) [1 - (1 - \rho)^n] - \frac{(1 - \alpha)c + 1}{n + 1} [1 - (1 - \rho)^{n+1}].
\end{aligned} \tag{45}$$

Using (43) and (45), we can lower bound the mis-coverage rate of  $\hat{C}_n(X_{n+1})$  as follows:

$$\begin{aligned}
\mathbb{P}\{Y_{n+1} \notin \hat{C}_n(X_{n+1})\} & \geq \alpha + \alpha a (1 - \rho) [1 - (1 - \rho)^N] - (1 - \alpha)b\rho [1 - \rho^N] \\
& \quad - 2[(1 - \alpha)c + 1]/[n + 1].
\end{aligned}$$

This proves the claim in the proposition. When  $c = -1$ , the interval  $\hat{C}_n(X_{n+1})$  is defined using the first  $n$  data points. In other words, we have

$$\hat{C}_n^-(X_{n+1}) = \left[ \hat{\mu}(X_{n+1}) \pm Q_{1-\alpha} \left( \sum_{i=1}^n w_i^- \delta_{R_i} \right) \right],$$

where  $w_i^- = w_i \times [N_0 + N_1 b + 1]/[N_0 + N_1 b]$ . When  $X_{n+1} \leq 0$ ,

$$\begin{aligned}
& \mathbb{P}\{Y_{n+1} \notin \hat{C}_n^-(X_{n+1}) \mid X_{n+1} \leq 0, N_0, N_1\} \\
& = \mathbb{P} \left\{ \sum_{i=1}^{n+1} w_i^- \mathbb{1}\{R_i \geq R_{n+1}\} \leq \alpha + \frac{1}{N_0 + N_1 b} \mid X_{n+1} \leq 0, N_0, N_1 \right\} \\
& = \mathbb{P} \left\{ \sum_{i=1}^{n+1} w_i \mathbb{1}\{R_i \geq R_{n+1}\} \leq \alpha' := \left[ \alpha + \frac{1}{N_0 + N_1 b} \right] \times \frac{N_0 + N_1 b}{N_0 + N_1 b + 1} \mid X_{n+1} \leq 0, N_0, N_1 \right\} \\
& \geq \alpha' - \frac{(1 - \alpha')N_1 b}{N_0 + 1} - \frac{1}{N_0 + 1} \\
& = -\frac{N_1 b + 1}{N_0 + 1} + \frac{\alpha(N_0 + N_1 b) + 1}{N_0 + 1} \\
& = \alpha + (1 - \alpha)b - \frac{(1 - \alpha)(n + 1)b + \alpha}{N_0 + 1}.
\end{aligned}$$

The inequality follows from (42) with  $c = 0$ . Similarly, we can show that

$$\mathbb{P}\{Y_{n+1} \notin \hat{C}_n^-(X_{n+1}) \mid X_{n+1} > 0, N_0, N_1\} \geq \alpha - \alpha a + \frac{\alpha(n+1)a - \alpha}{N_1 + 1},$$

using (44) with  $c = 0$ . Then,

$$\mathbb{P}\{Y_{n+1} \notin \hat{C}_n^-(X_{n+1})\} = \mathbb{E} \left[ \mathbb{P} \left\{ \sum_{i=1}^{n+1} w_i \mathbb{1}\{R_i \geq R_{n+1}\} \leq \alpha \mid X_{n+1}, N_0, N_1 \right\} \right]$$

$$\begin{aligned}
&\geq \alpha + (1 - \alpha)(1 - \rho)b - (1 - \rho)[(1 - \alpha)(n + 1)b + \alpha] \mathbb{E} \left[ \frac{1}{N_0 + 1} \right] \\
&= \alpha + \alpha a(1 - \rho) [1 - (1 - \rho)^N] - (1 - \alpha)b\rho [1 - \rho^N] - 2\alpha/[n + 1],
\end{aligned}$$

which confirms that the proposition holds with  $c = -1$ .  $\square$

## C.2 Proof of Proposition 1

*Proof.* By the definition  $w_i^*$ , we have  $w_1^*, \dots, w_{n+1}^* \perp\!\!\!\perp X_{n+1} \mid \pi^*(X_{n+1})$ . By the definition of  $\hat{C}_n^*(X_{n+1})$  in (5), we have

$$Y_{n+1} \notin \hat{C}_n^*(X_{n+1}) \iff \hat{P}_n^* := \sum_{i=1}^{n+1} w_i^* \mathbb{1}\{R_i \geq R_{n+1}\} \leq \alpha.$$

which shows that the miscoverage event  $\{Y_{n+1} \notin \hat{C}_n^*(X_{n+1})\}$  only depends on  $X_{n+1}$  through  $R_{n+1}$  and  $\pi^*(X_{n+1})$  in the weights  $w_1^*, \dots, w_{n+1}^*$ . Under the model (4),

$$R_{n+1} \perp\!\!\!\perp X_{n+1} \mid \pi^*(X_{n+1}).$$

The probability of miscoverage given  $\pi^*(X_{n+1})$  and  $X_{n+1}$  is independent of  $X_{n+1}$  :

$$\mathbb{P}\{\hat{P}_n^* \leq \alpha \mid X_{n+1}, \pi^*(X_{n+1})\} = \mathbb{P}\{\hat{P}_n^* \leq \alpha \mid \pi^*(X_{n+1})\}.$$

Conversely, the probability given  $\pi^*(X_{n+1})$  and  $X_{n+1}$  is independent of  $\pi^*(X_{n+1})$ :

$$\mathbb{P}\{\hat{P}_n^* \leq \alpha \mid X_{n+1}, \pi^*(X_{n+1})\} = \mathbb{P}\{\hat{P}_n^* \leq \alpha \mid X_{n+1}\}.$$

which proves the claim as required.  $\square$

## C.3 Proof of Theorem 1 and Proposition 2

*Proof.* Below, we prove Proposition 2, which also covers Theorem 1 by replacing  $\pi^y$  with  $\pi^*$ . Let  $z_i = (x_i, y_i)$  and  $r_i = |y_i - \hat{\mu}(x_i)|$ . Conditional on

$$Z_{[n+1]} \in \mathcal{D}_{\mathbf{z}} := \{z_1, \dots, z_{n+1}\} \quad \text{and} \quad \tilde{\pi}^{Y_{n+1}}(X_{n+1}) = \tilde{l}/m, \quad (46)$$

the probability of  $Z_{n+1} = z_j$  can be written as

$$\begin{aligned}
&\mathbb{P}\{Z_{n+1} = z_j \mid Z_{[n+1]} \in \mathcal{D}_{\mathbf{z}}, \tilde{\pi}^{Y_{n+1}}(X_{n+1}) = \tilde{l}/m\} \\
&= \frac{\sum_{\sigma: \sigma(n+1)=j} p_{Z_{[n+1]}}(z_{\sigma(1)}, \dots, z_{\sigma(n+1)}) \prod_{k=1}^K [\pi_k^{y_j}(x_j)]^{\tilde{l}_k}}{\sum_{i=1}^{n+1} \sum_{\sigma': \sigma'(n+1)=i} p_{Z_{[n+1]}}(z_{\sigma'(1)}, \dots, z_{\sigma'(n+1)}) \prod_{k'=1}^K [\pi_{k'}^{y_i}(x_i)]^{\tilde{l}_{k'}}} \quad (\text{By Bayes' rule})
\end{aligned}$$

$$\begin{aligned}
&= \frac{\sum_{\sigma: \sigma(n+1)=j} \prod_{k=1}^K [\pi_k^{y_j}(x_j)]^{\tilde{l}_k}}{\sum_{i=1}^{n+1} \sum_{\sigma': \sigma'(n+1)=i} \prod_{k'=1}^K [\pi_{k'}^{y_i}(x_i)]^{\tilde{l}_{k'}}} && \text{(By the exchangeability of } Z_{[n+1]}\text{)} \\
&= \frac{\prod_{k=1}^K [\pi_k(x_j)]^{\tilde{l}_k}}{\sum_{i=1}^{n+1} \prod_{k'=1}^K [\pi_{k'}(x_i)]^{\tilde{l}_{k'}}} && \text{(By the symmetry of } \mathcal{A}\text{)} \\
&= \tilde{w}_j(\{z_1, \dots, z_{n+1}\}) && \text{(By the definition of } \tilde{w}_j\text{).}
\end{aligned}$$

The probability of mis-coverage can be rewritten as

$$\begin{aligned}
&\mathbb{P}\{Y_{n+1} \notin \hat{C}_n^{\text{PCP}}(X_{n+1}) \mid Z_{[n+1]} \in \mathcal{D}_z, \tilde{\pi}^{Y_{n+1}}(X_{n+1}) = \tilde{l}/m\} \\
&= \sum_{j=1}^{n+1} \mathbb{P}\{Y_{n+1} \notin \hat{C}_n^{\text{PCP}}(X_{n+1}) \mid Z_{[n+1]} \in \mathcal{D}_z, \tilde{\pi}^{Y_{n+1}}(X_{n+1}) = \tilde{l}/m, Z_{n+1} = z_j\} \\
&\quad \times \mathbb{P}\{Z_{n+1} = z_j \mid \tilde{\pi}^{Y_{n+1}}(X_{n+1}) = \tilde{l}/m, Z_{[n+1]} \in \mathcal{D}_z\} \\
&= \sum_{j=1}^{n+1} \tilde{w}_j(\{z_1, \dots, z_{n+1}\}) \mathbb{1} \left\{ \sum_{i=1}^{n+1} \tilde{w}_i(\{z_1, \dots, z_{n+1}\}) \mathbb{1}\{r_i \geq r_j\} \leq \alpha \right\} \leq \alpha.
\end{aligned} \tag{47}$$

The last equality uses the weight expression above and that  $Y_{n+1} \notin \hat{C}_n^{\text{PCP}}(X_{n+1})$  is deterministic under the conditional event. More precisely, the non-random membership probabilities  $\pi = \pi^{Y_{n+1}}$  are functions of  $\mathcal{D}_z$ . As functions of  $\tilde{\pi}(X_{n+1}) = \tilde{l}/m$  and  $\mathcal{D}_z$ , the weights in our interval are also fixed. Finally,  $Z_{n+1} = z_j$  fixes the test point, which does not affect the weights of our interval given  $\tilde{\pi}(X_{n+1}) = \tilde{l}/m$ . The last step is achieved by the deterministic inequality in Lemma A.1 in [Harrison \[2012\]](#).

Following the proof of the same Lemma A.1, we lower bound the probability of miscoverage. Without loss of generality, we assume that  $r_1 < \dots < r_{n+1}$ . Otherwise, we can sort them from the smallest to the largest. Let  $j^*$  be the smallest  $j \in [n+1]$  such that  $\sum_{i=1}^{n+1} \tilde{w}_i \mathbb{1}\{r_i \geq r_j\} \leq \alpha$ . Then, we have

$$\sum_{j=1}^{n+1} \tilde{w}_j \mathbb{1} \left\{ \sum_{i=1}^{n+1} \tilde{w}_i \mathbb{1}\{r_i \geq r_j\} \leq \alpha \right\} = \sum_{j=j^*}^{n+1} \tilde{w}_j = \sum_{j=j^*-1}^{n+1} \tilde{w}_j - \tilde{w}_{j^*-1} > \alpha - \tilde{w}_{j^*-1}.$$

By the definition of  $j^*$ ,  $\sum_{j=j^*-1}^{n+1} \tilde{w}_j > \alpha$ , which gives the inequality above. Upper bounding  $\tilde{w}_{j^*-1}$  by  $\max_{i \in [n+1]} \tilde{w}_{i^*}$  proves the claim as required.  $\square$

## C.4 Proof of Theorem 2

By the definition (5), the interval  $\hat{C}_n^*(X_{n+1})$  is infinite when  $w_{n+1}^* \geq \alpha$ , i.e.,

$$\phi^*(X_{n+1}, X_{n+1}) \geq \frac{\alpha}{1-\alpha} \sum_{i=1}^n \phi^*(X_i, X_{n+1}).$$

By the expression of  $\phi^*(X_i, X_{n+1})$  in (12), that is when

$$H := - \sum_{k=1}^K \tilde{L}_k \log \pi_k^*(X_{n+1}) \leq - \log \left( \frac{\alpha}{1-\alpha} \sum_{i=1}^n \prod_{k=1}^{K^*} [\pi_k^*(X_i)]^{\tilde{L}_k} \right) := \epsilon(\alpha, X_{[n]}, \tilde{L}). \quad (48)$$

When  $\tilde{L}$  is fixed, the random variable  $H$  does not have a known distribution due to the mutual dependence between  $\pi_j^*(X_{n+1})$  and  $\pi_k^*(X_{n+1})$  for  $j \neq k$ . Nevertheless, we can compute the moment-generating function (MGF) of  $H$  as follows:

$$\begin{aligned} \mathbb{E}[e^{tH} \mid \tilde{L}] &= \mathbb{E} \left[ \prod_k^{K^*} [\pi_k^*(X_{n+1})]^{-t\tilde{L}_k} \mid \tilde{L} \right] \\ &= \int \prod_k^{K^*} \pi_k^{-t\tilde{L}_k} \text{Dir}(\pi; \Lambda + \tilde{L}) d\pi \\ &= \frac{1}{\text{B}(\Lambda + \tilde{L})} \int \prod_k^{K^*} \pi_k^{-t\tilde{L}_k} \prod_k^{K^*} \pi_k^{\Lambda_k + \tilde{L}_k - 1} d\pi \\ &= \text{B}(\Lambda + [1-t]\tilde{L}) / \text{B}(\Lambda + \tilde{L}) \\ &= \frac{\Gamma(\bar{\Lambda} + m)}{\Gamma(\bar{\Lambda} + [1-t]m)} \prod_{k=1}^{K^*} \frac{\Gamma(\Lambda_k + [1-t]\tilde{L}_k)}{\Gamma(\Lambda_k + \tilde{L}_k)}, \end{aligned}$$

where  $\bar{\Lambda} = \sum_{k=1}^{K^*} \Lambda_k$ . By minimizing  $H$  in terms of  $\pi^*(X_{n+1})$  subject to the constraints of the probability simplex, we can show that  $H$  is lower bounded by

$$H_{\min} := - \sum_{k=1}^K \tilde{L}_k \log \tilde{\pi}_k^*(X_{n+1}) = -m \sum_{k=1}^K \tilde{\pi}_k^*(X_{n+1}) \log \tilde{\pi}_k^*(X_{n+1}), \quad (49)$$

which is non-random given  $\tilde{L}$ . The MGF of  $H - H_{\min}$  is given by

$$\begin{aligned} M_{H-H_{\min}}(t) &= \mathbb{E}[e^{t[H-H_{\min}]} \mid \tilde{L}] \\ &= \prod_{k=1}^{K^*} [\tilde{\pi}_k^*(X_{n+1})]^{t\tilde{L}_k} \frac{\Gamma(\bar{\Lambda} + m)}{\Gamma(\bar{\Lambda} + [1-t]m)} \prod_{k=1}^{K^*} \frac{\Gamma(\Lambda_k + [1-t]\tilde{L}_k)}{\Gamma(\Lambda_k + \tilde{L}_k)}. \end{aligned} \quad (50)$$

We let  $M^{(j)}$  denote the  $j$ -th order derivative of  $M_{H-H_{\min}}(t)$  as follows:

$$M^{(0)} \equiv M_{H-H_{\min}}(t) \quad \text{and} \quad M^{(j)} := d^j M_{H-H_{\min}}(t) / dt^j \quad \text{for } j \in \mathbb{N}^+.$$

The following is the key lemma used to prove Theorem 2. We defer its proof to Appendix C.4.2. Ignoring the error term, the lemma shows that the moments of  $H - H_{\min}$  matches the moments of the exponential distribution  $\text{Exp}(1 + \bar{\Lambda}/m)$ .

**Lemma 1.** For  $b \in \mathbb{N}^+$ , the  $b$ -th moment of  $H - H_{\min}$  can be written as

$$\mathbb{E} \left[ (H - H_{\min})^b \mid \tilde{\pi}(X_{n+1}) = \Lambda/\bar{\Lambda} \right] = \frac{b!}{(1 + \bar{\Lambda}/m)^b} + O(1/m).$$

Using Lemma 1, we can write the characteristic function of  $H - H_{\min}$  as

$$\phi_{H-H_{\min}}(t) = 1 + \sum_{b=1}^{\infty} \frac{i^b \mathbb{E} \left[ (H - H_{\min})^b \mid \tilde{\pi}(X_{n+1}) = \Lambda/\bar{\Lambda} \right]}{b!} t^b = \frac{m + \bar{\Lambda}}{m + \bar{\Lambda} - mit} + O(1/m).$$

The CDF of  $H - H_{\min}$  is given by

$$F_{H-H_{\min}}(h) = \int_0^h \frac{1}{2\pi} \int_{-\infty}^{\infty} \exp(-ith') \phi_{H-H_{\min}}(t) dt dh' = 1 - \exp\{-(1 + \bar{\Lambda}/m)h\} + O(1/m).$$

Then, by the equivalence and the definition of  $\epsilon(\alpha, X_{[n]}, \tilde{L})$  in (48), we have

$$\begin{aligned} & \mathbb{P}\{|\hat{C}_n^*(X_{n+1})| < \infty \mid X_{[n]}, \tilde{\pi}(X_{n+1}) = \Lambda/\bar{\Lambda}\} \\ &= \mathbb{P}\left\{H - H_{\min} \geq \epsilon(\alpha, X_{[n]}, \tilde{L}) - H_{\min} \mid X_{[n]}, \tilde{\pi}(X_{n+1}) = \Lambda/\bar{\Lambda}\right\} \\ &= \exp\left\{(1 + \bar{\Lambda}/m) \log\left(\frac{\alpha}{1 - \alpha} \sum_{i=1}^n \prod_{k=1}^{K^*} [\pi_k(X_i)]^{\tilde{L}_k}\right) + (1 + \bar{\Lambda}/m)H_{\min}\right\} \wedge 1 + O(1/m) \\ &= \left\{\frac{\alpha}{1 - \alpha} \sum_{i=1}^n \prod_{k=1}^{K^*} [\pi_k(X_i)]^{\tilde{L}_k} / \prod_{k=1}^{K^*} [\tilde{\pi}_k(X_{n+1})]^{\tilde{L}_k}\right\}^{1 + \bar{\Lambda}/m} \wedge 1 + O(1/m) \\ &= \left\{\frac{\alpha}{1 - \alpha} \sum_{i=1}^n \exp\left(\sum_{k=1}^{K^*} \tilde{L}_k \log \frac{\pi_k(X_i)}{\tilde{\pi}_k(X_{n+1})}\right)\right\}^{1 + \bar{\Lambda}/m} \wedge 1 + O(1/m) \\ &= \min\left\{\frac{\alpha}{1 - \alpha} \sum_{i=1}^n \exp\left(-m \sum_{k=1}^{K^*} D_{\text{KL}}(\tilde{\pi}^*(X_{n+1}) \parallel \pi^*(X_i))\right), 1\right\}^{(m + \bar{\Lambda})/m} + O(1/m), \end{aligned} \tag{51}$$

whre the third equality is obtained by the definition of  $H_{\min}$  in (49).

#### C.4.1 Numerical experiments for Theorem 2

The proof of Theorem 2 is based on Lemma 1, which shows that  $H - H_{\min}$  (defined in (48) and (49)) approximately follows an exponential distribution  $\text{Exp}(1 + \bar{\Lambda}/m)$ . We next verify our theory on three different Dirichlet distributions. When  $\tilde{\pi}^*(X_{n+1}) = \Lambda/\bar{\Lambda}$ , the posterior distribution of  $\pi^*(X_{n+1})$  given  $\tilde{\pi}^*(X_{n+1})$  can be expressed as



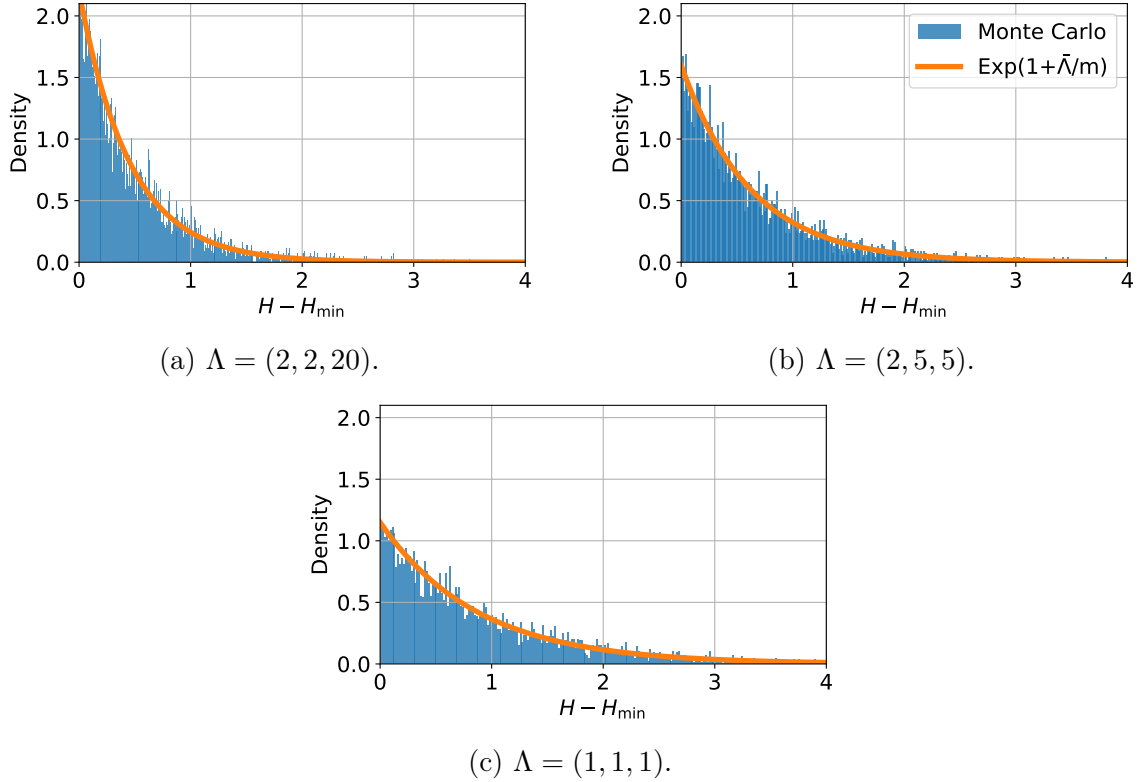


Figure 13: The exponential distribution  $\text{Exp}(1 + \bar{\Lambda}/m)$  and the Monte-Carlo simulations of  $H - H_{\min}$  under the Dirichlet posterior  $\text{Dir}(\Lambda + m\Lambda/\bar{\Lambda})$  with  $m = 20$ .

$\text{Dir}(\Lambda + m\Lambda/\bar{\Lambda})$ . We draw 5000 random samples from the posterior to construct a Monte-Carlo approximation of the distribution of  $H - H_{\min}$ . Figure 13 shows that the Monte-Carlo approximation aligns well with  $\text{Exp}(1 + \bar{\Lambda}/m)$  for  $m = 20$  and three different values of  $\Lambda$ . This result confirms that the first term in (51) gives an accurate approximation of the probability that our interval has a finite length.

#### C.4.2 Proof of Lemma 1

*Proof.* The derivative of each term in  $M_{H-H_{\min}}(t)$  in (50) involves itself. First,

$$\frac{d}{dt} \left( [\tilde{\pi}^*(X_{n+1})]^{t\tilde{L}_k} \right) = [\tilde{\pi}_k^*(X_{n+1})]^{t\tilde{L}_k} \times \tilde{L}_k \ln \tilde{\pi}_k^*(X_{n+1}).$$

The derivative of  $\Gamma(\Lambda + t\tilde{L})$  can be written as

$$\frac{d}{dt} \left( \frac{\Gamma(\bar{\Lambda} + m)}{\Gamma(\bar{\Lambda} + [1 - t]m)} \right) = \frac{\Gamma(\bar{\Lambda} + m)}{\Gamma(\bar{\Lambda} + [1 - t]m)} \times m\psi(\bar{\Lambda} + [1 - t]m),$$

where  $\psi(v) = d \ln \Gamma(v)/dv$  is the digamma function. Similarly, we have

$$\frac{d}{dt} \left( \frac{\Gamma(\Lambda_k + [1-t]\tilde{L}_k)}{\Gamma(\Lambda_k + \tilde{L}_k)} \right) = -\frac{\Gamma(\Lambda_k + [1-t]\tilde{L}_k)}{\Gamma(\Lambda_k + \tilde{L}_k)} \times \tilde{L}_k \psi(\bar{\Lambda}_k + [1-t]\tilde{L}_k).$$

By the last three equations, we can express the first-order derivative of  $M(t)$  as

$$M^{(1)} = G^{(0)} M^{(0)}, \quad (52)$$

where the function  $G^{(0)}$  is defined as

$$G^{(0)}(t) = \sum_{k=1}^K \tilde{L}_k \log \tilde{\pi}_k^*(X_{n+1}) + m \psi(\bar{\Lambda} + [1-t]m) - \sum_{k=1}^{K^*} \tilde{L}_k \psi(\Lambda_k + [1-t]\tilde{L}_k).$$

It is well-known that  $\psi$  can be approximated as follows:

$$\psi(v) = \ln(v) - \frac{1}{2v} - \frac{1}{12v^2} + \frac{1}{120v^4} - \frac{1}{252v^6} + \dots \approx \ln(v) - \frac{1}{2v}.$$

Then, we approximate the above expression of  $G^{(0)}$  as

$$\begin{aligned} G^{(0)} &\approx \sum_{k=1}^K \tilde{L}_k \log \tilde{\pi}_k^*(X_{n+1}) + \sum_{k=1}^{K^*} \tilde{L}_k \ln \left( \frac{\bar{\Lambda} + [1-t]m}{\Lambda_k + [1-t]\tilde{L}_k} \right) \\ &\quad + \sum_{k=1}^{K^*} \left( \frac{\tilde{L}_k}{2[\Lambda_k + [1-t]\tilde{L}_k]} \right) - \frac{m}{2[\bar{\Lambda} + [1-t]m]} \\ &= \sum_{k=1}^K \tilde{L}_k \log \tilde{\pi}_k^*(X_{n+1}) + \sum_{k=1}^{K^*} \tilde{L}_k \ln \left( \frac{\bar{\Lambda}/m + [1-t]}{\Lambda_k/\tilde{L}_k + [1-t]} \times \frac{1}{\tilde{\pi}_k^*(X_{n+1})} \right) \\ &\quad + \frac{(K^* - 1)m}{2\bar{\Lambda} + 2[1-t]m} \\ &= \frac{(K^* - 1)m}{2\bar{\Lambda} + 2[1-t]m}. \end{aligned} \quad (53)$$

The last equality is due to  $\bar{\Lambda}/m = \Lambda_k/\tilde{L}_k$ , which follows from the condition that  $\tilde{\pi}^*(X_{n+1}) = \tilde{L}_k/m = \Lambda_k/\bar{\Lambda}$ . The approximation error can be written as

$$\begin{aligned} G^{(0)} - \frac{(K^* - 1)m}{2\bar{\Lambda} + 2[1-t]m} &= \sum_{j=1}^{\infty} C_j \left\{ \sum_{k=1}^{K^*} \left( \frac{\tilde{L}_k}{[\Lambda_k + [1-t]\tilde{L}_k]^{2j}} \right) - \frac{m}{[\bar{\Lambda} + [1-t]m]^{2j}} \right\} \\ &= \sum_{j=1}^{\infty} C_j \left\{ \sum_{k=1}^{K^*} \frac{1}{\tilde{L}_k^{2j-1}} - \frac{1}{m^{2j-1}} \right\} \frac{m^{2j}}{[\bar{\Lambda} + [1-t]m]^{2j}} \end{aligned}$$

$$= \sum_{j=1}^{\infty} C_j \left\{ \sum_{k=1}^{K^*} (\bar{\Lambda}/\Lambda_k)^{2j-1} - 1 \right\} \frac{m}{[\bar{\Lambda} + [1-t]m]^{2j}} = O(1/m),$$

where  $C_2 = -1/12, C_4 = 1/120, \dots$ , are coefficients in the expansion of  $\psi$  above. The second equality is obtained by  $\bar{\Lambda}/m = \Lambda_k/\tilde{L}_k$ :

$$\begin{aligned} \frac{\tilde{L}_k}{[\Lambda_k + [1-t]\tilde{L}_k]^{2j}} &= \frac{1}{\tilde{L}_k^{2j-1}} \times \left[ \frac{m/\bar{\Lambda}}{1 + [1-t]m/\bar{\Lambda}} \right]^{2j} \\ &= \frac{1}{\tilde{L}_k^{2j-1}} \times \frac{m^{2j}}{[\bar{\Lambda} + [1-t]m]^{2j}}. \end{aligned}$$

When  $K^* = 3$ , using (53), the  $b$ -th order derivative of  $G^{(0)}$  is

$$\begin{aligned} G^{(b)} &= \frac{d^b}{dt^b} \left( \frac{m}{\bar{\Lambda} + [1-t]m} \right) + \sum_{j=1}^{\infty} C_j \left\{ \sum_{k=1}^{K^*} \frac{1}{\tilde{L}_k^{2j-1}} - \frac{1}{m^{2j-1}} \right\} \frac{(2j+k-1)!m^{b+1}}{(2j-1)![\bar{\Lambda} + [1-t]m]^{2j+b}} \\ &= \frac{b!m^{b+1}}{(\bar{\Lambda} + [1-t]m)^{b+1}} + O(1/m). \end{aligned} \tag{54}$$

Then,  $M^{(1)}(t)$  in (52) can be written as

$$M^{(1)}(t) = \frac{mM^{(0)}}{\bar{\Lambda} + [1-t]m} + O(1/m). \tag{55}$$

By  $M^{(0)}(0) = M_{H-H_{\min}}(0) = 1$ , we can express the first moment of  $H - H_{\min}$  as

$$\mathbb{E} [H - H_{\min} \mid X_{[n]}, \tilde{\pi}(X_{n+1}) = \Lambda/\bar{\Lambda}] = M^{(1)}(0) = \frac{m}{\bar{\Lambda} + m} + O(1/m),$$

which proves the claim for  $b = 1$ . We next use induction to prove the claim for  $b = 2, 3, \dots$ . More precisely, we will show that for any  $b \in \mathbb{N}^+$ ,

$$M^{(b)} = b! \left( \frac{m}{\bar{\Lambda} + [1-t]m} \right)^b M^{(0)} + O(1/m). \tag{56}$$

We first compute the second, third and fourth-order derivative of  $M_{H-H_{\min}}(t)$  to illustrate the idea. As shown in the first and second row in Figure 14, we differentiate  $M^{(0)}$  and  $G^{(0)}$  respectively to obtain the expression of  $M^{(2)}$  as follows:

$$M^{(2)} = G^{(1)}M^{(0)} + G^{(0)}M^{(1)} = 2 \left( \frac{m}{\bar{\Lambda} + [1-t]m} \right)^2 M^{(0)} + O(1/m),$$

by the expressions of  $G^{(b)}$  in (54) and  $M^{(1)}$  in (55). Similarly, in the third and fourth rows of the same figure, further differentiating  $M^{(b)}$  gives that

$$M^{(3)} = G^{(2)}M^{(0)} + 2G^{(1)}M^{(1)} + G^{(0)}M^{(2)},$$

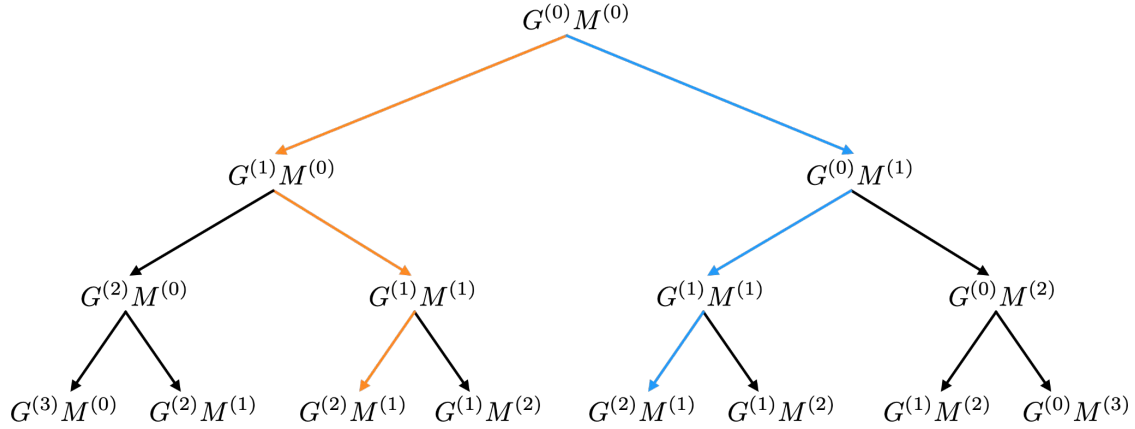


Figure 14: The paths of computing the  $j$ -th order derivatives of  $M_{H-H_{\min}}(t)$  for  $j \in [4]$ .

$$M^{(4)} = G^{(3)}M^{(0)} + 3G^{(2)}M^{(1)} + 3G^{(1)}M^{(2)} + G^{(0)}M^{(2)}.$$

Because of the multiplicative structure in (52), the expression of  $M^{(b)}$  involves terms

$$G^{(c)}M^{(d)}, \forall c, d \in \{0, 1, 2, \dots\} \text{ such that } c + d = b - 1.$$

In other words, we can write  $G^{(c)}M^{(d)} = G^{(c)}M^{(b-1-c)}$  in the expression of  $M^{(b)}$ . From  $G^{(0)}M^{(0)}$  in the first row to one of the  $G^{(c)}M^{(b-1-c)}$ 's in the  $b$ -th row in Figure 14, we need to go through the derivatives  $G^{(1)}, G^{(2)}, \dots, G^{(c-1)}$  in some previous rows. For example, the two coloured paths in the figure highlight two of the paths for obtaining the term  $G^{(2)}M^{(1)}$  in the expression of  $M^{(4)}$ . In the yellow path,  $G^{(1)}$  appears in the second row, and  $G^{(2)}$  appears in the fourth row, while in the blue path,  $G^{(1)}$  appears in the second row and  $G^{(2)}$  appears in the fourth row. In general, there are  $\binom{b-1}{c}$  paths to obtain the term  $G^{(c)}M^{(b-1-c)}$  in the  $b$ -th row. Therefore, we have the expression,

$$M^{(b)} = \sum_{c=0}^{b-1} \binom{b-1}{c} G^{(c)}M^{(b-1-c)}. \quad (57)$$

It is straightforward to show that (57) holds for the expression of  $M^{(b)}$  above for  $b \in [4]$ . Suppose that the expression holds for  $M^{(b)}$ . Differentiating the expression gives

$$\begin{aligned} M^{(b+1)} &= \sum_{c=0}^{b-1} \binom{b-1}{c} G^{(c+1)}M^{(b-1-c)} + \sum_{c=0}^{b-1} \binom{b-1}{c} G^{(c)}M^{(b-c)} \\ &= \sum_{c=1}^b \binom{b-1}{c-1} G^{(c)}M^{(b-c)} + \sum_{c=0}^{b-1} \binom{b-1}{c} G^{(c)}M^{(b-c)} \\ &= \sum_{c=1}^{b-1} \left[ \binom{b-1}{c-1} + \binom{b-1}{c} \right] G^{(c)}M^{(b-c)} + G^{(b)}M^{(0)} + G^{(0)}M^{(b)} \end{aligned}$$

$$= \sum_{c=0}^b \binom{b}{c} G^{(c)} M^{(b-c)},$$

which proves the expression (57) holds for  $b + 1$ .

Similarly, substituting  $G^{(c)}$  in (54) and  $M^{(b-c)}$  in (56) into (57), we have

$$\begin{aligned} M^{(b+1)} &= \sum_{c=0}^b \binom{b}{c} \left[ \frac{c! m^{c+1}}{(\bar{\Lambda} + [1-t]m)^{c+1}} \right] \left[ (b-c)! \left( \frac{m}{\bar{\Lambda} + [1-t]m} \right)^{b-c} M^{(0)} \right] + O(1/m) \\ &= \sum_{c=0}^b \binom{b}{c} c! (b-c)! \left( \frac{m}{\bar{\Lambda} + [1-t]m} \right)^{b+1} M^{(0)} + O(1/m) \\ &= b! \sum_{c=0}^b \left( \frac{m}{\bar{\Lambda} + [1-t]m} \right)^{b+1} M^{(0)} + O(1/m) \\ &= b! \left( \frac{m}{\bar{\Lambda} + [1-t]m} \right)^{b+1} M^{(0)} + O(1/m), \end{aligned}$$

which proves that the expression (56) holds for  $b + 1$  by induction.  $\square$

## C.5 Proof of Theorem 3

In Theorem 3, the KL-based weights are constructed using a fixed  $\pi$ , which does not depend on  $R_{[n+1]}$ . Below, we prove the theorem for any weighted interval,

$$\hat{C}_n(X_{n+1}) = \left\{ y : \sum_{i=1}^{n+1} w_i \mathbb{1}\{R_i \geq R_{n+1}^y\} > \alpha \right\},$$

where  $w_i := w_i(X_{[n+1]}, R_{[n] \setminus \{i\}})$  is a measurable function of  $X_{[n+1]}$  and  $R_{[n] \setminus \{i\}}$ , excluding  $R_i$  and  $R_{n+1}$ . This result means even if we allow the weights to depend on  $R_{[n+1]}$ , the coverage guarantee in the theorem can still hold approximately, provided that our mixture learning algorithm  $\mathcal{A}$  remains stable when leaving out  $R_i$  and  $R_{n+1}$ . Additionally, we require the last weight,  $w_{n+1}$ , to be the maximum of all the  $w_i$ , a condition satisfied by the KL-based weights used in the theorem.

*Proof.* By the definition of  $\hat{C}_n(X_{n+1})$  above, we have

$$Y_{n+1} \notin \hat{C}_n(X_{n+1}) \Leftrightarrow \sum_{i=1}^{n+1} w_i \mathbb{1}\{R_i \geq R_{n+1}\} \leq \alpha.$$

By the deterministic inequality in Lemma A.1 in [Harrison \[2012\]](#), we can upper bound the coverage gap  $\mathbb{P}\{Y_{n+1} \notin \hat{C}_n(X_{n+1}) \mid X_{[n+1]}\} - \alpha$  by

$$\begin{aligned}
& \mathbb{E} \left[ \mathbb{1} \left\{ \sum_{i=1}^{n+1} w_i \mathbb{1} \{R_i \geq R_{n+1}\} \leq \alpha \right\} - \sum_{j=1}^{n+1} w_j \mathbb{1} \left\{ \sum_{i'=1}^{n+1} w_{i'} \mathbb{1} \{R_{i'} \geq R_j\} \leq \alpha \right\} \mid X_{[n+1]} \right] \\
&= \sum_{j=1}^{n+1} \mathbb{E} \left[ w_j \left( \mathbb{1} \left\{ \sum_{i=1}^{n+1} w_i \mathbb{1} \{R_i \geq R_{n+1}\} \leq \alpha \right\} - \mathbb{1} \left\{ \sum_{i'=1}^{n+1} w_{i'} \mathbb{1} \{R_{i'} \geq R_j\} \leq \alpha \right\} \right) \mid X_{[n+1]} \right] \\
&\equiv \sum_{j=1}^{n+1} \mathbb{E} \left[ w_j(X_{[n+1]}, R_{[n]/\{j\}}) \epsilon_j(X_{[n+1]}, R_{[n+1]}) \mid X_{[n+1]} \right],
\end{aligned} \tag{58}$$

where  $\epsilon_j(X_{[n+1]}, R_{[n+1]})$  is defined as the expectation of the difference between the two indicator functions in the second line conditional on  $X_{[n+1]}$  and  $R_{[n]/\{j\}}$ . Under the mixture model (4), we can rewrite each residual  $R_j$  as

$$R_j \stackrel{d}{=} \sum_{k=1}^{K^*} \mathbb{1}\{U_j = k\} \tilde{R}_k, \tag{59}$$

where  $U_j \sim \sum_{k=1}^{K^*} \pi^*(X_j) \delta_k$  and  $\tilde{R}_k \sim f_k^*$  for  $k \in [K^*]$ . Denote

$$\begin{aligned}
\Delta(R_{-j}, R_j) &= \alpha - \sum_{i' \neq j}^n w_{i'} \mathbb{1} \{R_{i'} \geq R_j\} \quad \text{and} \\
\mathbb{P}_{k',k}^{-j} \{\cdot\} &= \mathbb{P} \left\{ \cdot \mid U_{n+1} = k', U_j = k, X_{[n+1]}, R_{[n]/\{j\}} \right\}.
\end{aligned}$$

The term  $\epsilon(X_{[n+1]}, R_{[n]/\{j\}})$  in (58) can be rewritten as

$$\begin{aligned}
& \sum_{k=1}^{K^*} \pi_k^*(X_{n+1}) \sum_{k'=1}^{K^*} \pi_{k'}^*(X_j) \mathbb{P}_{k',k}^{-j} \left\{ w_j \mathbb{1} \{R_j \geq R_{n+1}\} + w_{n+1} \leq \Delta(R_{-j}, R_{n+1}) \right\} \\
& - \sum_{k=1}^{K^*} \pi_k^*(X_j) \sum_{k'=1}^{K^*} \pi_{k'}^*(X_{n+1}) \mathbb{P}_{k',k}^{-j} \left\{ w_j + w_{n+1} \mathbb{1} \{R_{n+1} \geq R_j\} \leq \Delta(R_{-j}, R_j) \right\} \\
& \leq \sum_{k=1}^{K^*} \sum_{k'=1}^{K^*} \left[ \pi_k^*(X_{n+1}) \pi_{k'}^*(X_j) - \pi_k^*(X_j) \pi_{k'}^*(X_{n+1}) \right] \\
& \quad \times \mathbb{P}_{k',k}^{-j} \left\{ w_j + w_{n+1} \mathbb{1} \{R_{n+1} \geq R_j\} \leq \Delta(R_{-j}, R_j) \right\} \\
& \leq \sum_{k'=1}^{K^*} |\pi_{k'}^*(X_j) - \pi_{k'}^*(X_{n+1})| \mathbb{P} \left\{ w_j + w_{n+1} \mathbb{1} \{\tilde{R}_{k'} \geq R_{n+1}\} \leq \Delta(R_{-j}, R_{n+1}) \mid X_{[n+1]}, R_{[n]/\{j\}} \right\} \\
& \quad + \sum_{k=1}^{K^*} |\pi_k^*(X_{n+1}) - \pi_k^*(X_j)| \mathbb{P} \left\{ w_j + w_{n+1} \mathbb{1} \{R_{n+1} \geq \tilde{R}_k\} \leq \Delta(R_{-j}, \tilde{R}_k) \mid X_{[n+1]}, R_{[n]/\{j\}} \right\}
\end{aligned}$$

$$\begin{aligned}
&\leq 2 \sum_{k=1}^{K^*} |\pi_k^*(X_{n+1}) - \pi_k^*(X_j)| \mathbb{P} \left\{ w_j \leq \Delta(R_{-j}, \max\{R_{n+1}, \tilde{R}_k\}) \mid X_{[n+1]}, R_{[n]/\{j\}} \right\} \\
&\leq 2 \sum_{k=1}^{K^*} |\pi_k^*(X_{n+1}) - \pi_k^*(X_j)|.
\end{aligned}$$

The first inequality is obtained by  $w_{n+1} \geq w_j$  for all  $j$ , which implies that

$$\begin{aligned}
&(w_{n+1} - w_j)(1 - \mathbb{1}\{R_{n+1} \geq R_j\}) \geq 0 \\
&\Leftrightarrow w_j \mathbb{1}\{R_{n+1} \geq R_j\} + w_{n+1} \geq w_j + w_{n+1} \mathbb{1}\{R_{n+1} \geq R_j\}.
\end{aligned}$$

The second inequality is achieved by applying

$$\begin{aligned}
&\pi_k^*(X_{n+1})\pi_{k'}^*(X_j) - \pi_k^*(X_j)\pi_{k'}^*(X_{n+1}) \\
&\leq |\pi_{k'}^*(X_j) - \pi_{k'}^*(X_{n+1})|\pi_k^*(X_{n+1}) + |\pi_k^*(X_{n+1}) - \pi_k^*(X_j)|\pi_{k'}^*(X_{n+1}),
\end{aligned}$$

along with (59) and the definition of  $\mathbb{P}_{k',k}^{-j}$ . Finally, we prove the claim by substituting the upper bound of  $\epsilon(X_{[n+1]}, R_{[n]/\{j\}})$  above into (58).  $\square$

## C.6 Proof of Theorem 4

*Proof.* The proof below follows from the one of Theorem 6 of Barber et al. [2023]. Under the mixture model (4), we have  $R_j \stackrel{\text{d}}{=} \sum_{k=1}^{K^*} \mathbb{1}\{U_j = k\} \tilde{R}_k$ , where  $U_j \sim \sum_{k=1}^{K^*} \pi^*(X_j) \delta_k$  and  $\tilde{R}_k \sim f_k^*$  for  $k \in [K^*]$ . Let  $B_i = \mathbb{1}\{U_i = U_{n+1}\}$ . We have

$$\begin{aligned}
Y_{n+1} \notin \hat{C}_n(X_{n+1}) &\Rightarrow \sum_{i=1}^{n+1} w_{\text{KL},i} B_i \mathbb{1}\{R_i \geq R_{n+1}\} \leq \alpha \\
&\Leftrightarrow \sum_{i=1}^{n+1} w_i B_i \mathbb{1}\{R_i \geq R_{n+1}\} \\
&\leq \alpha \frac{\sum_{i=1}^n \phi_i + 1}{\sum_{j=1}^n \phi_j B_j + 1} \equiv \alpha \delta(X_{[n+1]}, U_{[n+1]}),
\end{aligned} \tag{60}$$

where  $\phi_i = \phi(X_i, X_{n+1}) = \exp\{-m D_{\text{KL}}(\pi(X_{n+1}) \parallel \pi(X_i))\}$  and  $w_i$  is the renormalized weights over the data points with  $U_i = U_{n+1}$ .

Let  $\mathcal{U}_k = \{i \in [n+1] : U_i = k\}$ . All  $R_i$ 's for  $i \in \mathcal{U}_k$  are i.i.d. drawn from  $f_k^*$ . Then,

$$\begin{aligned}
&\mathbb{P}\{Y_{n+1} \notin \hat{C}_n(X_{n+1}) \mid X_{[n+1]}, U_{[n]}, U_{n+1} = k\} \\
&\leq \mathbb{P} \left\{ \sum_{i \in \mathcal{U}_k} w_i \mathbb{1}\{R_i \geq R_{n+1}\} \leq \alpha \delta(X_{[n+1]}, U_{[n+1]}) \mid X_{[n+1]}, U_{[n]}, U_{n+1} = k \right\}
\end{aligned}$$

$$\begin{aligned}
&= \sum_{j \in \mathcal{U}_k} w_j \mathbb{P} \left\{ \sum_{i \in \mathcal{U}_k} w_i \mathbb{1} \{R_i \geq R_j\} \leq \alpha \delta(X_{[n+1]}, U_{[n+1]}) \mid X_{[n+1]}, U_{[n]}, U_{n+1} = k \right\} \\
&= \mathbb{E} \left[ \sum_{j \in \mathcal{U}_k} w_j \mathbb{1} \left\{ \sum_{i \in \mathcal{U}_k} w_i \mathbb{1} \{R_i \geq R_j\} \leq \alpha \delta(X_{[n+1]}, U_{[n+1]}) \right\} \mid X_{[n+1]}, U_{[n]}, U_{n+1} = k \right] \\
&\leq \alpha \delta(X_{[n+1]}, U_{[n]}, k),
\end{aligned}$$

by the deterministic inequality in Lemma A.1 in [Harrison \[2012\]](#). Then,

$$\mathbb{P}\{Y_{n+1} \notin \hat{C}_n(X_{n+1}) \mid X_{[n]}, U_{n+1}\} \leq \alpha \mathbb{E} \left\{ \delta(X_{[n+1]}, U_{[n+1]}) \mid X_{[n+1]}, U_{n+1} \right\}. \quad (61)$$

Next, we use induction to prove an upper bound for the expectation in the RHS of (61). Without loss of generality, we assume that the probabilities  $\pi_k^*(X_i)$  are ordered such that  $\pi_k^*(X_1) \leq \dots \leq \pi_k^*(X_n)$ . When  $n = 1$ , for any  $b \geq 0$ ,

$$\begin{aligned}
\mathbb{E} \left\{ \frac{\phi_1 + b + 1}{\phi_1 B_1 + b + 1} \mid X_{[n]}, U_{n+1} = k \right\} &= \pi_k(X_1) + [1 - \pi_k(X_1)] \frac{\phi_1 + b + 1}{b + 1} \\
&= \frac{[1 - \pi_k(X_1)]\phi_1 + b + 1}{b + 1} \\
&\leq \frac{[1 - \pi_k(X_1)]\phi_1 + b + \pi_k(X_1)\phi_1}{b + \pi_k(X_1)\phi_1} \\
&= \frac{\phi_1 + b}{\phi_1 \pi_k(X_1) + b}.
\end{aligned} \quad (62)$$

The inequality is obtained by  $\pi_k(X_1)\phi_1 \leq 1$  and that  $f(x) = [x + a]/[x + b]$  is a decreasing function of  $x$ , with a negative derivative  $(b - a)/(b + x)^2$  for any  $a > b \geq 0$ .

When  $n \geq 2$  and  $U_{n+1} = k$ , we have  $B_i \stackrel{d}{=} A_i B_n^{(i)}$  for all  $i \in [n - 1]$ , where  $A_i \sim \text{Bern}(\pi_k(X_i)/\pi_k(X_n))$  and  $B_n^{(i)} \sim \text{Bern}(\pi_k(X_n))$ . For any  $b \geq 0$ , we have

$$\begin{aligned}
&\mathbb{E} \left\{ \frac{\sum_{j=1}^n \phi_j + b + 1}{\sum_{i=1}^n \phi_i B_i + b + 1} \mid X_{[n]}, U_{n+1} = k \right\} \\
&= \mathbb{E} \left\{ \frac{\sum_{j=1}^n \phi_j + b + 1}{\sum_{i=1}^{n-1} \phi_i A_i B_n^{(i)} + \phi_n B_n + b + 1} \mid X_{[n]}, U_{n+1} = k \right\} \\
&= \mathbb{E} \left\{ \mathbb{E} \left[ \frac{\sum_{j=1}^{n-1} \phi_j A_j + \phi_n + b + 1}{\sum_{i=1}^{n-1} \phi_i A_i B_n^{(i)} + \phi_n B_n + b + 1} \mid X_{[n+1]}, A_{[n-1]} \right] \right. \\
&\quad \left. \times \frac{\sum_{j=1}^n \phi_j + b + 1}{\sum_{j=1}^{n-1} \phi_j A_j + \phi_n + b + 1} \mid X_{[n]}, U_{n+1} = k \right\} \\
&\leq \mathbb{E} \left\{ \frac{\sum_{j=1}^{n-1} \phi_j A_j + \phi_n + b}{(\sum_{i=1}^{n-1} \phi_i A_i + \phi_n) \pi_k(X_n) + b} \times \frac{\sum_{j=1}^n \phi_j + b + 1}{\sum_{j=1}^{n-1} \phi_j A_j + \phi_n + b + 1} \mid X_{[n]}, U_{n+1} = k \right\}
\end{aligned}$$



$$\begin{aligned}
&\leq \mathbb{E} \left\{ \frac{\sum_{j=1}^{n-1} \phi_j A_j + \phi_n + b}{(\sum_{i=1}^{n-1} \phi_i A_i + \phi_n) \pi_k(X_n) + b} \middle| X_{[n]}, U_{n+1} = k \right\} \\
&\quad \times \mathbb{E} \left\{ \frac{\sum_{j=1}^n \phi_j + b + 1}{\sum_{j=1}^{n-1} \phi_j A_j + \phi_n + b + 1} \middle| X_{[n]}, U_{n+1} = k \right\} \\
&\leq \frac{\sum_{j=1}^{n-1} \phi_j \pi_k(X_j) / \pi_k(X_n) + \phi_n + b}{(\sum_{i=1}^{n-1} \phi_i \pi_k(X_i) / \pi_k(X_n) + \phi_n) \pi_k(X_n) + b} \times \frac{\sum_{j=1}^n \phi_j + b}{\sum_{j=1}^{n-1} \phi_j \pi_k(X_j) / \pi_k(X_n) + \phi_n + b} \\
&= \frac{\sum_{j=1}^n \phi_j + b}{\sum_{i=1}^n \phi_i \pi_k(X_i) + b}. \tag{63}
\end{aligned}$$

In the second equality, only the i.i.d. Bernoulli random variables  $B_n^{(1)}, \dots, B_n^{(n)}, B_n$  are random given  $X_{n+1}$  and  $A_{[n-1]}$ . We then apply case 2 of Lemma 3 in Barber et al. [2023] (i.e. the inverse binomial lemma in Ramdas et al. [2019]) to obtain the first inequality. In the fourth line, the first term is an increasing function of  $\sum_{j=1}^{n-1} \phi_j A_j$  if  $\pi_k(X_n) < 1$ , otherwise a constant function 1 if  $\pi_k(X_n) = 1$ . The second term is a decreasing function of  $\sum_{j=1}^{n-1} \phi_j A_j$ . The covariance between the first and second terms is zero or negative, which gives the second inequality above. In the last inequality, the first term is obtained by Jensen's inequality. When  $n = 2$ , the second term is obtained by (62) with  $B_1$  changed to  $A_1$  and  $b$  changed to  $b + \phi_2$ .

Once eq. (63) holds for  $n = 2$ , we can apply it to bound the second term in the last inequality for  $n = 3$ , with  $(B_1, B_2)$  changed to  $(A_1, A_2)$  and  $b$  changed to  $b + \phi_3$ . By induction, we can prove that eq. (63) holds for any positive integer  $n$ . Then using the definition of  $\delta(X_{[n+1]}, U_{[n+1]})$  in (60), (61) and (63) for  $b = 0$ , we obtain

$$\mathbb{E} \{ \delta(X_{[n+1]}, U_{[n+1]}) \mid X_{[n+1]}, U_{n+1} \} \leq \frac{\sum_{j=1}^n \phi_j}{\sum_{i=1}^n \phi_i \pi_{U_{n+1}}(X_i)} \leq \frac{1}{\sum_{i=1}^n w_{\text{KL}, i} \pi_{U_{n+1}}(X_i)}.$$

Marginalizing out  $U_{n+1}$  given  $X_{n+1}$  gives the bound in the theorem.  $\square$

## D PAC guarantees

In this section, we first review the PAC guarantee for the unweighted SCP interval, and extend the proof to weighted prediction intervals. In general, the proofs of PAC guarantees rely on concentration inequalities without requiring any algorithm to be a symmetric function of the data  $Z_{[n+1]}$ . In the following, we mainly use the notation  $Z_{[n+1]}$  instead of  $\mathcal{D}_{[n+1]}$ . For the intervals  $\hat{C}_n(X_{n+1})$  considered in this paper, the miscoverage event  $\{Y_{n+1} \notin \hat{C}_n(X_{n+1})\}$  is equivalent to

$$p(Z_{[n+1]}) := \sum_{i=1}^{n+1} w_i(Z_{[n+1]}) \mathbb{1}\{R_i \geq R_{n+1}\} \leq \alpha. \tag{64}$$

We define a slightly different p-value which assigns zero weight to  $R_{n+1}$ ,

$$p'(Z_{[n+1]}) := \sum_{i=1}^n w'_i(Z_{[n+1]}) \mathbb{1}\{R_i \geq R_{n+1}\}, \quad (65)$$

where  $w'_i$  are renormalized over the first  $n$  residuals. For the SCP interval in (1),  $w_i(Z_{[n+1]}) = 1/(n+1)$  and  $w'_i(Z_{[n+1]}) = 1/n$ . We define

$$\alpha(Z_{[n]}) = \mathbb{P}\{p(Z_{[n+1]}) \leq \alpha \mid Z_{[n]}\} \quad \text{and} \quad \alpha'(Z_{[n]}) = \mathbb{P}\{p'(Z_{[n+1]}) \leq \alpha \mid Z_{[n]}\}. \quad (66)$$

We begin with a simple lemma that will be used in the results below.

**Lemma 2.** *With probability 1,  $p(Z_{[n+1]}) \geq p'(Z_{[n+1]})$ .*

*Proof.* Since  $w_i(Z_{[n+1]})$  is normalized over all the data points while  $w'_i(Z_{[n+1]})$  is only normalized over first  $n$  points, we have  $w_i(Z_{[n+1]}) \leq w'_i(Z_{[n+1]})$ ,  $\forall i \in [n]$ . Then,

$$\begin{aligned} p(Z_{[n+1]}) - p'(Z_{[n+1]}) &= w_{n+1}(Z_{[n+1]}) + \sum_{i=1}^n [w_i(Z_{[n+1]}) - w'_i(Z_{[n+1]})] \mathbb{1}\{R_i \geq R_{n+1}\} \\ &\geq w_{n+1}(Z_{[n+1]}) + \sum_{i=1}^n [w_i(Z_{[n+1]}) - w'_i(Z_{[n+1]})] = 0, \end{aligned}$$

which proves the claim as required.  $\square$

## D.1 Recap

**Proposition 6** (Proposition 2a in Vovk [2012]). *If the data points  $Z_{[n+1]}$  are i.i.d., for any  $\delta \in (0, 0.5]$ , with probability at least  $1 - \delta$ , the SCP interval in (1) satisfies*

$$\alpha(Z_{[n]}) = \mathbb{P}\{Y_{n+1} \notin \hat{C}_n^{\text{SCP}}(X_{n+1}) \mid Z_{[n]}\} \leq \alpha + \sqrt{\frac{\log(1/\delta)}{2n}}. \quad (67)$$

The guarantee in (67) means that the coverage rate over many test points is close to  $\alpha$  for large sample size  $n$ . We next revisit two standard proofs of Proposition 6.

*Proof.* By Lemma 2, it suffices to prove (67) holds for  $\alpha'(Z_{[n]})$  in (66), where  $p'(Z_{[n+1]}) = n^{-1} \sum_{i=1}^n \mathbb{1}\{R_i \geq R_{n+1}\} \leq \alpha$ . Proposition 2a in Vovk [2012] shows that

$$\alpha'(Z_{[n]}) \sim \text{Beta}(n_\alpha, n + 1 - n_\alpha) \quad \text{for } n_\alpha = \lfloor \alpha(n + 1) \rfloor, \quad (68)$$

which is the distribution of the  $n_\alpha$ -smallest sample in  $n + 1$  i.i.d. standard uniform random variables. The event  $\{\alpha'(Z_{[n]}) \leq \alpha\}$  occurs when the sample quantile of  $R_{[n]}$  is larger than the true marginal quantile of  $R_{n+1}$ . We have

$$F_{\alpha'(Z_{[n]})}(\alpha + \Delta; n_\alpha, n + 1 - n_\alpha) = 1 - \text{Binomial}(n_\alpha - 1; n, \alpha + \Delta).$$

The LHS is the probability that the  $n_\alpha$ -smallest standard uniform random variable  $\alpha'(Z_{[n]}) \leq \alpha + \Delta$ . The RHS is the probability that at least  $n_\alpha$  standard uniform random variables fall into  $[0, \alpha + \Delta]$ . The two events are equivalent, so they have the same probability. For  $B_n \sim \text{Binomial}(\cdot; n, \alpha + \Delta)$  and  $\Delta = \sqrt{\log(1/\delta)/(2n)}$ ,

$$\mathbb{P}\{\alpha'(Z_{[n]}) \leq \alpha + \Delta\} = \mathbb{P}\{B_n \geq n_\alpha\} \geq 1 - \mathbb{P}\{B_n - (\alpha + \Delta)n \leq -\Delta n\} \geq 1 - \delta.$$

The last step is obtained by Hoeffding's inequality.  $\square$

*Proof.* Denote the marginal CDF  $F_R(\cdot)$  and  $G_R(\cdot) = 1 - F_R(\cdot)$ . Then,

$$\begin{aligned} \alpha'(Z_{[n]}) &= \mathbb{P}\{G_R(R_{n+1}) \leq \alpha + G_R(R_{n+1}) - p'(Z_{[n+1]}) \mid Z_{[n]}\} \\ &\leq \alpha + \sup_{(x,y)} \left\{ G_R(|y - \hat{\mu}(x)|) - p'(Z_{[n]}, (x, y)) \right\}, \end{aligned}$$

by the probability integral transform. Then, we have

$$\mathbb{P}\{\alpha'(Z_{[n]}) \leq \alpha + \Delta\} \geq \mathbb{P}\left\{ \sup_{(x,y)} \left\{ G_R(|y - \hat{\mu}(x)|) - p'_n(Z_{[n]}, (x, y)) \right\} \leq \Delta \right\} \geq 1 - \delta,$$

by the  $\Delta$  above and the Dvoretzky-Kiefer-Wolfowitz inequality [Massart, 1990].  $\square$

## D.2 PCP guarantee of weighted intervals

For the weighted p-value in (65), the conditional probability  $\alpha'(Z_{[n]})$  in (66) does not have a tractable distribution as in (68) and  $p'(Z_{[n]}, (x, y))$  is not an unbiased estimator of  $G_R(|y - \hat{\mu}(x)|)$ . The proofs in Appendix D.1 are non-applicable to weighted p-values.

Given marginal validity  $\mathbb{E}[\alpha(Z_{[n]})] \leq \alpha$ , the PAC guarantee in (29) is implied by

$$\mathbb{P}\{\alpha(Z_{[n]}) - \mathbb{E}[\alpha(Z_{[n]})] \leq o(1)\} \geq 1 - o(1). \quad (69)$$

It is known [Talagrand, 1995] that a random variable  $\alpha(Z_{[n]})$  that smoothly depends on many independent random variables  $Z_{[n]}$  concentrates at its expectation. Following this principle, we write  $\alpha(Z_{[n]}) - \mathbb{E}[\alpha(Z_{[n]})]$  as

$$\alpha(Z_{[n]}) - \alpha(Z_{[n-1]}) + \cdots + \alpha(Z_1) - \mathbb{E}[\alpha(Z_{[n]})] \equiv \sum_{i=1}^n \nu(Z_{[i]}).$$

The martingale differences  $\nu(Z_{[i]}), i \in [n]$ , are bounded if we make a stability assumption on the weights in the p-values. Then, we can apply the bounded difference inequality to prove a weighted prediction interval is PAC.

## D.2.1 PAC guarantee of covariate weighted intervals

To illustrate, we first prove a result by assuming the weights only depend on the features, e.g.,  $w_i(Z_{[n+1]}) \propto \phi(X_i, X_{n+1}) = \exp(-\lambda \|X_i - X_{n+1}\|)$ . If  $\lambda$  is small, the sum of distances  $\psi(X_{-j}, X_{n+1})$  defined below increases at a fast rate, which can lead to a PAC guarantee. For example, we have  $\rho_1 = 1$  below for the SCP interval using  $\lambda = 0$ .

**Theorem 5.** *Assume that  $Z_{[n+1]}$  are i.i.d. and  $p(Z_{[n+1]})$  in (64) based on  $\phi(X_i, X_{n+1})$  has a continuous distribution given  $Z_{[n]}$  a.s.. Then,  $\alpha(Z_{[n]})$  in (66) satisfies*

$$\mathbb{P} \left\{ \alpha(Z_{[n]}) \lesssim \alpha + \sqrt{n^{1-2\rho_1} \log(1/\delta)} \right\} \geq 1 - \delta,$$

if  $\psi(X_{-j}, X_{n+1}) := \sum_{i \neq j} \phi(X_i, X_{n+1}) \gtrsim n^{\rho_1}$  for all  $j \in [n]$  and some  $\rho_1 > 1/2$  a.s..<sup>9</sup>

*Proof.* For any  $j \in [n]$ , we can define a leave-one-out p-value

$$p_{-j}(Z_{[n+1]}) := \sum_{i \neq j} w_{-j}(X_i, X_{n+1}) \mathbb{1}\{R_i \geq R_{n+1}\},$$

where  $w_{-j}$  is the renormalized weights. By

$$w(X_i, X_{n+1}) = \frac{\phi(X_i, X_{n+1})}{\phi(X_j, X_{n+1}) + \psi(X_{-j}, X_{n+1})} = \frac{w_{-j}(X_i, X_{n+1})}{1 + \phi(X_j, X_{n+1})/\psi(X_{-j}, X_{n+1})}, \quad (70)$$

we can rewrite the event in (64) as

$$p_{-j}(Z_{[n+1]}) \leq [\alpha - w(X_j, X_{n+1}) \mathbb{1}\{R_j \geq R_{n+1}\}] \times \left[ 1 + \frac{\phi(X_j, X_{n+1})}{\psi(X_{-j}, X_{n+1})} \right]. \quad (71)$$

Observe that the event in (71) implies the following event  $E_+$ :

$$p_{-j}(Z_{[n+1]}) \leq [\alpha - 0] \times [1 + 1/\psi(X_{-j}, X_{n+1})] = \alpha + \alpha/\psi(X_{-j}, X_{n+1}).$$

Conversely, the event in (71) is implied by

$$p_{-j}(Z_{[n+1]}) \leq \alpha \times \left[ 1 + \frac{\phi(X_j, X_{n+1})}{\psi(X_{-j}, X_{n+1})} \right] - \frac{\phi(X_j, X_{n+1})}{\psi(X_{-j}, X_{n+1})},$$

using  $\mathbb{1}\{R_j \geq R_{n+1}\} \leq 1$  and the expression of  $w(X_j, X_{n+1})$  in the first equality in (70). Hence, the event in (71) is also implied by the following event  $E_-$ :

$$p_{-j}(Z_{[n+1]}) \leq \alpha + (\alpha - 1)/\psi(X_{-j}, X_{n+1}).$$

---

<sup>9</sup>We use  $\sum_{i \neq j}$  to denote the sum from 1 to  $n+1$  without including  $j$ -th element. We let  $a \lesssim b$  indicate that  $a \leq Cb$  for some universal constant  $C$ .

Then, we know from the equivalence in (71) that

$$\mathbb{P}\{E_- \mid Z_{[n]\setminus\{j\}}\} \leq \alpha(Z_{[n]}) \leq \mathbb{P}\{E_+ \mid Z_{[n]\setminus\{j\}}\},$$

where the upper and lower bound hold because  $p_{-j}(Z_{[n+1]})$  does not depend on  $Z_j$ . Their difference can be bounded using the rate condition on  $\psi(X_{-j}, X_{n+1})$ ,

$$\mathbb{P}\{\alpha + (\alpha - 1)/\psi(X_{-j}, X_{n+1}) < p_{-j}(Z_{[n+1]}) \leq \alpha + \alpha/\psi(X_{-j}, X_{n+1})\} \lesssim n^{-\rho_1}.$$

The last two equations show that  $\alpha(Z_{[n]})$  satisfies the bounded difference condition in McDiarmid's inequality. That is, modifying the value of one argument of  $\alpha(Z_{[n]})$  changes the value of  $\alpha(Z_{[n]})$  at most  $cn^{-\rho_1}$  for some universal constant  $c$ . Applying McDiarmid's inequality, we prove the claim as required.  $\square$

## D.2.2 PAC guarantee of PCP

We next prove that our PCP interval has a PAC guarantee when the membership probabilities in our mixture model satisfies a stability assumption. Our theorem is inspired by the following series of works on full conformal prediction (FCP) [Vovk et al., 2005]. First, Lei et al. [2018] demonstrate that if the predictive model  $\hat{\mu}$  is stable against perturbation of one response data point in the training set, FCP can achieve an interval length comparable to the oracle interval that uses the true conditional quantile of the residual. More recently, Bian and Barber [2023] shows that FCP is impossible to obtain the PAC guarantee of SCP in distribution-free settings. Liang and Barber [2023] then proves that FCP can have a PAC guarantee if  $\hat{\mu}$  is stable against the change of adding multiple data points into the training set.

We note that the setup of our problem is different from that of FCP. Regarding the assumption, we will require the weights in our p-values to be stable rather than the predictive model  $\hat{\mu}$ . Unlike the results above, we now allow the weights to depend on any data in  $Z_{[n+1]}$ . In what follows, we use the general notation introduced in (64-66). We denote the non-normalized PCP weights in (64) and their sum as

$$\phi_i(Z_{[n+1]}) = \prod_{k=1}^K [\pi_k^{Y_{n+1}}(X_i)]^{\tilde{L}_k} \quad \text{and} \quad \psi_{-j} = n^{-1} \sum_{i \neq j} \phi_i(Z_{[n+1]}).$$

**Assumption 1.** The sum  $\psi_{-j} \in [C_1, C_2]$  for all  $j \in [n+1]$  and some  $C_1, C_2 > 0$  a.s..

**Assumption 2.** (Leave-two-out stability). For sufficiently large  $n$  and some  $\rho > 1/2$ ,

$$\mathbb{P}\{\|\pi^{-(j,n+1)}(X_i) - \pi(X_i)\|_1 \lesssim n^{-\rho}, \forall i, j \in [n] \text{ and } i \neq j\} = 1 - o(1).$$

The notation  $\lesssim$  is introduced below Theorem 5, and  $\pi$  denote the probabilities fitted to  $Z_{[n+1]}$  while  $\pi^{-(j,n+1)}$  denote the probabilities fitted to  $Z_{[n]\setminus\{j\}}$ . Both of them are fitted to  $Z_i$ , so they have a small difference when evaluated at  $X_i$ .

**Theorem 6.** *Suppose Assumptions 1 and 2 holds and the data points  $Z_{[n+1]}$  are i.i.d.. Suppose the  $p$ -value  $p(Z_{[n+1]})$  in (64) based on the PCP weights in (17) is continuous given  $Z_{[n]}$  a.s.. Then, the PCP interval defined in (16), i.e.,  $\alpha(Z_{[n]})$  in (66), satisfies*

$$\mathbb{P} \left\{ \alpha(Z_{[n]}) = \mathbb{P} \{ Y_{n+1} \notin \hat{C}_n^{\text{PCP}}(X_{n+1}) \mid Z_{[n]} \} \lesssim \alpha + n^{-\min\{\rho-1/2, 1\}} \right\} \geq 1 - o(1). \quad (72)$$

*Proof.* We let  $\phi_j = \phi_j(Z_{[n+1]})$  and  $\psi_{-j} = \psi_{-j}(Z_{[n+1]})$ . Observe that

$$\begin{aligned} p'(Z_{[n+1]}) \leq \alpha &\Leftrightarrow p(Z_{[n+1]}) \leq [\alpha + w'_{n+1}(Z_{[n+1]})] \times \frac{\psi_{-(n+1)}}{\psi_{-(n+1)} + \phi_{n+1}} \\ &\Leftrightarrow p(Z_{[n+1]}) \leq \alpha - (1 - \alpha)w_{n+1}(Z_{[n+1]}). \end{aligned}$$

Then, by the definition in (66) and Assumption 1, we have

$$\mathbb{E}[\alpha'(Z_{[n]})] - \mathbb{E}[\alpha(Z_{[n]})] = \mathbb{P} \{ \alpha < p(Z_{[n+1]}) \leq \alpha + (1 - \alpha)w_{n+1}(Z_{[n+1]}) \} \lesssim n^{-1}. \quad (73)$$

By Lemma 2 and marginal validity  $\mathbb{E}[\alpha(Z_{[n]})] \leq \alpha$ , the guarantee (72) is implied by

$$\mathbb{P} \{ \alpha'(Z_{[n]}) - \mathbb{E}[\alpha'(Z_{[n]})] \lesssim n^{-\min\{\rho-1/2, 1\}} \} \geq 1 - o(1). \quad (74)$$

We fix the value of  $\tilde{\pi}_k(X_{n+1})$  at  $\tilde{l}_k/m$ . We denote the non-normalized weight,

$$\phi_i^{-(j, n+1)} = \prod_{k=1}^K [\pi_k^{-(j, n+1)}(X_i)]^{\tilde{l}_k},$$

for the leave-two-out estimator  $\pi^{-(j, n+1)}$ . We decompose the difference between the two non-normalized weights into two error terms:

$$\begin{aligned} \phi_i^{-(j, n+1)} - \phi_i &= \prod_{k=1}^{K-1} [\pi_k^{-(j, n+1)}(X_i)]^{\tilde{l}_k} \times \left\{ [\pi_K^{-(j, n+1)}(X_i)]^{\tilde{l}_K} - [\pi_K(X_i)]^{\tilde{l}_K} \right\} \\ &\quad - [\pi_K(X_i)]^{\tilde{l}_K} \times \left\{ \prod_{k=1}^{K-1} [\pi_k^{-(j, n+1)}(X_i)]^{\tilde{l}_k} - \prod_{k=1}^{K-1} [\pi_k(X_i)]^{\tilde{l}_k} \right\} \\ &\leq \sum_{k=1}^K O(|\pi_K^{-(j, n+1)}(X_i)]^{\tilde{l}_k} - [\pi_K(X_i)]^{\tilde{l}_k}|) \lesssim n^{-\rho}. \end{aligned}$$

To obtain the first inequality, we expand the second line using the first equality. The second inequality uses  $a^m - b^m = (a - b)(a^{m-1}b + a^{m-2}b + \dots + ab^{m-2} + ab^{m-1})$  and Assumption 2. Let  $w_{-j, i}^{-(j, n+1)}$  be the normalized version of  $\phi_i^{-(j, n+1)}$ . By Assumptions 1

and 2, we can bound the difference of the normalized weights:

$$\begin{aligned}
& \sum_{i \neq j} \left| w_{-j,i} - w_{-j,i}^{-(j,n+1)} \right| \\
&= \sum_{i \neq j} \left| \phi_{-j,i} / \psi_{-j} - \phi_{-j,i}^{-(j,n+1)} / \psi_{-j}^{-(j,n+1)} \right| \\
&= n^{-1} \sum_{i \neq j} \left| \frac{\phi_{-j,i} - \phi_{-j,i}^{-(j,n+1)}}{\psi_{-j} / n} + \frac{\phi_{-j,i}^{-(j,n+1)}}{\psi_{-j} \times \psi_{-j}^{-(j,n+1)} / n^2} \times \left[ \psi_{-j}^{-(j,n+1)} - \psi_{-j} \right] / n \right| \tag{75} \\
&= n^{-1} \sum_{i \neq j} O(|\phi_{-j,i} - \phi_{-j,i}^{-(j,n+1)}|) \lesssim n^{-\rho}.
\end{aligned}$$

The remaining steps follow from the proof of Theorem 5. First,

$$\begin{aligned}
p'(Z_{[n+1]}) \leq \alpha &\Leftrightarrow \sum_{i \neq j} \phi_i \mathbb{1}\{R_i \geq R_{n+1}\} + \phi_j \mathbb{1}\{R_j \geq R_{n+1}\} \leq \alpha(\psi_{-j} + \phi_j) \\
&\Leftrightarrow \sum_{i \neq j} w_{-j,i} \mathbb{1}\{R_i \geq R_{n+1}\} \leq \alpha + [\alpha - \mathbb{1}\{R_j \geq R_{n+1}\}] \phi_j / \psi_{-j}.
\end{aligned}$$

By (75), the event in the second line can be implied by

$$p_j^{-(j,n+1)} := \sum_{i \neq j} w_{-j,i}^{-(j,n+1)} \mathbb{1}\{R_i \geq R_{n+1}\} \leq \alpha - c_1 n^{-\min\{\rho-1/2, 1\}},$$

for some positive constants  $c_1$ . Conversely, the event in the second line implies that

$$p_j^{-(j,n+1)} \leq \alpha + c_2 n^{-\min\{\rho-1/2, 1\}},$$

for some positive constants  $c_2$ . The last two equations exclude  $Z_j$  and show that  $\alpha'(Z_{[n]})$  satisfies the bounded difference condition in McDiarmid's inequality:

$$|\alpha'(Z_{[n] \setminus \{j\}}, z_j) - \alpha'(Z_{[n] \setminus \{j\}}, z'_j)| \lesssim n^{-\min\{\rho-1/2, 1\}}, \forall z_j, z'_j \in \mathcal{X} \times \mathcal{Y}.$$

We can then apply the inequality to prove (74), which implies the desired guarantee.  $\square$

## E Additional experiments

In the experiments from Sections 1 and 2.2, we compare posterior conformal prediction (PCP) with split conformal prediction (SCP) [Vovk et al., 2005], SCP+conditional calibration (CC) [Gibbs et al., 2023] and randomly-localized conformal prediction (RLCP) [Hore and Barber, 2023]. Here, we describe the implementation of these methods and discuss the remaining experiments.

**Methods.** The SCP interval is defined in (1). The SCP+CC interval is constructed using a linear quantile regression model fitted to the features and residuals in the validation set. Our implementation also includes the randomization strategy suggested by the authors, which makes the interval have exact coverage at  $1 - \alpha$ . The RLCP interval is described in Section 1.4, where the bandwidth  $\beta$  in the kernel weights is chosen to keep the effective sample size of the interval at 100; we refer to equation (21) in Hore and Barber [2023] for more details on this bandwidth selection method. We implement PCP and select its hyperparameters as described in Appendix B. As detailed there, our mixture model is based on multiple linear models mapping  $X_{n+1}$  to predict whether the residual  $R_{n+1}$  is smaller than some quantiles defined below (35). Our PCP interval in (16) is defined non-parametrically using a weighted empirical distribution. In this sense, we can think of PCP as a semiparametric method, whereas our implementation of SCP+CC is parametric, and RLCP is nonparametric.

**Worst-slice conditional coverage rate.** Following the steps outlined in Section S1.2 of Romano et al. [2020b], we partition the test data into two subsets, with 20% used to compute the worst slice and 80% used to evaluate the conditional coverage. We generate slices  $\{x : v^\top x \in [a, b]\}$  for 2500 random vectors  $v$  on the unit sphere. For every slice, we choose  $a$  and  $b$  to minimize the within-slice coverage rate, subject to the slice containing at least 10% of the data in the first subset. The worst-slice coverage rate is the minimum within-slice coverage rate across all slices.

## E.1 Setting 2

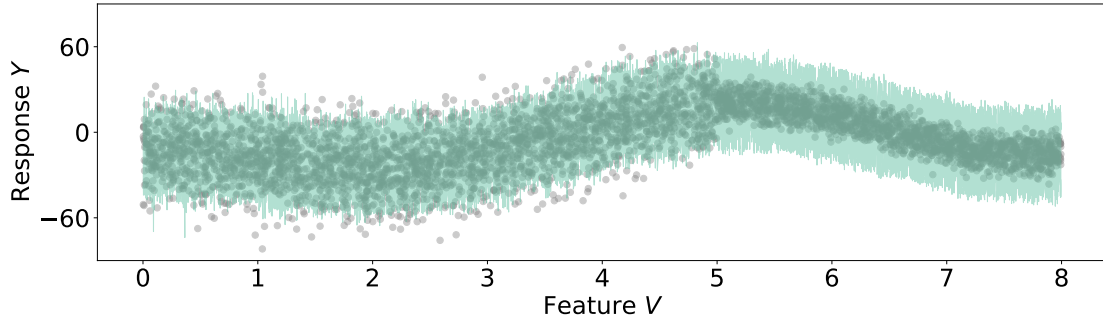
The 6-dimensional features and the drift function  $f(V)$  are generated in the same way as Setting 1. Here we generate the response  $Y$  with a change point in variance:

$$Y = f(V) + 4(1 + 3\mathbb{1}\{V \leq 5\})\epsilon_i \quad \text{and} \quad \epsilon_i \sim \mathcal{N}(0, 1).$$

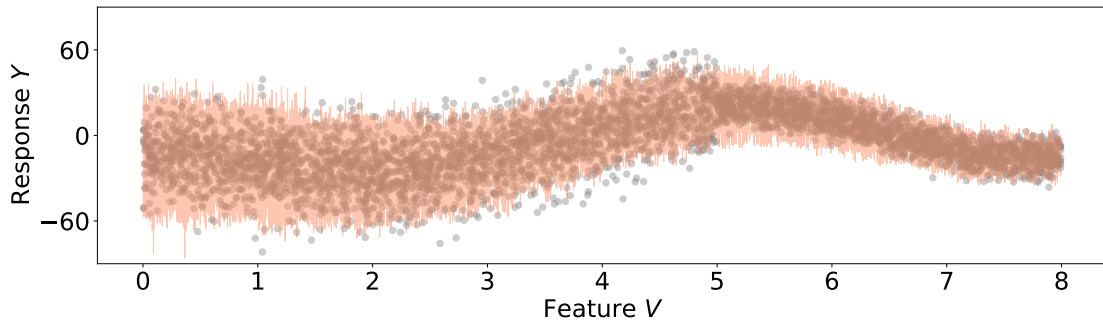
As in Setting 1, we generate 5000 random copies of  $(X, Y)$  as our training, validation, and test sets, respectively. We use the training set to fit a random forest model  $\hat{\mu}$ , which can accurately approximate the function  $f(V)$ . We can imagine the residual  $R = |Y - \hat{\mu}(X)|$  roughly follows a mixture model in (4), where  $\pi_k^*(X)$  is either 0 or 1 for  $V > 5$ , leading to the sparse scenario described in Theorem 4.

Figure 15 depicts the test responses and their prediction intervals. The intervals of SCP, SCP+CC and PCP are stable locally with small variations from the predictions by  $\hat{\mu}$ . In comparison, the interval of RLCP exhibits more variability due to matching all the features and randomizing the location of the test point. Figure 16 shows the local average coverage rates of the intervals over the 250 nearest test points based on the feature  $V$ . SCP uses the same empirical quantile to generate the intervals for all the test points. We can see that these intervals are poorly calibrated with coverage of

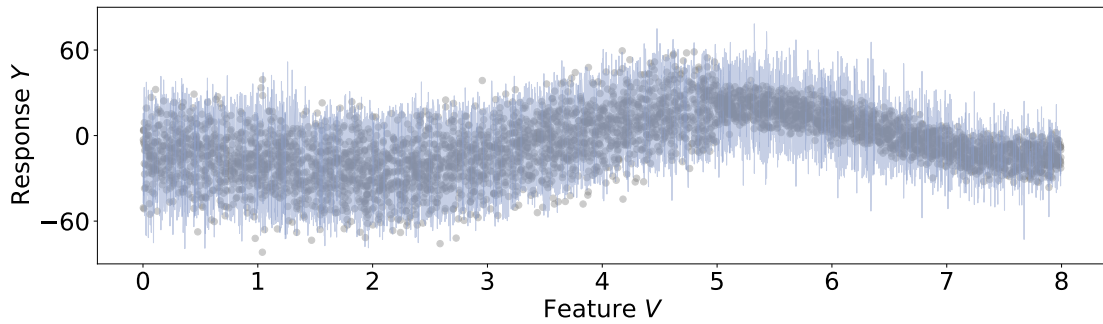




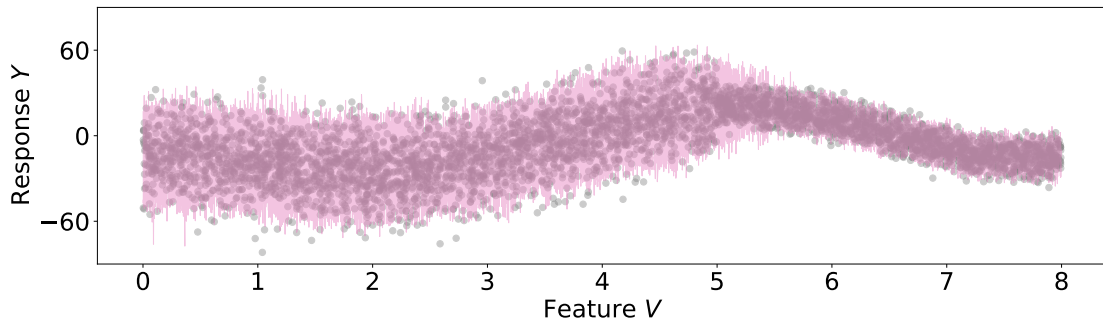
(a) Split conformal prediction (SCP).



(b) SCP+conditional calibration (SCP+CC).



(c) Randomly-localized conformal prediction (RLCP).



(d) Posterior conformal prediction (PCP).

Figure 15: Prediction intervals of conformal prediction methods in Setting 2.

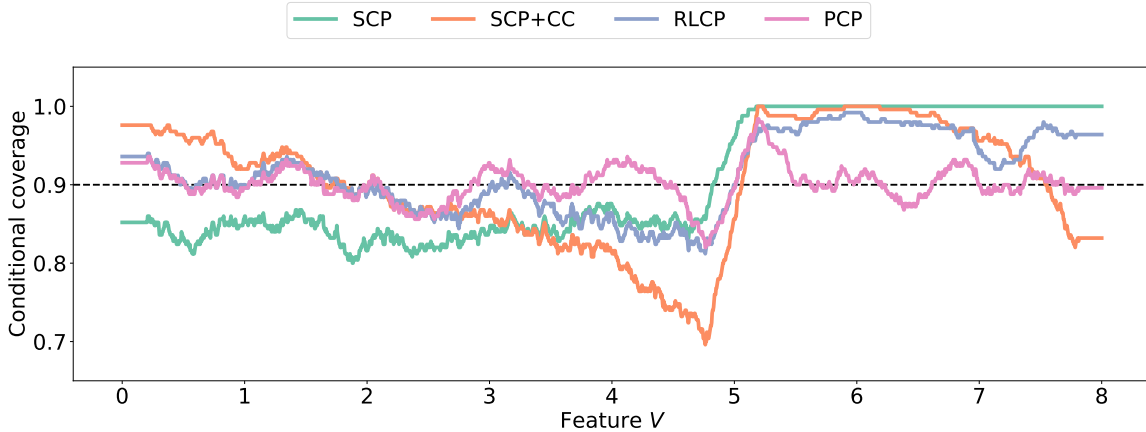


Figure 16: Local average coverage rates of conformal prediction methods in Setting 2.

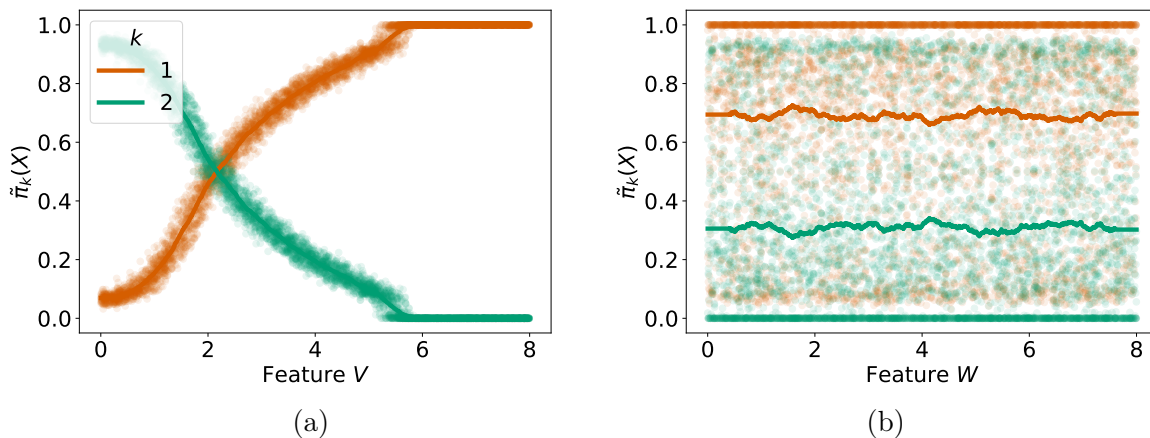
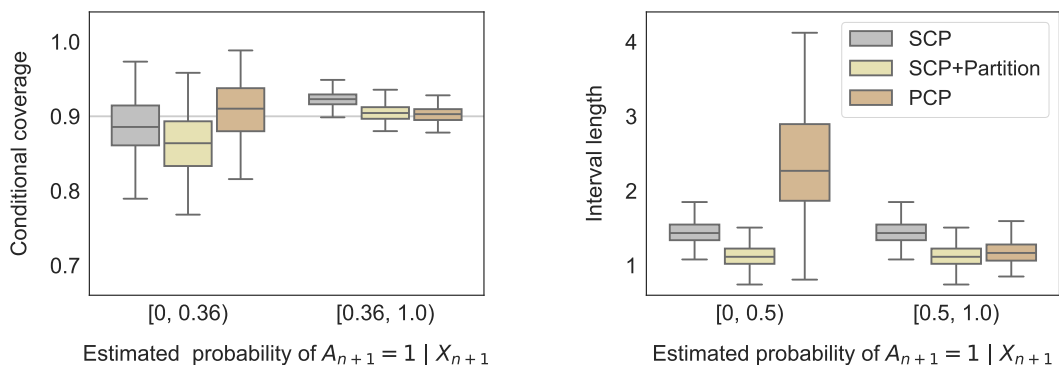


Figure 17: PCP membership probabilities in Setting 2.

around either 0.8 or 1. In SCP+CC, the linear quantile model fails to capture the nonlinear changes in the conditional residual distribution. Consequently, its coverage rate drops significantly at the changepoint  $V = 5$ . RLCP also has coverage gaps because matching all the features makes it difficult to detect the changes in the conditional residual distribution due to the first feature  $V$ .

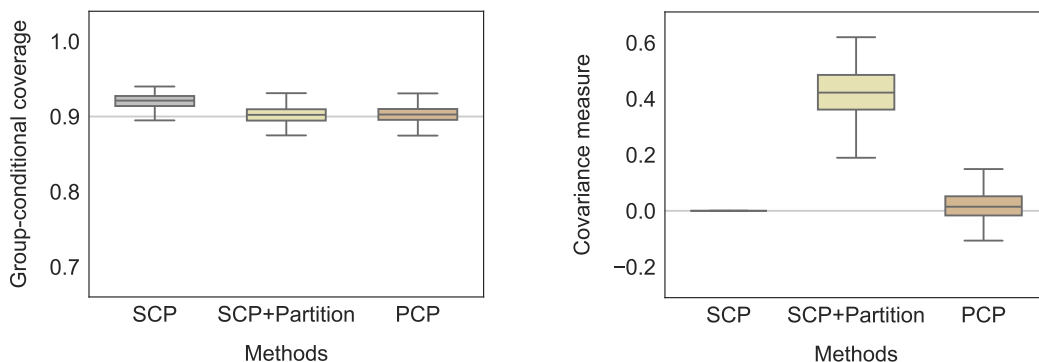
PCP consistently achieves a coverage rate near 0.9 at most values of  $V$ . We interpret this result by visualizing the membership probabilities in Figure 17. The probabilities vary continuously over  $V$  while changing randomly over  $W$ . This means our mixture model learns that  $V$  is the important feature of the conditional residual distribution. The hyperparameter selection procedure in Appendix B.1 chooses a large value of the precision parameter,  $m = 500$ . Thus, the membership probabilities  $\tilde{\pi}_1(X)$  have small deviations from the local average in Figure 17a. With the large  $m$  and  $\tilde{\pi}_1(X) = 1$ , PCP achieves approximate conditional validity and short interval length for  $V \in [5, 8]$ , where the residuals are (approximately) drawn from the same distribution.

## E.2 Medical expenditure panel survey dataset



(a) Coverage rate given  $A_{n+1} = 1$  and  $\tilde{e}(X_{n+1}) < \theta = 0.36$ .

(b) Interval length given  $A_{n+1} = 1$  and  $\tilde{e}(X_{n+1}) < \theta = 0.36$ .



(c) Group-conditional coverage rate given  $A_{n+1} = 1$  (female).

(d) Measure of dependence between intervals and  $A_{n+1}$  given  $X_{n+1}$ .

Figure 18: Comparison of conformal prediction methods on a racial feature in the Medical Expenditure Panel Survey (MEPS) 19.

We replicate the MEPS experiment in Section 3, with the variable  $A_{n+1}$  indicating whether the test point is from a white or non-white person. We let  $\theta = 0.36$  in (22) since white individuals make up approximately 36% of the full population. We divide the white group ( $A_{n+1} = 1$ ) in the test set into two subgroups based on whether  $\tilde{e}(X_{n+1}) < 0.36$  or not, where  $\tilde{e}(X_{n+1})$  is the estimator of  $e(X_{n+1})$  defined below (23). Figure 18a shows that SCP+Partition decreases the coverage rate for white individuals with  $A_{n+1} = 1$  and  $\tilde{e}(X_{n+1}) < 0.36$ . PCP closes this gap by weighting, which significantly increases the interval length in Figure 18b. Nevertheless, the coverage rate of PCP is around 0.9, meaning it is non-conservative. The PCP interval maintains the group-conditional coverage guarantee of SCP+Partition in Figure 9c, while being independent of  $A_{n+1}$  asymptotically, as shown in Figure 9d.